UCRL-18918
cy. 2

LIBRARY AND
DOCUMENTS SECTION

THE DESIGN OF AN IMPROVED DEVICE FOR ABSORPTION WITH CHEMICAL REACTION

Edward J. Palkot, Jr.* and C. Judson King

RECEIVED
LAWRENCE
RADIATION LABORATORY
JUL 15 1969
LIBRARY AND
DOCUMENTS SECTION

June 1969

AEC Contract No. W-7405-eng-48

*M.S. Thesis

TWO-WEEK LOAN COPY

This is a Library Circulating Copy which may be borrowed for two weeks. For a personal retention copy, call Tech. Info. Division, Ext. 5545

UCRL-18918
cy. 2

LAWRENCE RADIATION LABORATORY
UNIVERSITY of CALIFORNIA BERKELEY

DISCLAIMER

This document was prepared as an account of work sponsored by the United States Government. While this document is believed to contain correct information, neither the United States Government nor any agency thereof, nor the Regents of the University of California, nor any of their employees, makes any warranty, express or implied, or assumes any legal responsibility for the accuracy, completeness, or usefulness of any information, apparatus, product, or process disclosed, or represents that its use would not infringe privately owned rights. Reference herein to any specific commercial product, process, or service by its trade name, trademark, manufacturer, or otherwise, does not necessarily constitute or imply its endorsement, recommendation, or favoring by the United States Government or any agency thereof, or the Regents of the University of California. The views and opinions of authors expressed herein do not necessarily state or reflect those of the United States Government or any agency thereof or the Regents of the University of California.

UCRL-18918

UNIVERSITY OF CALIFORNIA

Lawrence Radiation Laboratory
Berkeley, California 94720

AEC Contract No. W-7405-eng-48

THE DESIGN OF AN IMPROVED DEVICE FOR ABSORPTION WITH CHEMICAL REACTION

Edward J. Palkot, Jr. and C. Judson King

(M.S. Thesis)

June 1969

THE DESIGN OF AN IMPROVED DEVICE FOR ABSORPTION WITH CHEMICAL REACTION

Contents

Abstract vi

List of Figures viii

I. Introduction 1

A. Project Motivation 1

B. Purpose and Scope of Investigation 10

II. Carbon Dioxide Absorption 12

A. Process Specification 12

B. Design Basis 13

1. General Consideration 13

2. Multi-staging 23

C. Chemical and Physical Properties 24

III. HCl Absorption 26

A. Process Specification 26

B. Design Basis 27

1. General Consideration 27

2. Heat and Mass Balances 35

C. Chemical and Physical Properties 43

IV. Discussion and Design of Absorption Devices 44

A. Co-current Packed Column 44

1. General Consideration 44

2. HCl-water System 52

3. CO_2 Absorption System 60

B. Open Pipe Contactors 69

1. General Consideration 69

2. Annular Flow 78

3. Froth Flow 97

C. Dispersed Phase Systems 109

1. General Considerations 109

2. Spray Towers 114

3. Spray Tower--CO_2 Absorption 117

V. Evaluation and Conclusions 123

A. General Considerations 123

B. CO_2 Absorbers 126

1. Basis of Evaluation 126

2. Results 130

C. HCl Absorbers 133

1. Basis of Evaluation 133

2. Results 135

D. General Conclusions 138

Acknowledgments 140

Appendices 141

I. A. Rate Considerations for CO_2 Absorption 141

I. B. Test of Criterion for Treating Absorption of CO_2 into Potassium Carbonate Solution as Pseudo First-Order . . . 146

II. Physical Solubility of CO_2 in K_2CO_3 147

III. Chemical Equilibrium in the CO_2-K_2CO_3 System 149

IV. Physical Properties--CO_2-K_2CO_3 System 151

V. Algorithm for Determining Over-all Heat and Mass Balances for the Two-contactor HCl Absorption Process 153

VI. Equilibrium in the HCl-water System 157

VII. HCl-water System Enthalpy Data 159

VIII. Physical Properties--HCl-water System 164

IX. Physical Properties for Coefficient Correction 169

X. Fourth-order Runge-Kutta Integration for HCl Absorption in a Packed Column 171

XI. Flow Equations and Determination of Column Lengths for the CO_2-K_2CO_3 System 175

XII. Nomenclature 180

References 187

THE DESIGN OF AN IMPROVED DEVICE FOR ABSORPTION WITH CHEMICAL REACTION

Edward J. Palkot, Jr. and C. Judson King

Lawrence Radiation Laboratory and,
Department of Chemical Engineering
University of California
Berkeley, California 94720

June 1969

ABSTRACT

When absorption is accompanied by chemical reaction in the liquid phase, the nature of the gas-liquid equilibrium data is often such that a high degree of gas purification may be accomplished in one or a very few equilibrium stages. Examples of such absorption systems that were considered in this study are the scrubbing of CO_2 from gas streams using hot, catalyzed potassium carbonate and the scrubbing of HCl from gas streams using water. The scrubbing of CO_2 is important in the manufacture of high purity hydrogen for process uses such as the manufacture of ammonia, and HCl absorption is important in many processes, including a scheme for the reprocessing of enriched reactor fuels which has been considered by the AEC. Less commonly used devices for carrying out these absorption processes were considered which had features likely to result in high absorption rates and, consequently, high efficiency. The implementation of devices with these characteristics might be expected to result in considerable savings in investment and/or operating costs when compared to equipment currently used to effect the desired gas purifications.

The devices considered were the co-current packed column, open pipe contractors with co-current flow of gas and liquid in the froth and annular regimes, and the spray tower. Based on information dealing with these devices in the literature and models which were proposed to fill gaps in the literature, device sizes necessary to scrub gases of quantities and compositions likely to be encountered in industry were calculated. Hierarchies of attractiveness of the devices for each of the systems studied were determined by assigning relevant cost variables to each contractor. It was shown that some of the devices could well be attractive in reducing the costs of absorption in the processes considered.

LIST OF FIGURES

Fig. 1. Solubility of CO_2 in water at low pressure.

Fig. 2. CO_2 vapor pressure in the K_2CO_3-$KHCO_3$-CO_2-H_2O system.

Fig. 3. Partial pressure of HCl over aqueous HCl solutions.

Fig. 4. Vetrocoke absorption system.

Fig. 5. Single and staged CO_2 contactors.

Fig. 6. Staged HCl contactors.

Fig. 7. Concentration and temperature profiles in a single packed column for HCl absorption; diameter = .888 ft.

Fig. 8. Flow patterns in two-phase gas-liquid horizontal flow.

Fig. 9. Baker correlation of flow patterns in gas-liquid horizontal flow.

Fig. 10. Concentration and temperature profiles in a single annular-flow contactor for HCl absorption.

Fig. 11. Bubble diameter vs. $(D)^{1/2}/V_l$; James and Silberman data; 0, 2-1/2 in. pipe; Δ, 4 in. pipe.

Fig. 12. Flow diagram for absorption of CO_2 in two froth-flow contactors.

Fig. 13. Flow diagram for HCl absorption in froth-flow contactor.

Fig. 14. Regions of Baker correlation to which open pipe contactor designs correspond.

Fig. 15. Dispersed-phase contacting devices.

Fig. 16. Depiction of operating and investment variables for CO_2 absorbers.

Fig. 17. Depiction of operating and investment variables for HCl absorbers.

I. INTRODUCTION

A. Project Motivation

In the general consideration of separation processes, the concept of the "equilibrium stage" is frequently invoked as a thermodynamic measure of the feasibility of separating a stream of given composition into streams with compositions different than the input stream. By definition, any single equilibrium stage process is limited by the constraint that the compositions of the product streams can at best only be in equilibrium with each other. The desire to obtain better separation than that corresponding to equilibrium between the products necessitates the implementation of devices which will provide multiple equilibrium stages.

For purely physical absorption more than one equilibrium stage will commonly be required to effect desired separations of components from gas streams. A typical physical absorption process is represented by the CO_2 - H_2O system, for which equilibrium data are shown in Fig. 1. A counter-current operating line has been drawn which corresponds to using an inlet stream of pure water to reduce the CO_2 content of a gas stream from 10% to 1% at 10 atmospheres total pressure and a liquid to gas ratio (assumed constant) of twice the minimum. Approximately 5 equilibrium stages would be required to effect the desired separation.

The absorption of carbon dioxide into water may be contrasted to the absorption of CO_2 into potassium carbonate or HCl into water. In both of these cases, absorption is accompanied by chemical reaction in

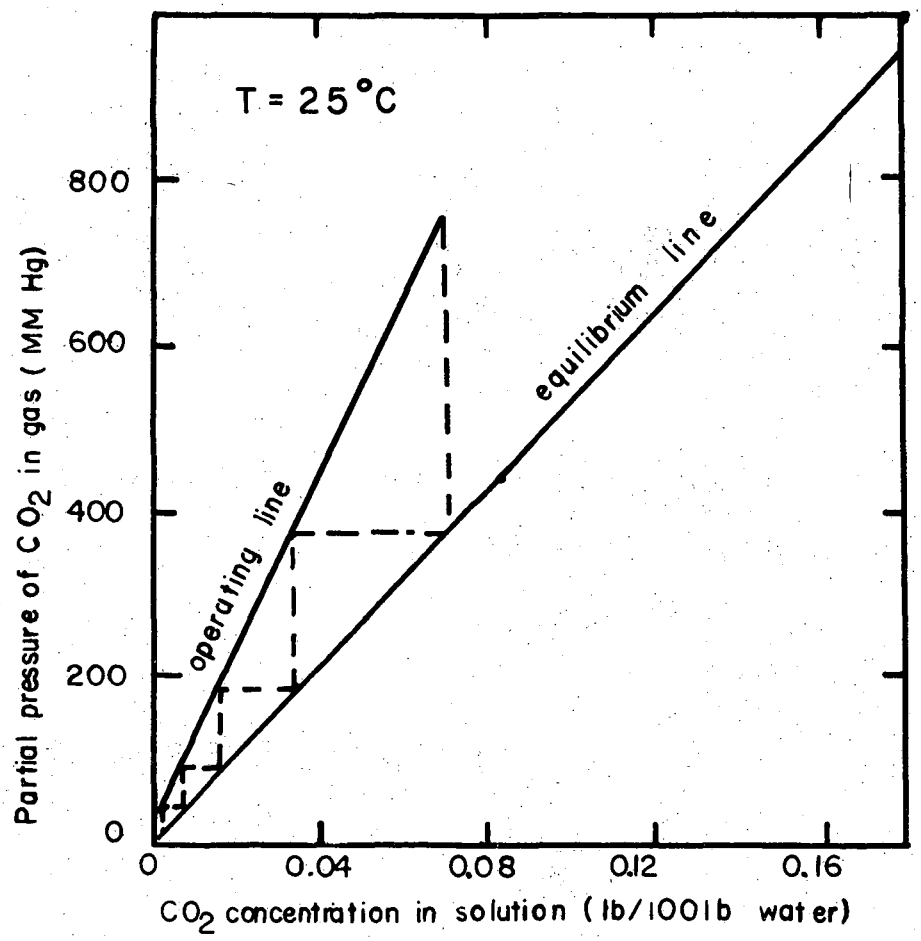

XBL 695-575

Fig. 1. Solubility of CO_2 in water at low pressure.

the liquid phase, according to the equations:

$$(CO_2\text{-}K_2CO_3) \qquad CO_2(g) = CO_{2(soln)} \tag{1}$$

$$CO_{2(soln)} + K_2CO_3 + H_2O = 2KHCO_3 \tag{2}$$

$$(HCl\text{-}H_2O) \qquad HCl_{(g)} = HCl_{(soln)} \tag{3}$$

$$HCl_{(soln)} + H_2O = H_3O^+ + Cl^- \quad . \tag{4}$$

These equations may be generalized as:

$$A_{(g)} = A_{(soln)} \tag{5}$$

$$A_{(soln)} + R = B + C \quad . \tag{6}$$

The equilibrium condition of Eq. (5) may be represented as

$$p_A = \frac{1}{H}\,[A_{(soln)}] \tag{7}$$

where p_A is the partial pressure of A in the gas phase, H is a solubility constant and the bracketed term represents a concentration variable. The equilibrium state of Eq. (6) may be represented as

$$K = \frac{[B][C]}{[A][R]} \tag{8}$$

where K is the equilibrium constant, and the bracketed terms represent concentration variables. Combining Eqs. (7) and (8), the partial pressure of A may be expressed as

$$p_A = \frac{[B][C]}{HK[R]} \quad . \tag{9}$$

If the concentration of the reagent, R, is large relative to the amounts of B and C formed during reaction, implying that the forward reaction is pseudo-first order with respect to the solute A, Eq. (9) implies that the equilibrium curve should be approximately parabolic. The equilibrium curves for the CO_2-K_2CO_3 and HCl-water systems are shown in Figs. 2 and 3. Their shapes confirm the predictions of the preceding analysis.

The shapes of the equilibrium curves characteristic of absorption with chemical reaction in the liquid phase have important implications regarding the necessity of staging. Possible operating lines are drawn on Figs. 2 and 3, corresponding to using initially unreacted absorbents to reduce the respective gas concentrations from 10% to 1% at liquid to gas ratios (assumed constant) equal to twice the minimum. A total pressure of ten atmospheres is assumed for the CO_2 case, and a total pressure of one atmosphere and a constant temperature of 70°F for the HCl case. With this choice of parameters, the desired separations may be accomplished in approximately one equilibrium stage.

The analysis of the necessity of staging has, to this point, neglected rate considerations--i.e., the extent to which equilibrium will be approached in a contacting device. The extent of approach to equilibrium may be represented by the Murphree stage efficiency, written (in terms of the gas-phase compositions) as

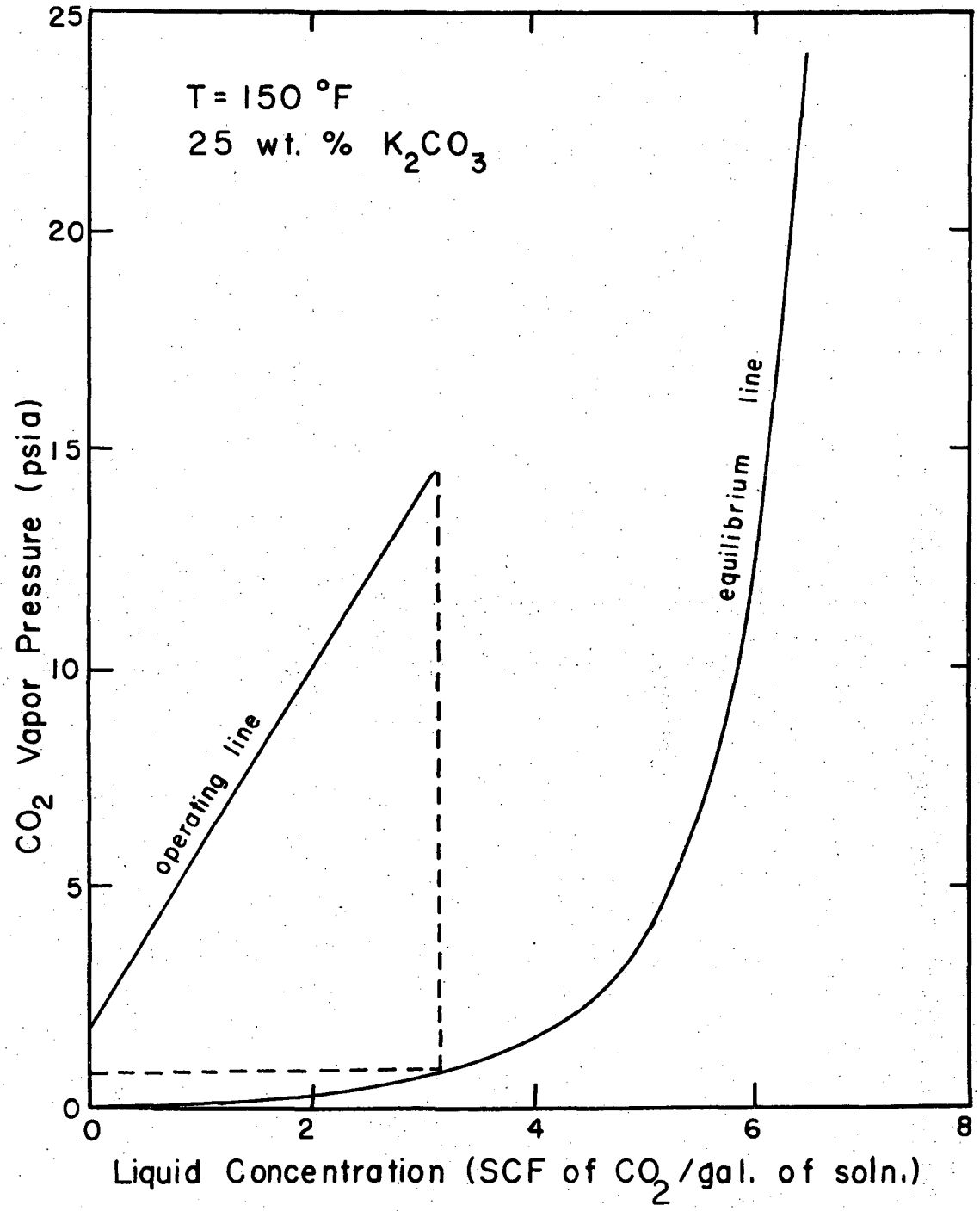

XBL 695-574

Fig. 2. CO_2 vapor pressure in the K_2CO_3-$KHCO_3$-CO_2-H_2O system.

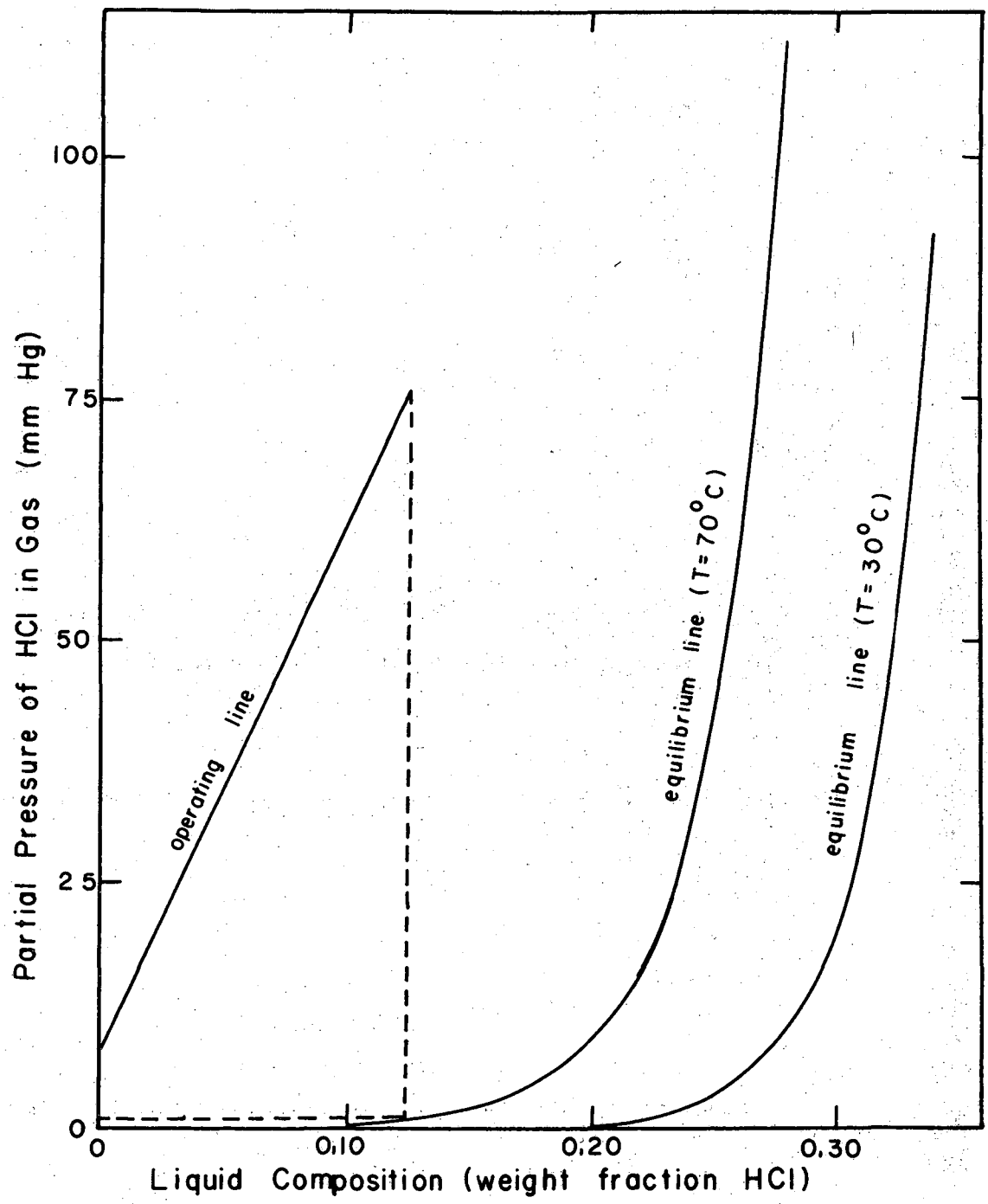

XBL 695-570

Fig. 3. Partial pressure of HCl over aqueous HCl solutions.

$$E_{MV} = \frac{y_{in} - y_{out}}{y_{in} - y^*_{out}} \tag{10}$$

where y_{in} and y_{out} are the inlet and outlet gas compositions of the solute to be absorbed and y^*_{out} is the gas composition in equilibrium with the outlet liquid. The rate of mass transfer of solute from the gas stream may be written as

$$d(G_m y) = SK_g aP(y - y^*)\, dz \tag{11}$$

where G_m = molar gas flow rate, moles/(time)

K_g = over-all mass-transfer coefficient, moles/(time) (unit pressure)(unit area)

P = total pressure

a = interfacial area per unit volume available for mass transfer

y = mole fraction of solute in bulk gas

y^* = mole fraction of solute in equilibrium with liquid at point in reactor

z = length coordinate

S = cross sectional area of contactor.

The approach of y_{out} to y^*_{out} will depend on the rate of mass transfer, $SK_g aP(y - y^*)$. In the case of absorption with chemical reaction in the liquid phase, a gas phase solute must, upon entering the liquid under the impetus of a concentration difference corresponding to the purely physical solubility of the solute, react with the reagent in the

liquid to achieve full chemical equilibrium. If the chemical reaction is infinitely fast, as is the ionization reaction between HCl and water, and the solvent reagent (e.g., water) concentration is large relative to that of the solute, the solute will achieve full equilibrium immediately upon entering the liquid phase. The rate of absorption will effectively be determined by the full concentration difference corresponding to the attainment of total equilibrium, rather than that corresponding only to the physical solubility of the solute. The process may be treated as if it were purely physical absorption, with no consideration of the actual kinetics necessary. If, on the other hand, the chemical reaction rate is finite, as is the case with the reaction of CO_2 with K_2CO_3, the solute will not achieve full chemical equilibrium immediately upon entering the liquid. The concentration driving force will in this case be that corresponding only to the physical solubility of the solute. Equation (11) implies that for given values of the transport coefficient, effective interfacial area and degree of purification desired, the vessel length will be increased compared to that calculated if the absorption were accompanied by an infinitely fast chemical reaction with a large excess of dissolved reactant at the gas-liquid interface. Conversely, the reduced concentration driving force relative to the change in bulk gas composition desired implies that the stage efficiency is reduced. This conclusion has been verified by Kohl and Riesenfeld, who report stage efficiencies for the simultaneous absorption of CO_2 and H_2S into MEA as 15% and 40% respectively, with the greater efficiency for H_2S absorption corresponding to the faster rate of reaction of H_2S with MEA.[1]

Based on equilibrium consideration, then, it is possible to carry out absorption with chemical reaction in devices providing one, or only a few, equilibrium stages. However, to obtain the capacity and degree of separation corresponding to the multiple-stage devices currently used for absorption with a finite chemical reaction rate, while making few-stage devices competitive in terms of capital and operating costs, the efficiency of these devices must be greater than those currently used for the process.

In recent years, a number of devices and methods of contacting have been considered which, by increasing the transport coefficients and effective interfacial area, improve absorption efficiency. Many of these devices may be particularly applicable to carrying out absorption with chemical reaction.

The shapes of the equilibrium curves, which imply that staging is unnecessary, also suggest that the over-all driving force corresponding to co-current flow patterns may be similar to that obtainable with counter-current flow. This results from a change in the equilibrium partial pressure or concentration of the active component along the length of the contactor smaller than occurs in the case of physical absorption. In a co-current flow scheme, flow rates of the phases are not limited by flooding considerations, as in counter-current flow, and much higher linear velocities may be brought about, with a great flexibility in gas-liquid ratios. The turbulent interfacial conditions obtainable with the higher phase velocities act to decrease the resistance of each phase to mass transfer, and the mixing that may occur as a result

of the turbulence will greatly increase the area available for mass transfer. These advantages of increased efficiency must be weighed against possibly greater pressure drops due to the increased velocities necessary to be able to accrue the advantages of co-current flow.

B. Purpose and Scope of Investigation

The purpose of this investigation was to utilize available data to estimate the attractiveness of less-commonly-used devices for carrying out specific absorption processes. Although a myriad of devices have been proposed for efficient gas-liquid contacting, data necessary for theoretically predicting absorption performance are not frequently available. The choice of the specific contacting schemes studied--the co-current packed column, two-phase co-current flow in open pipes and the spray tower--was based both on the potential attractiveness of these devices for carrying out efficient mass transfer in stages of compact size and on the availability of data potentially useful for design purposes.

The choice of the particular systems studied--the absorption of CO_2 into hot, catalyzed potassium carbonate and HCl into weak hydrochloric acid--was based on the potential theoretical and practical fruits of the investigation. From a theoretical standpoint, these systems represent the extremes of almost complete control of the transfer process in either the liquid or the gas phase, and a distinction between a finite and an infinite rate of chemical reaction. The difference in applicability of specific contacting devices for systems with these

distinct characteristics is of interest. From a practical standpoint, the systems studied represent gas-cleaning problems of considerable interest in various processing operations, including a number of interest to the AEC.

For each absorption system studied, separation problems, expressed in terms of gas flow rates, compositions and purification requirements, were defined by reference to available literature. Process operating conditions, physical and chemical properties were similarly determined. The necessary absorbent flow rates were determined by implicitly setting the efficiency of the absorption devices and assuming a concentration of solute in the available absorbent. The effect of using multiple stages was considered in light of variables affecting the economics of both the absorber and over-all process. For example, a reduced absorbent flow rate associated with multiple stages of efficiency comparable to a single stage may have important implications regarding stripper-reboiler duties and, in the case of HCl absorption, the production of an acid of commercially valuable strength. With the flow rates determined, the size and operating characteristics of specific devices were determined. No optimization was attempted, either on an over-all process or device basis, but the effect of certain variables, such as column diameter, was investigated. The relative attractiveness of the various contacting schemes considered was evaluated by comparing their investment and operating requirements.

II. CARBON DIOXIDE ABSORPTION

A. Process Specification

The most commonly used process to produce hydrogen involves the reforming of light hydrocarbons, such as methane, ethane or naphtha, to produce a gas mixture consisting mainly of hydrogen, carbon monoxide, carbon dioxide, nitrogen and unreacted or cracked hydrocarbons. Carbon dioxide and carbon monoxide must be removed or converted to produce an ammonia synthesis gas with a high hydrogen purity. The bulk of the carbon monoxide is converted, in a "shift converter", by reaction with steam to form carbon dioxide. The bulk of the carbon dioxide is removed by absorption into an alkaline solvent, after which the remaining quantities of carbon dioxide and monoxide are converted to methane.

The absorption of CO_2 in this purification train is an important consideration in the economics of ammonia production, and the possible savings in capital and/or operating costs with a more efficient process than currently used deserves investigation.[2]

In recent years, various modifications of the hot potassium carbonate process, developed by the U. S. Bureau of Mines in their effort to provide a commercially useful Fischer-Tropsch process, have replaced the ethanolamine absorption process as the most widely used for CO_2 removal. The unmodified hot potassium carbonate process has been widely discussed.[3,4,1] One licensed modification of the hot carbonate process is the Giammarco-Vetrocoke process, which uses either small amounts of organic catalysts or, more effectively, large amounts of inorganic catalysts, such as arsenic trioxide, to increase the rate of reaction in the liquid phase.[1]

The necessity of increasing the catalyzed rate of reaction of CO_2 with potassium carbonate dictates the use of high process temperatures--although not as high as in the unpromoted hot carbonate process--in spite of the decrease in gas solubility with elevation in temperature. Furthermore, the existence of high pressure in the synthesis gas process stream suggests the use of high pressure in the absorber. As a consequence of these temperature and pressure conditions and the nature of the CO_2 - carbonate equilibrium relationships, the bulk of the absorbent regeneration may be accomplished by flashing the liquid to low pressure (about 1 atmosphere). This results in a 30% - 40% saving in regeneration costs relative to the amine system, where regeneration must be carried out at high temperatures because of equilibrium and solubility considerations.[5]

The Vetrocoke absorption process has been carried out commercially in counter-current plate or packed columns, despite the low efficiencies which have been measured in these devices.

B. Design Basis

1. General Consideration

Many of the parameters significant for design were based on a hydrogen plant of the Phillips Petroleum Company discussed by Hyman.[6] A schematic diagram of the absorber-stripper combination is shown in Fig. 4. The composition of the gas leaving the cold shift converter and entering the Vetrocoke absorber was taken from the Phillips flow sheet,

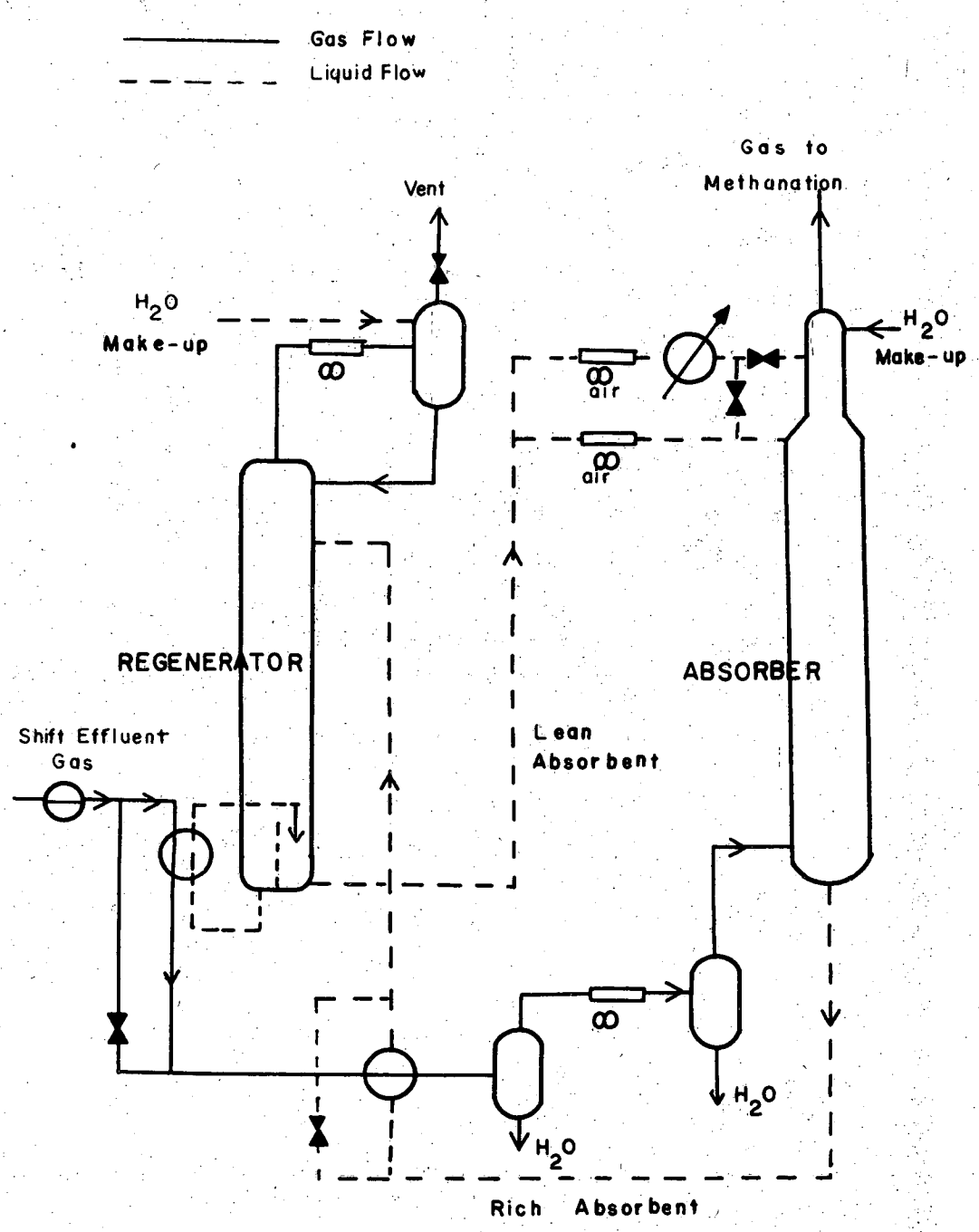

XBL 695-577

Fig. 4. Vetrocoke absorption system.

with the exception that the water vapor was neglected and design was considered on a dry basis. The outlet CO_2 specification was altered to make the outlet CO_2 mole fraction approximately 1%, rather than 2% as shown for the Phillips process. The higher outlet CO_2 content was sufficient in the Phillips case because of the use of an amine absorber to purify the Vetrocoke tail gas. All gas flow rates were scaled down to yield flow rates corresponding more closely to the ranges of variables studied in the available literature dealing with less commonly used absorption equipment. A summary of the gas flow rates and compositions is given in Table 1.

To simplify the calculation procedures, the process was assumed to be isothermal. Because of the high liquid to gas ratio and the relatively small heat of absorption of CO_2, the error of this assumption is probably small compared to other errors involved in the estimate of equipment sizes. The temperature was taken to be 150°F, based on the inlet gas temperature to the Phillips absorber.

The average pressure in the contactor was taken to be about 140 psia, based on the flow sheet range of 140-150 psia.

The concentration of K_2CO_3 used for the absorbent is constrained by solubility, temperature and conversion relationships, as demonstrated by Kohl and Riesenfeld.[1] It was assumed that the effect of dissolved catalyst would not significantly alter the conclusions regarding solubility obtained for the situation with unpromoted carbonate. For example, at 150°F, a 40%-by-weight solution of K_2CO_3 can only be about 43% converted to $KHCO_3$ before precipitation will occur, while a 25%

solution may be completely converted at this temperature. Buch and Leitch[7] have concluded that 30% equivalent K_2CO_3 concentration should be the maximum used, and have observed no appreciable effect on absorptive capacity from reducing the concentration to 20%. The carbonate solution was thus assumed to be 25% equivalent K_2CO_3 by weight.

The catalyst was assumed to be arsenious acid, $As(OH)_3$, which dissociates to form arsenite ion, the actual catalyzing agent. Because of the proprietary nature of the Vetrocoke process, no information is available regarding catalyst strengths used in commercial absorbers. A concentration of 1 gram mole per liter was assumed, based on the value used for sample calculations by Danckwerts and Sharma.[33]

The practical lower limit for the regeneration of carbonate solutions is about 2 standard cubic feet of CO_2/gallon of solution.[4] This was taken as the inlet carbonate concentration.

The outlet concentration of carbonate in a co-current device must be such that an adequate driving force toward total equilibrium is maintained at the outlet of the contactor. An analysis of the system indicates that setting the approach to equilibrium, all inlet conditions except liquid flow rate and the degree of gas purification desired sets the liquid flow rate. The outlet liquid composition was assumed to be that which would be in equilibrium with a gas composition equal to half the desired outlet CO_2 mole fraction. This assumption of equilibrium approach is arbitrary, and is equivalent to setting the Murphree vapor-phase efficiency, defined by Eq. (10), to a value dependent only on the change in CO_2 concentration in the gas stream.

Figure 5a depicts a single co-current reactor, assuming a 5 psi pressure drop. As a result of the formulation of the problem, the mass balance for the system may be determined uniquely without consideration of the rate equation. This is not the case for the HCl absorption system discussed in Section III. Writing the equations necessary to formulate the problem (neglecting those for which a one-to-one correspondence between variables and equations exists):

Rate Equation

$$L_{out}x_{out} - L_{in}x_{in} = MS\int_{in}^{out} (Ra)\, dz \quad ^{\dagger} \tag{12}$$

Component Mass Balance (only CO_2 is transferred)

$$L_{out}x_{out} - L_{in}x_{in} = -(G_{out}y_{out} - G_{in}y_{in}) \tag{13}$$

Total Mass Balance

$$L_{in} + G_{in} = L_{out} + G_{out} \tag{14}$$

Specification of Constant Inert Gas Flow

$$G_{in}(1 - y_{in}) = G_{out}(1 - y_{out}) \tag{15}$$

Outlet Equilibrium Specification

$$x_{out} = f(y_{out}, T, P, k_e) \tag{16}$$

---

† The rate equation is discussed in Section II-C and Appendix I.

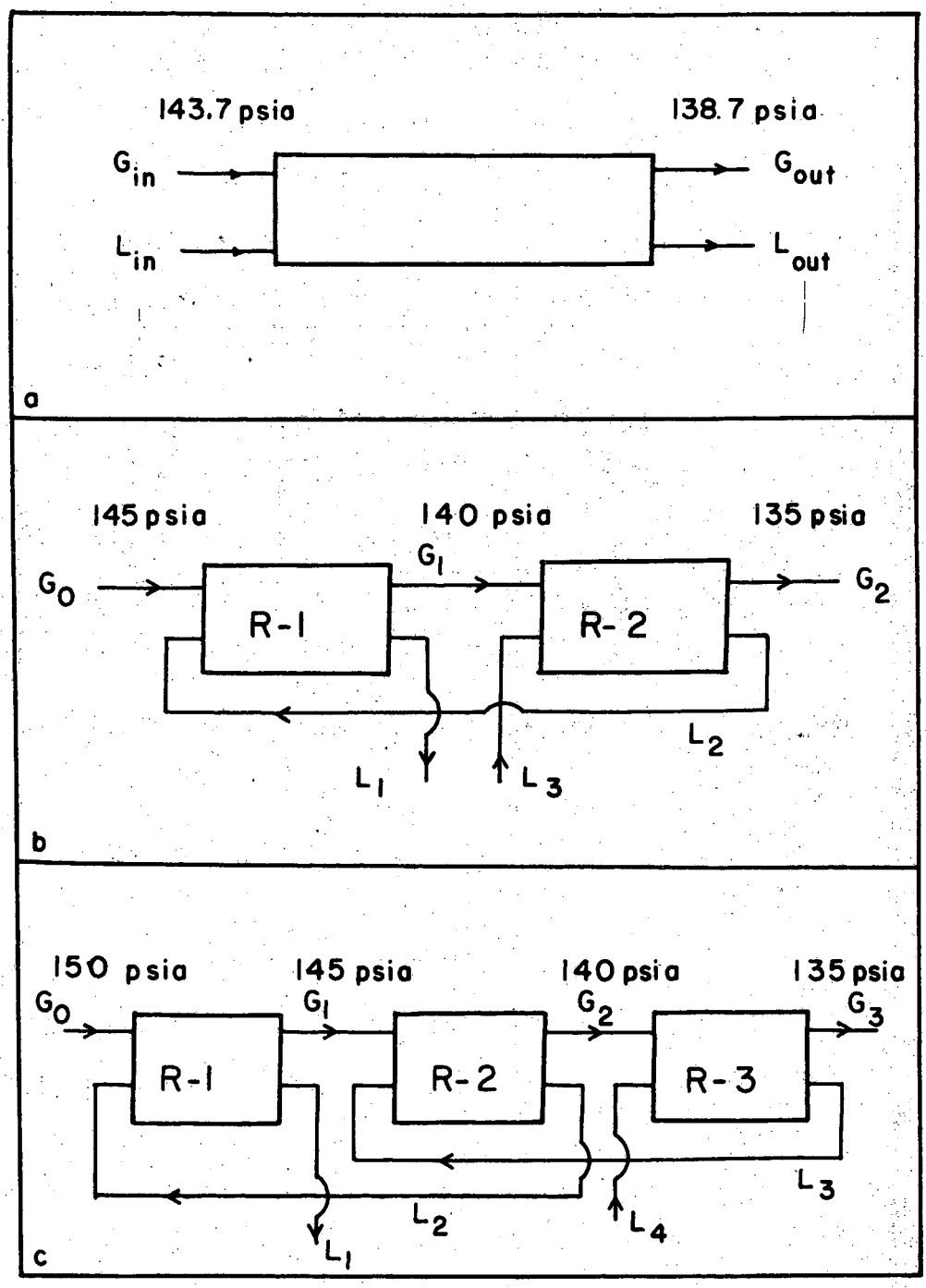

XBL 695-572

Fig. 5. Single and staged CO_2 contactors.

where: x,y = weight fractions of CO_2 in the liquid and gas phase

L,G = total mass liquid and gas flow rates

P = total pressure

T = temperature

k_e = variable representing approach to equilibrium of outlet gas stream

R = absorption rate, moles/(time)(area)

a = effective interfacial area per unit volume

z = length coordinate

S = cross sectional area of contactor

M = molecular weight of transferring component.

The pertinent variables may be itemized as:

L_{in}	L_{out}
G_{in}	G_{out}
x_{in}	x_{out}
y_{in}	y_{out}
z	
T	
P	
k_e	

Sum = 12 .

Since there are five independent equations characterizing the system, 12 - 5 = 7 independent variables must be specified. If, as discussed above, we choose P, T, G_{in}, x_{in}, y_{in}, y_{out}, and k_e, the system

is fully specified, and we may solve for the liquid compositions, flow rates and the contactor size. If we do not consider Eq. (12), the rate equation, we are left with 4 equations in 11 unknowns, and the same seven variables may be specified. Thus, in determining the liquid flow rate through the contactor, the result is independent of the rate equation, and the calculation may be done as if the contactor were a "black box", yielding the necessary boundary conditions for the rate equation. This conclusion is based on the assumption that the outlet pressure, needed to evaluate Eq. (16), is independent of reactor internals. Although this will not be the case, if the pressure drop is only a small fraction of the total pressure the error incurred by this assumption is small.

Rather than calculating L_{in} and L_{out}, the average liquid flow rate was calculated for use in design calculations. Reference to Fig. 5a and Table 1 shows that the outlet partial pressure of carbon dioxide for a single reactor is (0.0101)(138.7) = 1.40 psia. The outlet carbonate concentration in equilibrium with $P_{CO_2}/2$, or 0.7 psia, is about 3.0 standard cubic feet of CO_2/gallon of solution.[38] Since the amount of CO_2 absorbed is 162.16 pound moles of CO_2 per hour, or 61,458.64 SCF of CO_2 per hour, the average solution flow rate is 61,458.64 gallons per hour. The Murphree stage efficiency is calculated from Eq. (10) as

$$E_{MV} = \frac{0.0101 - 0.1961}{0.00505 - 0.1961} \times 100 = 97.35\% \quad .$$

Table 1. Summary of over-all mass balances, CO_2 absorption system.

Inert Gas Flow		lb moles/hr	lb/hr
	CO	2.58	72.2
	CH_4	10.37	165.9
	N_2	5.35	149.8
	H_2	675.36	1361.5
	Total	693.66	1749.4

A. Single Contactor (Fig. 5a)

Gas Flow

	Inlet			Outlet		
	lb moles/hr	lb/hr	Mole %	lb moles/hr	lb/hr	Mole %
CO_2	169.24	7446.6	19.6	7.08	311.5	1.0
Inert	693.66	1749.4	80.4	693.66	1749.4	99.0
Total	862.90	9196.0	100.0	700.74	2060.9	100.0

Inlet Liquid Composition = 2.00 SCF of CO_2/gallon

Outlet Liquid Composition = 3.00 SCF of CO_2/gallon

Average Liquid Flow Rate = 61,460 gallons/hr = 618,000 lb/hr

B. Two Contactors (Fig. 5b)

Gas Flow

	Inlet			Inter-stage		
	lb moles/hr	lb/hr	Mole %	lb moles/hr	lb/hr	Mole %
CO_2	169.24	7446.6	19.6	53.81	2367.6	7.2
Inert	693.66	1749.4	80.4	693.66	1749.4	92.8
Total	862.90	9196.0	100.0	747.47	1749.4	100.0

(continued)

Table 1. Continued.

	Outlet		
	lb moles/hr	lb/hr	Mole %
CO_2	7.08	311.5	1.0
Inert	693.66	1749.4	99.0
Total	700.74	2060.9	100.0

Inlet Liquid Composition = 2.00 SCF of CO_2/gallon
Inter-stage Liquid Composition (X_2) = 2.97 SCF of CO_2/gallon
Outlet Liquid Composition = 5.37 SCF of CO_2/gallon
Average Liquid Flow Rate = 18,240 gallons/hr = 183,430 lb/hr

C. Three Contactors (Fig. 5c)

Gas Flow

	Inlet			Inter-stage (G_1)		
	lb moles/hr	lb/hr	Mole %	lb moles/hr	lb/hr	Mole %
CO_2	169.24	7446.6	19.6	128.92	5672.5	15.7
Inert	693.66	1749.4	80.4	693.66	1749.4	84.3
Total	862.90	9196.0	100.0	822.58	7421.9	100.0

	Inter-stage (G_2)			Outlet		
	lb moles/hr	lb/hr	Mole %	lb moles/hr	lb/hr	Mole %
CO_2	44.39	1953.2	6.0	7.08	311.5	1.0
Inert	693.66	1749.4	94.0	693.66	1749.4	99.0
Total	738.05	3702.6	100.0	700.74	2060.9	100.0

Inlet Liquid Composition = 2.00 SCF of CO_2/gallon
Inter-stage Liquid Composition (X_3) = 2.97 SCF of CO_2/gallon
Inter-stage Liquid Composition (X_2) = 5.19 SCF of CO_2/gallon
Outlet Liquid Composition = 6.25 SCF of CO_2/gallon
Average Liquid Flow Rate = 14,460 gallons/hr = 145,460 lb/hr.

2. Multi-staging

Using multiple stages to carry out a separation feasibly done in a single stage will have the benefit of decreasing the amount of separating agent required, if the efficiencies of the multiple stages are comparable to that of the single stage. For the Vetrocoke absorption process, reduced absorbent consumptions would have the economic advantages of reducing liquid pumping costs and heating requirements in the carbonate regenerator. One way of staging, while maintaining the advantages of co-current flow within the contactors, is to operate multiple co-current contactors with counter-current absorbent flow, as shown in Fig. 5 b, c. The efficiencies of these multiple contactors were implicitely set, as in the single contactor case, by assuming that the liquid composition out of each contactor was in equilibrium with a gas composition equal to half the value of the actual outlet gas composition. Using a digital computer with the aid of curve-fitted equilibrium data, an iterative procedure was devised to determine the inter-stage gas and liquid compositions and the average liquid flow rate. As summarized in Table 1, the use of two contactors reduces the necessary absorbent flow rate by a factor of about 3.4 over the single-contactor case, while the decrease with three reactors as compared to one is by a factor of 4.2. Based solely on the consumption of separating agent, it appears that the approximate optimal number of contactors to use is two, because of the large reduction in absorbent flow rate which this combination yields. The true optimal number of contactors to use can only be determined by an economic study accounting for the increased capital and reduced operating costs in a multi-stage system.

Because of the manner of specification of the equilibrium approach, the stage efficiency of each of the two multiple contactors is reduced in comparison to the single contactor.

$$E_{MV}(R\text{-}1) = \frac{0.07198 - 0.1961}{0.03599 - 0.1961} \times 100 = 77.52\%$$

$$E_{MV}(R\text{-}2) = \frac{0.0101 - 0.07198}{0.00505 - 0.07198} \times 100 = 92.45\% \quad .$$

Recall that the efficiency of the single stage was 97.35%.

C. Chemical and Physical Properties

The rate equation describing the absorption of CO_2 into potassium carbonate promoted by arsenious acid may be written as

$$Ra = \frac{a(HPy - C_b)\eta}{1 + \frac{aH\eta}{k_g a}} \tag{17}$$

where: $\eta = (k_1^2 + D_1 k_{OH}(OH^-) + D_1 k_{As}(As(OH)_2O^-))^{1/2}$, cm/sec

R = absorption rate, gm moles/cm^2-sec

a = interfacial area available for mass transfer, cm^2/cm^3

H = Henry's law solubility constant, gm moles/cm^{3}atm

P = total pressure, atm

y = mole fraction of solute in bulk gas

C_b = concentration of dissolved, but unreacted CO_2 in solution, gm moles/cm^3

$k_g a$ = gas phase mass-transfer coefficient, gm moles/sec atm cm^3

k_1 = physical liquid phase mass-transfer coefficient, cm/sec

D_1 = diffusivity of CO_2 in liquid, cm^2/sec

k_{OH} = rate constant for consumption of CO_2 by reaction with hydroxide ions, cm^3/gm mole sec

k_{As} = rate coefficient accounting for arsenite catalysis, cm^3/gm mole sec.

A discussion of this expression and the conditions under which it applies may be found in Appendix I. The means of estimating the Henry's law solubility of CO_2 in potassium carbonate is treated in Appendix II. A discussion of the chemical equilibrium of the CO_2-K_2CO_3 reaction, together with equations derived to fit the equilibrium data, is presented in Appendix III. The relevant physical properties of the gas and liquid are presented in Appendix IV.

III. HCl ABSORPTION

A. Process Specification

The Atomic Energy Commission has exhibited a considerable amount of interest during the last several years in developing more economical processes for the recovery of U-235 from enriched reactor fuels. The most important of these fuels consist of 5% to 10% U-235, and small amounts of plutonium, clad in Zircaloy-2 (an alloy of high zirconium content) or aluminum.[13] A process of this nature has been studied extensively by the Argonne National Laboratory.[13,14,15,16,17] In this "Volatility Process", the clad fuel, suspended in an inert bed of alumina particles, is reacted with gaseous HCl of the concentration necessary to produce adequate reaction rates at about 350°C. This produces gaseous $ZrCl_4$ or $AlCl_3$ and solid UCl_3. After the cladding materials have been separated by volatilization, the uranium chloride is reacted successively with HF, to produce UF_4, and fluorine, to produce UF_6 for use in fuel element manufacture. The gaseous $ZrCl_4$ or $AlCl_3$, after having been filtered to remove entrained UCl_3 solids, may be converted to the solid oxide by reaction with steam in a pyrolysis converter, producing HCl for recycle. The off-gases are sent to a tower for scrubbing. The equations describing the process are (for Zircaloy-2 cladding)

$$\text{U-Zr} + HCl = ZrCl_{4(g)} + H_2 + UCl_{3(s)} \tag{18}$$

$$ZrCl_4 + H_2O = ZrO_{2(s)} + HCl \tag{19}$$

$$UCl_3 + HF = UF_4 + HCl + H_2 \tag{20}$$

$$UF_4 + F_2 = UF_6 \quad . \tag{21}$$

Because this process has potential utility as a commercial-scale re-processing scheme, the consumption of HCl, which is typically used with a stoichiometric efficiency of only 30% to 50%, may represent an important economic factor. Recycle of HCl of desired purity may be a significant step toward improving the economics of this stage of the process. A means of obtaining HCl of desired purity is to employ an absorber-stripper system in the process stream. A system of this nature, which results in the regeneration of HCl of 99% purity, has been described in relation to another process.[18]

B. Design Basis

1. General Considerations

No detailed information was available regarding the flow rates and compositions encountered in HCl absorbers currently used in conjunction with the Volatility Process. The bases for determining the relative amounts of HCl and H_2 entering the scrubber were:

(1) An assumption that the fuel to be processes was 5% U-235 clad in Zircaloy-2 (Zr-98.25%; Sb-1.5%; Cr-.10%).

(2) The result reported by the Argonne National Laboratory of a pilot plant chlorination of a 13 Kg. sample of Zircaloy-2 in 2.6 hours.[13]

(3) As estimated HCl utilization efficiency of 40%, based on reported efficiencies of 30-56%.[16,13]

(4) As assumption that $ZrCl_4$ was completely converted to the oxide in the pyrolysis converter, limiting the consumption of HCl to that used in the formation of UCl_3.

(5) An assumption that the steam in the pyrolysis reactor is efficiently used, leaving the gas entering the absorber saturated with water vapor. (Saturation was defined as the equilibrium water vapor pressure of that liquid which would be in equilibrium with the mole fraction of gaseous HCl entering the contactor.)

It has been reported that HCl of 5-75 volume per cent has been used in the process reactor, although 100% HCl has been used in some installations.[15] It was assumed that the mole fraction of HCl entering the scrubber was 0.20, with air as a diluant.

The scrubber was assumed to operate with an inlet temperature of 30°C. The result of this temperature selection was to insure operating temperatures in the range of commercial installations.[18] This temperature would require that the gas leaving the pyrolysis converter be cooled before entering the scrubber. This could be done economically to provide a substantial amount of the heat required for the stripper reboiler. Pressure was assumed to be atmospheric.

Based on the preceding assumptions, an estimate of the gas flow rate and composition entering the absorber was made. For design calculations, the flow rate was scaled up by a factor of 50 to achieve a rate corresponding more closely to ranges studied in the literature, and in conformity with the desire to estimate conditions likely to be encountered in a commercial scale process. The resultant inlet gas flow rate and composition are shown in Tables 2A and 2B.

The mole fraction of HCl leaving the absorber was taken to be 0.01. It was felt that this assumption defined a reasonable separation problem.

Table 2. Summary of over-all heat and mass balances, HCl absorption system.

A. Assumption that outlet water vapor is in equilibrium with liquid of outlet composition

1. Single Contactor

		Inlet				Outlet		
		lb/moles/hr	lb/hr	Mole %		lb moles/hr	lb/hr	Mole %
	HCl	30.08	1097.2	20.0	HCl	1.44	52.5	1.0
	H_2O	1.28	23.1	0.8	H_2O	23.53	423.5	16.3
Gas Flow	H_2	6.02	12.2	4.0	H_2	6.03	12.2	4.2
	Air	113.00	3273.7	75.1	Air	113.00	3273.7	78.5
	Total	150.38	4406.2	99.9	Total	144.00	3761.9	100.0

	Inlet	Outlet
Liquid Flow Rate	6911.0 lb/hr	7555.3 lb/hr
Liquid Composition	5.0 w/o HCl	18.4 w/o HCl
Temperature	30.0°C	64.9°C

(continued)

Table 2. Continued.

2. Two-contactor case

a. High-HCl-partial-pressure contactor

		Inlet				Outlet		
		lb moles/hr	lb/hr	Mole %		lb moles/hr	lb/hr	Mole %
	HCl	30.08	1097.2	20.0	HCl	18.69	681.6	12.8
	H_2O	1.28	23.1	0.8	H_2O	8.06	145.0	5.5
Gas Flow	H_2	6.02	12.2	4.0	H_2	6.02	12.2	4.1
	Air	113.02	3274.4	75.1	Air	113.02	3274.4	77.5
	Total	150.40	4406.9	99.9	Total	145.79	4113.2	99.9

b. Low-HCl-partial-pressure contactor

		Inlet				Outlet		
		lb moles/hr	lb/hr	Mole %		lb moles/hr	lb/hr	Mole %
	HCl	18.69	681.6	13.4	HCl	1.37	50.1	1.0
	H_2O	1.31	23.6	0.9	H_2O	16.84	302.8	12.3
Gas Flow	H_2	6.02	12.2	4.3	H_2	6.02	12.2	4.4
	Air	113.02	3274.4	81.3	Air	113.02	3274.4	82.3
	Total	139.04	3991.8	99.9	Total	137.23	3639.5	100.0

(continued)

Table 2. Continued.

	Inlet	Interstage	Outlet
Liquid Flow Rate	3703.7 lb/hr	4055.9 lb/hr	4349.8 lb/hr
Liquid Composition	5.0 w/o HCl	20.1 w/o HCl	28.3 w/o HCl
Temperature	30.0°C	59.4°C	53.0°C

B. Assumption that outlet water vapor is in equilibrium with liquid in equilibrium with outlet HCl gas composition.

1. Single Contactor

		Inlet				Outlet		
		lb moles/hr	lb/hr	Mole %		lb moles/hr	lb/hr	Mole %
	HCl	30.08	1097.2	20.0	HCl	1.43	52.2	1.0
	H_2O	1.28	23.1	0.8	H_2O	22.68	408.2	15.8
Gas Flow	H_2	6.02	12.2	4.0	H_2	6.02	12.2	4.2
	Air	113.00	3273.7	75.1	Air	113.00	3273.7	78.9
	Total	150.38	4406.2	99.9	Total	143.13	3746.3	99.9

	Inlet	Outlet
Liquid Flow Rate	7008.0 lb/hr	7667.9 lb/hr
Liquid Composition	5.0 w/o HCl	18.2 w/o HCl
Temperature	30.0°C	65.8°C

(continued)

Table 2. Continued

2. Two-contactor case

a. High-HCl-partial-pressure contactor

		Inlet				Outlet		
		lb moles/hr	lb/hr	Mole %		lb moles/hr	lb/hr	Mole %
	HCl	30.08	1097.2	20.0	HCl	18.62	679.0	12.8
	H_2O	1.28	23.1	0.8	H_2O	7.64	137.5	5.3
Gas Flow	H_2	6.02	12.2	4.0	H_2	6.02	12.2	4.1
	Air	113.02	3274.4	75.1	Air	113.02	3274.4	77.8
	Total	150.41	4406.9	99.9	Total	145.30	4103.1	100.0

b. Low-HCl-partial-pressure contactor

	Inlet				Outlet		
	lb moles/hr	lb/hr	Mole %		lb moles/hr	lb/hr	Mole %
HCl	18.62	679.0	13.4	HCl	1.37	49.9	1.0
H_2O	1.31	23.8	0.9	H_2O	16.27	292.8	11.9
H_2	6.02	12.2	4.3	H_2	6.02	12.2	4.4
Air	113.02	3274.4	81.3	Air	113.02	3274.4	82.7
Total	138.97	3989.4	99.9	Total	136.68	3629.3	100.0

(continued)

Table 2. Continued

Liquid Flow Rate	3879.7 lb/hr	4086.8 lb/hr	4390.7 lb/hr
Liquid Composition	5.0 w/o HCl	20.0 w/o HCl	28.1 w/o HCl
Temperature	30.0°C	60.5°C	54.4°C

The absorbent was HCl solution, with an assumed inlet concentration of 5% by weight.

Since the heat of absorption of HCl into water or weak HCl solutions is relatively large (about 420 calories/gm), devices used to effect HCl absorption must provide a means of dissipating heat. The three conventional ways of doing this are:

(1) The continuous removal of the heat by the circulation of a cooling fluid around the absorption device. This results in a nearly isothermal operation.

(2) Cooling the liquid leaving the absorption device by external exchangers, and returning this liquid to the device or a device in series with it.

(3) Allowing the cooling to be effected by the evaporation of solvent, which will occur if the absorbent, like water, has a high vapor pressure and the heat of absorption is large. This results in nearly adiabatic operation.

The currently used cooled absorbers are tubular falling film absorbers, in which gas and liquid are contacted either co-currently or counter-currently in banks of tubes jacketed by cooling water. To effect complete absorption, a packed tails tower is often added to the system.[18,19,26]

Adiabatic absorbers, which have usually been packed columns, have frequently been used, particularly when a substantial amount of inerts is present in the gas stream.[26,67,68]

The actual situation in HCl absorption is somewhere between the extremes of purely adiabatic and purely isothermal operation, regardless of the method of contacting. The calculation of the devices was selected to be on the basis of adiabatic operation. This choice is more suitable for co-current than counter-current HCl absorption. The gas and liquid conditions in counter-current absorbers may result in a temperature peak which must be eliminated by cooling for efficient operation.[28] No such peaking will occur in co-current absorption. The choice of adiabatic operation simplifies the calculation procedures by making the consideration of heat transfer through the absorber walls unnecessary. However, the changing nature of the gas-liquid equilibrium curves with temperature must be more carefully considered than in the cooled-absorber case.

2. Heat and Mass Balances

Obtaining over-all mass and heat balances for the case of adiabatic absorption necessitates accounting for the HCl absorbed, the concomitant heat of absorption, the water vaporized as a result of this heat and the changes in temperature of the liquid and gas phases associated with these compensating effects. At any point in a contactor, the heat liberated by absorption must be equal to the sum of the heat consumed by vaporization and the heat transferred from the liquid to the gas phase. These quantities, in turn, depend on the rate of absorption of HCl, the rate of vaporization of water and the interfacial heat-transfer coefficient. The resistances to these transfer processes are characteristic of the particular devices in which the simultaneous mass and heat transfer is occurring.

A simplification was made by assuming that the gas and liquid phases enter the absorber at the same temperature, and that the heat-transfer coefficients for the devices to be considered are of sufficiently large magnitude to justify assuming perfect heat transfer between phases. According to the calculations of Norman,[26] The error incurred by the latter assumption is probably small. Even with this assumption, it is not possible to specify all inlet conditions and the gas outlet conditions independently in order to solve for the solution flow rates. This fact can be seen by itemizing the equations specifying the process. Constant pressure and mass-transfer coefficients were assumed.

Over-all Mass Balance

$$L_{in} + G_{in} = L_{out} + G_{out} \tag{22}$$

HCl Mass Balances

$$(Lx_{HCl})_{out} - (Lx_{HCl})_{in} = -\left[(Gy_{HCl})_{out} - (Gy_{HCl})_{in}\right] \tag{23}$$

$$(Lx_{HCl})_{out} - (Lx_{HCl})_{in} = K_g a_{HCl} M_{HCl} SP \int_{in}^{out} (y_{HCl} - y^*_{HCl})\, dz \tag{24}$$

H_2O Mass Balances

$$(Gy_{H_2O})_{out} - (Gy_{H_2O})_{in} = -\left[(L(1 - x_{HCl}))_{out} - (L(1 - x_{HCl}))_{in}\right] \tag{25}$$

$$(Gy_{H_2O})_{out} - (Gy_{H_2O})_{in} = K_g a_{H_2O} M_{H_2O} SP \int_{in}^{out} (y^*_{H_2O} - y_{H_2O})\, dz \tag{26}$$

Specification of Constant Inert Flow

$$G' = G(1 - y_{H_2O} - y_{HCl}) \tag{27}$$

Equilibrium Relationships

$$y^*_{HCl} = f(x_{HCl}, T) \tag{28}$$

$$y^*_{H_2O} = f(x_{HCl}, T) \tag{29}$$

Heat Balance

$$L_{out}H_L(x_{HCl},T)_{out} - L_{in}H_L(x_{HCl},T)_{in} + (G_{out} - G')H_g(y_{HCl},T)_{out}$$

$$+ (G_{in} - G')H_g(y_{HCl},T)_{in} + G'(H_g'(T)_{out} - H_g'(T)_{in}) = 0 \tag{30}$$

Specification of Outlet Equilibrium Approach

$$x_{HCl,out} = f(y_{HCl},T,P,k_e) \tag{31}$$

where: L = total mass liquid flow rate

G = total mass gas flow rate

G' = mass flow rate of gaseous inerts

x_{HCl} = weight fraction of HCl in the liquid

y_i = mass or mole fraction of component i in the gas, with units to keep equations dimensionally consistant

$K_g a_i$ = mass transfer coefficient of component i, moles/(time)(volume)(pressure)

S = cross sectional area of absorber

P = total pressure

M_i = molecular weight of species i

z = length coordinate of contactor

H_L = liquid enthalpy per unit mass

H_g = inert free gas enthalpy per unit mass

H_g' = inert gas enthalpy per unit mass

y_i^* = mole fraction of component i in equilibrium with liquid of composition x_{HCl}.

The variables may be itemized as

L_{in}	L_{out}
G_{in}	G_{out}
$y_{HCl,in}$	$y_{HCl,out}$
$y_{H_2O,in}$	$y_{H_2O,out}$
y^*_{HCl}	$y^*_{H_2O}$
$x_{HCl,in}$	$x_{HCl,out}$
T_{in}	T_{out}
G'	P
k_e	z

Sum = 18

Since the number of variables is 18, the the number of independent equations which have been written to specify the process is 10, the number of variables which must be set to determine a unique solution to the set of equations is 8. Based on process considerations, the 8 variables which could be logically set were: P, G_{in}, $x_{HCl,in}$,

$y_{HCl,in}$, $y_{HCl,out}$, T_{in}, $y_{H_2O,in}$ and k_e. Since neither G_{out} nor y_{H_2O} were set, it is impossible to solve for the necessary absorbent flow rate without consideration of Eqs. (24) and (26)--the rate equations. This conclusion contrasts with the result of the analysis of the CO_2 absorption system, in Section II-B-1. The complete specification of the heat and material balances in this case involves a trial and error calculations, iterating on the dependent variables L and T until the solution set is satisfied. Because of the non-analytical nature of the integrals in Eqs. (24) and (26), each trial must incorporate a numerical integration procedure.

To minimize the difficulty of this calculation and to permit calculation for cases in which a complete knowledge of the transport coefficients was not available, another method was used to estimate the values of the liquid flow rates. If the contactor were considered a "black box", the process would be specified by Eqs. (22), (23), (25), (27), (30) and (31). The number of variables in this set of equations is 15, so that the number of variables which must be set independently is now 9. If the additional variable, or relationship, set specifies the water vapor content at the contactor outlet, the dependent variables, including the liquid flow rate, may be solved for by a simple iteration on the dependent variable T_{out}. The assumption made at the outlet was that that the gas was saturated with water vapor--i.e., the water vapor mole fraction in the outlet gas was either in equilibrium with the outlet liquid or in equilibrium with a liquid composition in equilibrium with the outlet gas phase HCl composition. The choice of the definition of saturation to use depended on considerations of the mass-transfer

mechanisms associated with specific devices, and the effect of the choice on the results was only slight. Figure 7 shows the concentration profiles in a co-current packed column, calculated using Eqs. (24) and (26) with boundary conditions determined from the "black box" mass balance, with the assumption that the outlet water vapor was in equilibrium with the outlet absorbent. The assumption of saturation of water vapor at the outlet is seen to be quite good, as measured by the approach of $y^*_{H_2O}$ to y_{H_2O}. The reasons for the validity of this assumption are:

(1) The inlet gas was assumed to be saturated with water vapor.

(2) $K_g a_{H_2O}$ was large enough to insure enough transfer of water to maintain a saturated condition at the outlet.

(3) $y^*_{H_2O}$ decreases with increasing HCl concentration, but increases with temperature. In situations where the liquid HCl concentration is increasing more rapidly than the temperature, such as near the ends of the co-current contactors, the former effect may predominate, resulting in a closer approach of $y^*_{H_2O}$ to y_{H_2O} than had occurred at intermediate points in the contactor.

Over-all heat and material balances were calculated for a single reactor and for two reactors with interstage cooling, as shown in Fig. 6. The two-stage situation was considered because of:

(1) The potential savings in operating costs which might result from lower absorbent flow rates.

(2) The desirability, for many processes, of producing liquid HCl of a greater concentration than can be made in a single stage.

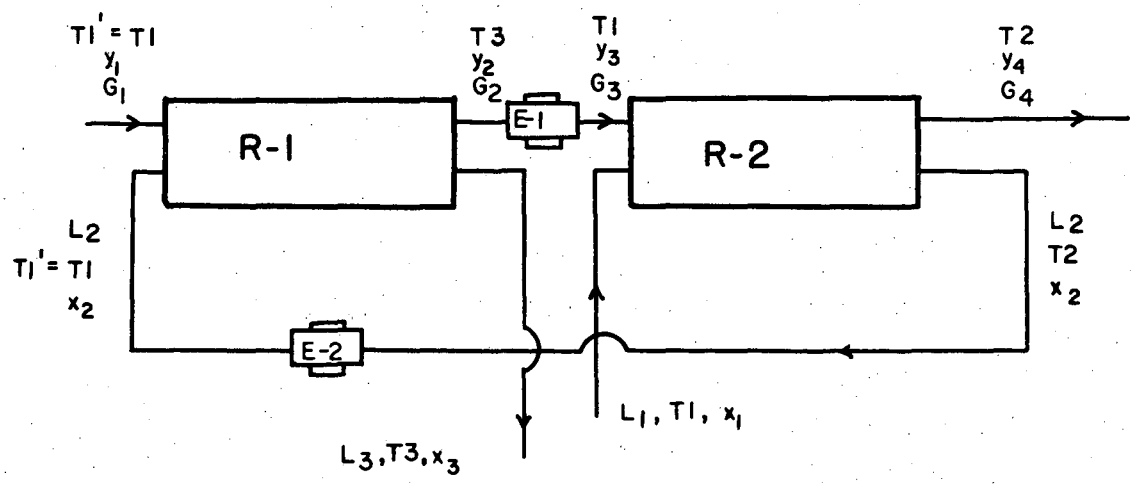

XBL 695-576

Fig. 6. Staged HCl contactors.

The implementation of heat exchangers in the two-stage case is necessary, because of the assumption that all streams enter and leave the contactors at the same temperature. The positions of these heat exchangers is, however, not unique. Referring to Fig. 6, it can be seen that if only T1 is to be specified, E-1 must be provided; if only T1' is to be specified, only E-2 need be provided; if both T1 and T1' are to be specified, both exchangers must be provided. Both E-1 and E-2 were provided, to enable the specification T1' = T1.

The algorithm for solving the two-contactor case, which is directly analogous to the solution procedure for the single-contactor case, is presented in Appendix V. The results of the computer solution are shown in Tables 2A and 2B. The use of two contactors reduces the necessary absorbent flow rate by a factor of 1.9, and results in the outlet HCl solution having a concentration of about 28% by weight, as opposed to about 18% with a single contactor. The decision of the number of contactors to use must be based on the increased capital costs involved in a multiple contactor system, including both the contactors and heat exchangers, the reduced absorbent pumping and supply requirements and the advantages of producing HCl of a concentration higher than obtainable with a single stage.

The Murphree-stage efficiency may be calculated using Eq. (10), since the specification of the outlet approach to equilibrium was assumed, as in the CO_2 absorption case, to be such that the outlet liquid was in equilibrium with a gas-phase mole fraction of HCl equal to half the actual outlet HCl mole fraction. The stage efficiencies for the single,

high-HCl-partial-pressure and low-HCl-partial-pressure contactors were 97.5%, 53% and 96.9% respectively.

C. Chemical and Physical Properties

The reaction of HCl with water to produce an ionized acid may be regarded as infinitely fast and reversible, with no water depletion at the interface.[1,61] From a mass-transfer standpoint, this implies that no distinction is necessary between physical solubility and total equilibrium, so that the actual kinetics of the chemical reaction need not be considered in designing absorption equipment. It also implies that no distinction between a physical and "chemical" mass-transfer coefficient need be made. The rate equation may be written as

$$Ra = K_g a_{HCl} P(y_{HCl} - y^*_{HCl}) \tag{32}$$

where R has units of moles/time area, a, the effective interfacial area, has units of area/volume and all other units are defined consistently with Eq. (24).

A discussion of the equilibrium of the HCl-water system is presented in Appendix VI. Enthalpy data are discussed in Appendix VII. Physical properties are presented in Appendix VIII.

IV. DISCUSSION AND DESIGN OF ABSORPTION DEVICES

A. Co-current Packed Column

1. General Consideration

Absorption in conventional counter-current packed columns, with a down-flow of liquid due to gravity and an up-flow of gas due to an imposed pressure gradient, suffers from a hydrodynamic limitation on the gas and liquid flows which constrains the gas velocity to a magnitude below that which produces flooding in the column. This disadvantage may be overcome by introducing both phases at the top of the packed column and allowing the phases to flow co-currently under the combined forces of gravity and imposed pressure gradient. The only constraint on flows, up to the limit of choked flow, is the available pumping power. This implies that the phase turbulence and, hence, the effective interfacial area and transport coefficients, can be much greater than in a counter-current packed column.

Riess[20] has presented a summary of the limited amount of data available in the literature dealing with co-current gas-liquid downflow in packed beds, including references useful for analysis of pressure deop, liquid holdup, liquid distribution and mass transfer.

a. Liquid distribution. The pressure drop and resistance to mass transfer in a co-current packed column are functions of the liquid distribution within the column. Larkins, et al.[21] have characterized four types of flow pattern--homogenous, transition, slug and close slugs, or blur--which may be observed by increasing the gas rate from a zero value while maintaining a constant liquid rate. At low gas rates, the

flow in the column is uniform, with the liquid clinging to the packing particles in a film of a thickness which decreases with increasing gas rate. As the gas rate is increased, the liquid distribution at the top of the column will remain uniform, while the material at the bottom of the column will exhibit a "slugging" flow, with observable plugs of higher density material moving through the column. As the gas rate is increased further, the slugging phenomenon will occur in the whole column, and at the highest gas rates, these slugs will appear to blur together, producing a wavy, or quivering, appearance in the column. At the highest gas rates, the liquid film on the packing surface is very thin, and the voids are filled with a heavy liquid mist.

Wen, et al.,[22] have observed a decrease in the height of the transfer unit, defined equivalently to the length of the transfer unit, as in Eq. (98) and (99) below, with increasing gas rate. This results from the increase in interfacial area corresponding to the turbulence associated with the flow patterns at higher gas rates. However, a channeling effect was noticed when the liquid rate was increased at constant gas rate. This channeling was found to increase the height of the transfer unit, due to the effects of reducing the phase turbulence and decreasing the area available for mass transfer, and was found to be more pronounced at higher gas rates. Riess[20] observed that, above a certain liquid rate, liquid distribution improves with increased liquid rate, and suggested that an increasing height of a transfer unit with increasing liquid rate will only occur under conditions where the actual wetting area of the packing is important--i.e., at lower values of the liquid flow rate than are likely to be encountered in industrial equipment.

Larkins, et al.,[21] have observed that the transitions in flow regimes do not produce any significant change in the functional relationship between flow rate and pressure drop. The exception to this occurs with foaming systems, in which the column will tend to fill and empty of foam, creating pressure surges of ± 40% from the average.

b. Pressure drop and liquid holdup. Data on pressure drop and liquid holdup for two-phase flow in packed beds were correlated by Larkins, et al.,[21] combining the analysis used by Lockhart and Martinelli[23] for two-phase pressure drop in open pipes with the single-phase pressure drop correlation developed by Ergun.[24] The pressure drop in each phase is calculated as if it were flowing alone by the Ergun equation:

$$\frac{\Delta P}{\Delta L}\left(\frac{g_c \rho D_p^3}{\mu^2}\right)\left(\frac{\varepsilon}{1-\varepsilon}\right)^3 = \alpha\ \mathrm{Re} + \beta\ \mathrm{Re}^2 \qquad (33)$$

where: $\mathrm{Re} = \dfrac{D_p V \rho}{\mu(1-\varepsilon)}$

D_p = equivalent spherical particle diameter of the packing $= 6(1-\varepsilon)/a_o$, ft

ε = packing void fraction

α,β = constants dependent on type and manner of packing

$\frac{\Delta P}{\Delta L}$ = single-phase pressure drop, $lb/ft^2 ft$

g_c = 32.17 $lb_m\ ft/lb_f sec^2$

μ = viscosity, lb/ft sec

a_o = packing surface area/unit volume, ft^{-1}

ρ = density, lb/ft^3.

Defining the two-phase parameter $\chi = [(\Delta P/\Delta L)_l/(\Delta P/\Delta L)_g]^{1/2}$, the two-phase pressure drop is calculated as:

$$\log_{10}\left[\frac{\left(\frac{\Delta P}{\Delta L}\right)_{tp}}{\left(\frac{\Delta P}{\Delta L}\right)_l + \left(\frac{\Delta P}{\Delta L}\right)_g}\right] = \frac{0.416}{(\log_{10}\chi)^2 + 0.666} \qquad (34)$$

The liquid holdup, defined as the fraction of the column occupied by the liquid at a given instant, is correlated by:

$$\log_{10} R_l = -0.774 + 0.525 \log_{10}\chi - 0.109 (\log_{10}\chi)^2. \qquad (35)$$

The accuracy of these correlations was claimed to be within a 13% standard deviation for pressure drop and 16% for liquid holdup.

c. Mass transfer. Calderbank and Moo-Young[25] have shown how a mean velocity component for isotropic turbulence may be defined in terms of the energy dissipation per unit volume associated with turbulent eddies. Given this velocity, a Reynolds number may be defined and, since the gas and liquid phase transport coefficients have been empirically shown to be related to the Reynolds number, the coefficients k_l and k_g may be related to the energy dissipation per unit volume.

For a single-phase system in a packed column, energy dissipation may be related to pressure drop by:

$$\frac{(\text{Power})}{(\text{volume})} = \frac{\Delta P G}{\Delta L \rho \varepsilon} \qquad (36)$$

Where G is the mass flow rate and the other units are consistently defined. Kinetic energy, heat input, shaft work and density head have been neglected in writing this form of the energy balance.

Riess[20] has defined a modified energy dissipation by

$$E_g = V_g(\Delta P/\Delta L)_{tp} \tag{37}$$

$$E_l = V_l(\Delta P/\Delta L)_{tp} \tag{38}$$

where: V_l = superficial liquid velocity, ft/sec

V_g = superficial gas velocity, ft/sec

E_g, E_l = energy dissipation per unit volume associated with the gas and liquid phases, ft lb_f/ft^3sec.

Liquid and gas phase mass-transfer coefficients were correlated by

$$k_l a = 0.12\ E_l^{1/2} \quad \text{For } O_2 \text{ desorption at } 77°F. \tag{39}$$

$$k_c a = 2.0 + 0.91\ E_g^{2/3} \quad \text{For } NH_3 \text{ absorption at } 70°F. \tag{40}$$

where: $k_l a = sec^{-1}$

$k_c a = sec^{-1}$.

These equations correlate Riess' data to within 25%. To convert the gas-phase mass-transfer coefficient $k_c a$ to the more useful coefficient $k_g a$, the following relation may be used.[35]

$$k_g a = \frac{k_c a}{RT}(453.59)(3600) \tag{41}$$

where: $k_g a$ = gm moles/ft^3 atm hr

R = gas constant, 1.314 atm ft^3/lb mole °K

T = system temperature, °K.

The Riess correlations, together with the pressure-drop correlations of Larkins, et al., were used to predict $k_l a$ and $k_g a$ for the co-current packed columns in this study. The values of $k_l a$ and $k_g a$ obtained from the correlations are valid only for oxygen desorption and ammonia absorption at the specified temperatures and pressure (one atmosphere), and must be corrected for differences in system temperature, pressure and physical properties.

For liquid-phase resistance to mass transfer in gas-liquid counter-current flow in packed beds, Norman[26] reports that experimental mass-transfer measurements may be correlated by

$$\frac{k_l a}{D_l} = \phi \left(\frac{V_l \rho_l}{\mu_l}\right)^{1-n} \left(\frac{\mu_l}{\rho_l D_l}\right)^{0.5} \tag{42}$$

where ϕ and n are characteristic of the packing. For 1" rings, which were arbitrarily selected for the columns of this study Norman reports that $n = 0.22$.

Equation (42) was assumed to be satisfactory for adjusting the value of $k_l a$ in a co-current packed column for physical properties at constant temperature. The Schmidt group is a strong function of temperature. This temperature dependence was taken to be of the form:

$$k_l a \sim e^{0.02T} \quad (T = °C) \tag{43}$$

as reported by Vivian and King for counter-current packed columns.[27]

Thus, k_1a may be corrected for physical properties, at constant temperature, and for temperature by

$$k_1a \sim D_1 \left(\frac{V_1\rho_1}{\mu_1}\right)^{0.78} \left(\frac{\mu_1}{\rho_1 D_1}\right)^{0.5} e^{0.02T} \tag{44}$$

or, neglecting the effects of superficial velocity

$$k_1a \sim D_1^{0.5}\ \rho_1^{0.28}\ \mu_1^{-0.28}\ e^{0.02T} \quad . \tag{45}$$

Various correlations describing the dependence of k_g on physical properties and pressure in counter-current packed columns have been summarized in Perry.[28] Based on the results of Gamson, Thodos and Hougen[29] and Taecker and Hougen,[30] the following dimensional result can be written to describe the effects of physical properties and pressure at constant temperature.

$$k_g \sim \left(\frac{\mu_g}{\rho_g D_g}\right)^{-2/3} \left(\frac{\rho_g}{\mu_g}\right)^{-0.41} \left(\frac{1}{P}\right) \quad . \tag{46}$$

It was assumed that this functionality was valid for co-current packed columns, and that the form of the relationship was independent of interfacial area.

Heuss, et al.[31] have reported the temperature dependence of k_ga in co-current froth flow in open pipes to be

$$k_ga \sim e^{(-0.01\pm0.002)T} \ (T = {}^\circ C) \quad . \tag{47}$$

The data of Dwyer and Dodge[32] for counter-current packed columns indicated the relationship

$$k_g a \sim e^{-0.013T} \quad (T = {}^\circ C) \quad . \tag{48}$$

An average of the temperature coefficients determined from these investigations was used to relate $k_g a$ to temperature by

$$k_g a \sim e^{-0.0115T} \quad (T = {}^\circ C) \quad . \tag{49}$$

The correction of $k_g a$ for temperature and for pressure and physical properties, at constant temperature, may be summarized as

$$k_g a \sim \left(\frac{\mu_g}{\rho_g D_g} \right)^{-2/3} \left(\frac{\rho_g}{\mu_g} \right)^{-0.41} e^{-0.0115T} P^{-1} \quad . \tag{50}$$

A summary of the physical properties used to correct the CO_2 and HCl absorption coefficients from values obtained for ammonia absorption and oxygen desorption data is presented in Appendix IX.

The selection of the column diameter to be used was limited by the range of superficial velocities for which the Riess correlation was applicable. Riess' data covered values of V_g from 1 - 20 ft/sec, and V_l from 0 to 1 ft/sec, although the lowest non-zero value of V_l was 0.141 ft/sec. Extrapolation to lower values of V_l is particularly precarious because of the possibilities of entering the channelling regimes noted by Wen, et al.[22]

2. HCl - Water System

a. Design considerations. Equations (24) and (26) represent the rate equations describing the absorption of HCl and the simultaneous vaporization of water. Since nearly all of the resistance to mass transfer is in the gas phase, the over-all coefficient, $K_g a$, was assumed equal to the gas-phase coefficient, $k_g a$. Using the addition-of-resistances concept,[34] this assumption was shown to be valid.

The two-phase pressure drop and the mass-transfer coefficient for HCl absorption were calculated by the methods outlined in Section IV-A-1. The packing was assumed to be 1" stacked rings, for which the Ergun constants necessary to evaluate Eq. (33) are[20]

$$\varepsilon = 0.787$$

$$D_p = 0.0147 \text{ ft}$$

$$\alpha = 129.0$$

$$\beta = 0.117 \quad .$$

The value of a_o, the surface area per unit volume of packing is $47.8 \text{ ft}^2/\text{ft}^3$.

The mass-transfer coefficient for water vaporization was related to the coefficient for HCl absorption by

$$k_g a_{H_2O} = k_g a_{HCl} \left(D_{g_{H_2O}}/D_{gHCl}\right)^{2/3} \quad . \tag{51}$$

This relationship implies that the difference in resistance to mass transfer of two species in a gas phase of given mixture density and viscosity is solely due to different diffusivities of the components, and is consistent with Eq. (46).

Because of the gas and liquid flow rates encountered for HCl absorption (i.e., low L/G), it was impossible to choose a column diameter such that the superficial flow velocities would be completely with the range of Riess'[20] data. A diameter of 0.888 feet, felt to yield flow velocities sufficiently near the Riess range, was selected for the multiple-contactor calculation, and the effect of column diameter was considered by using a few different diameters for the single-contactor calculation.

b. Calculation. Using initial liquid flow rates determined from the mass-and heat-balance calculations described in Section III-B-2, with the assumption that the outlet water-vapor partial pressure was in equilibrium with the outlet liquid composition, the set of design equations was numerically integrated. The transport coefficients were calculated from the flow rates, physical properties and pressure drop at each stage of the step-wise integration. The fourth-order Runge-Kutta integration technique that was used is described in Appendix X. The performance of the method was evaluated by varying the step size. Satisfactory convergence was obtained by choosing an initial step size of 0.05 feet.

c. Observations. The results of the calculations for the single- and two-contactor cases are presented in Table 3. Figure 7 shows concentration and temperature profiles for a single-contactor (D = 0.888 feet) case as a function of column length. As observed in Section III-B-2, the concentration profiles for y_{H_2O} and $y^*_{H_2O}$ indicate that the assumption, used to determine the initial absorbent flow rates, of

Table 3. HCl absorption in co-current packed columns.

A. Single column case

		Inlet				Outlet		
		lb moles/hr	lb/hr	Mole %		lb moles/hr	lb/hr	Mole%
	HCl	30.08	1097.2	20.0	HCl	1.40	51.1	1.0
	H_2O	1.28	23.1	0.8	H_2O	23.36	420.4	16.3
Gas Flow	H_2	6.02	12.2	4.0	H_2	6.02	12.2	4.2
	Air	113.00	3273.7	75.1	Air	113.00	3273.7	78.7
	Total	150.38	4406.2	99.9	Total	143.78	3757.4	100.2

	Inlet	Outlet
Liquid Flow Rate	6911.0	7560.0
Liquid Composition	5.0 w/o HCl	18.4 w/o HCl
Temperature	30.0°C	65.5°C

(continued)

Table 3. Continued.

	Diameter = 0.5 ft		Diameter = 0.888 ft		Diameter = 1.5 ft	
	Inlet	Outlet	Inlet	Outlet	Inlet	Outlet
V_l	0.15 ft/s	0.16 ft/s	0.048 ft/s	0.052 ft/s	0.017 ft/s	0.018 ft/s
V_g	84.4 ft/s	90.3 ft/s	26.7 ft/s	28.7 ft/s	9.37 ft/s	10.0 ft/s
†$K_g a_{HCl}$	2493.6	1505.8	285.3	172.7	53.3	32.4
†$K_g a_{H_2O}$	3141.7	1897.2	359.4	217.6	66.9	41.8
$\Delta P/\Delta L$	0.646 psi/ft	0.612 psi/ft	0.073 psi/ft	0.070 psi/ft	0.011 psi/ft	0.011 psi/ft
Height	1.49 feet		4.22 feet		7.92 feet	
ΔP	0.92 psi		0.30 psi		0.09 psi	

B. Two column case

1. High-HCl-Partial-Pressure Column--Diameter = 0.888 Feet

		lb moles/hr	lb/hr	Mole %		lb moles/hr	lb/hr	Mole %
	HCl	30.08	1097.2	20.0	HCl	18.64	679.9	13.0
	H_2O	1.28	23.1	0.8	H_2O	5.78	104.0	4.0
Gas Flow	H_2	6.02	12.2	4.0	H_2	6.02	12.2	4.2
	Air	113.02	3274.4	75.1	Air	113.02	3274.4	78.8
	Total	150.40	4406.9	99.9	Total	143.46	4070.5	100.0

†lb moles/ft^3 atm hr.

(continued)

Table 3. Continued.

	Inlet	Outlet
Liquid Flow	4055.9 lb/hr	4392.4 lb/hr
Liquid Composition	20.1 w/o HCl	28.1 w/o HCl
Temperature	30.0°C	59.9°C
V_l	0.028 ft/s	0.032 ft/s
V_g	26.7 ft/s	28.0 ft/s
†$K_g a_{HCl}$	269.9	181.4
†$K_g a_{H_2O}$	340.1	228.6
$\Delta P/\Delta L$	0.067 psi/ft	0.066 psi/ft
Height	0.73 feet	
ΔP	0.048 psi	

2. Low-HCl-Partial-Pressure Column--Diameter = 0.888 Feet

		Inlet				Outlet		
		lb moles/hr	lb/hr	Mole %		lb/moles hr	lb/hr	Mole %
	HCl	18.69	681.6	13.4	HCl	1.39	50.7	1.0
	H_2O	1.31	23.6	0.9	H_2O	16.44	296.0	12.0
Gas Flow	H_2	6.02	12.2	4.3	H_2	6.02	12.2	4.4
	Air	113.02	3274.4	81.3	Air	113.02	3274.4	82.6
	Total	139.04	3991.8	99.9	Total	136.87	3633.3	100.0

†lb moles/ft^3 atm hr.

(continued)

Table 3. Continued.

Liquid Flow	3703.7 lb/hr	4062.1 lb/hr
Liquid Composition	5.0 w/o HCl	19.2 w/o HCl
Temperature	30.0°C	60.7°C
V_l	0.025 ft/sec	0.028 ft/sec
V_g	24.8 ft/sec	26.9 ft/sec
†$K_g a_{HCl}$	232.3	157.9
†$K_g a_{H_2O}$	292.7	199.0
$\Delta P/\Delta L$	0.057 psi/ft	0.058 psi/ft
Height	4.07 feet	
ΔP	0.23 psi	

†lb moles/ft^{3}atm hr.

Exchanger Duties: Interstage cooler: 34,675,000 cal/hr

Liquid cooler: 23,732,000 cal/hr

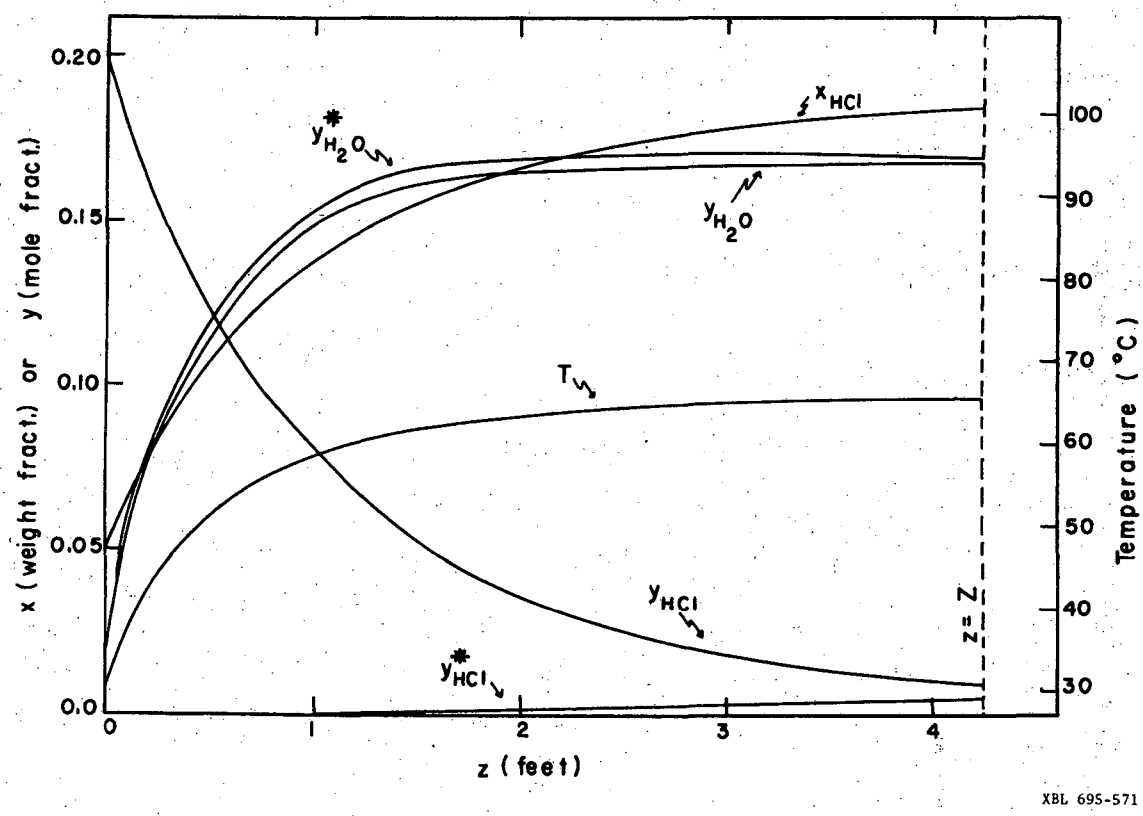

Fig. 7. Concentration and temperature profiles in a single packed column for HCl absorption; Diameter = 0.888 ft.

saturation of water vapor at the contactor outlet was a good one. As a result of this, the gas and liquid compositions predicted by the "black box" mass and heat balances, shown in Table 2A, agree closely with the values obtained in the actual calculation, shown in Table 3. The concentration profiles also show that the change in all variables is greatest in the early part of the contactor, with temperature and y_{H_2O} exhibiting almost their total change and x_{HCl} and y_{HCl} showing about 80% of their total change in the first half of the contactor. This suggests why, with the approach to equilibrium at the outlet of the contactors that was specified, the second (low-HCl-partial-pressure) contactor in the two-contactor case must be larger than the first.

An increase in column diameter for the single contactors results in a decrease in the mass-transfer coefficients, with a three-fold increase in diameter resulting in a 50-fold decrease in the coefficients. This effect, compensated somewhat by the increase in column area, results in an increasing column height with increasing diameter. The decrease in the transfer coefficients is due to the inter-related effects of decreased phase velocities and two-phase pressure drop.

In the two-contactor case, the required liquid flow rate is reduced. Because the gas rate is about the same, the change, at constant diameter, in the rate coefficient for this gas-phase controlled process is due chiefly to the decrease in the two-phase pressure drop. The average amount of this decrease was small. The total change in the bulk concentration of HCl in the gas phase will be the same in the single- and multiple-contactor cases. Since, as shown by Fig. 7, the

value of y^*_{HCl} is negligible over most of the contactor length, the greater change in absorbent concentration in the two-contactor case will have little effect on the average over-all driving force, $y_{HCl} - y^*_{HCl}$. Thus, the combined column heights for the two-contactor absorption are only slightly greater than for the single-contactor absorption in a column of the same diameter.

3. CO_2 Absorption System

a. Design considerations. Combining Eqs. (12) and (17), the mass balance for the Vetrocoke absorption system may be written as

$$\frac{d(Lx)}{MS} = d(V_1 C_o) = \frac{a(HPy - C_b)\eta}{1 + \frac{aH\eta}{k_g a}} \, dz \qquad (52)$$

where C_o is the concentration of the reagent, $CO_3^=$, in the liquid (gm moles/cm^3), V_1 is the volumetric liquid flow rate per unit area (ft/sec) and all other quantities are defined in a way consistent with Eqs. (12) and (17).

The form of Eq. (52) necessitates knowing k_1 and a separately. The procedure employed was to calculate $k_1 a$ and back out k_1 as $k_1 a/a$ by estimating the interfacial area.

The two-phase pressure drop and transport coefficients were calculated according to the procedures outlined in Section IV-A-1. The packing was assumed to be 1" dumped rings, for which the relevant Ergun constants are

$\varepsilon = 0.883$

$D_p = 0.0147$ feet

$\alpha = 920$

$\beta = 5.51$

$a_o = 47.8\ ft^2/ft^3 = 1.5682\ cm^{-1}$.

Column diameters in the range of 1 to 3 feet would yield superficial flow velocities within the range of Riess' data. Diameters of 1.333 and 2.666 feet were considered for the single and multiple contactor cases.

b. Interfacial area. Reported data and correlations usable for predicting interfacial area in counter-current packed columns are limited.[28,26,33] For co-current packed columns, no data were found describing the effective interfacial area available for mass transfer. The estimate of this quantity can be critical. If k_1^2 is much greater than $D_1k_2C_o$, the term η in Eq. (52) will be approximately equal to k_1a, and no separate knowledge of interfacial area is necessary. However, in the Vetrocoke absorption process, the value of $D_1k_2C_o$ is frequently of the same order of magnitude as or much greater than k_1^2. In this case, interfacial area must be known separately, and the height of the contactor will be approximately inversely proportional to the interfacial area, to a degree dependent on the magnitude of the term $1 + \frac{aH\eta}{k_g a}$, which indicates the extent of gas phase control. Indeed, unless k_1^2 can be increased to the point where it will be at least of the same order of magnitude as $D_1k_2C_o$, absorption efficiency can more significantly be improved by increasing interfacial area, rather than k_1.

Based on the flow patterns observed by Riess,[20] Wen, et al.,[22] and Larkins, et al.,[21] it was assumed that the minimum effective interfacial area available for mass transfer was the dry packing area, a_o. Mist or slugging effects would be expected to contribute substantially to the interfacial area. To estimate the magnitude of these effects, an analogy to a froth flow system (see Section IV-B-3) was postulated as follows.

For a system of N_i dispersed spherical particles of diameter d_i, the mean surface-volume diameter is defined as

$$d_{sv} = \frac{\Sigma N_i d_i^3}{\Sigma N_i d_i^2} \quad . \tag{53}$$

For a volume fraction of dispersed phase R_d, the interfacial area per unit volume is defined as

$$a = \frac{6R_d}{d_{sv}} \quad . \tag{54}$$

Heuss, et al. found that in froth flow, d_{sv} was equivalent to a diameter exceeded by only 5% or 10% of the bubbles ($d_{95} - d_{90}$). The magnitude of d_{95} was found to be related to a "homogeneous" gas-liquid velocity, U_{hom}, by

$$d_{95} \sim U_{hom}^{-3/2} \tag{55}$$

where

$$U_{hom} = \frac{\frac{L + G}{S}}{\rho_l R_l + \rho_g R_g} \tag{56}$$

in which: U_{hom} = homogeneous velocity, ft/sec

L = mass liquid rate, lb/sec

G = mass gas rate, lb/sec

R_l, R_g = fraction of pipe occupied by the liquid or gas phase

S = cross sectional area of pipe, ft^2

ρ_g, ρ_l = densities of gas and liquid phases, lb/ft^3 .

U_{hom} and the energy dissipation per unit volume were found to be related by

$$U_{hom} \sim E^{1/3} \tag{57}$$

where

$$E = \frac{g_c(\Delta P/\Delta L)_{tp} U_{hom}}{\rho_l R_l} \; ft^2/sec^3 \quad . \tag{58}$$

Combining Eqs. (55) and (57), d_{95} may be related to the energy dissipation per unit volume by

$$d_{95} = AE^{-1/2} \quad . \tag{59}$$

Based on bubble size distribution data of James and Silberman[37] and the relationship between U_{hom} and E discovered by Heuss, et al., A was evaluated to yield the result

$$d_{95} = 6.31 \; E^{-1/2} \tag{60}$$

where

$$d_{95} = \text{cm}$$
$$E = \text{ft}^2/\text{sec}^3 \quad .$$

Since d_{95} is approximately equal to d_{sv}, Eqs. (54) and (60) imply that the interfacial area in a froth flow device, with $R_d = R_g$, may be related directly to the energy dissipation per unit volume. The situations in froth flow in open tubes and flow in co-current packed columns would be expected to be quite different, because of the presence of packing material and the serious violation of the assumption of isotropic turbulence on which energy dissipation models are usually based. However, it was felt that because of the nature of the patterns of turbulent flow that have been observed in co-current packed columns, a satisfactory first approximation of the interfacial area generated in these devices could be obtained by relating the interfacial area to the energy dissipation predicted for these devices. To do this, a modified definition of U_{hom}, for use in Eq. (58), was made as

$$U'_{hom} = U_{hom}/\varepsilon \tag{61}$$

where ε is the bed porosity. d_{95} was obtained from Eq. (59), and was corrected for system temperature, pressure and void fractions different than encountered in the James and Silberman work (see Section IV-B-3-a). Interfacial areas were calculated from Eq. (54), with $R_d = R_g$ and $d_{sv} = d_{95}$.

c. Calculation. The transport coefficients and interfacial areas in the single-and multiple-contactor cases were calculated on the basis of average flow conditions and physical properties. The term $D_1 k_{OH}(OH^-)$ was found to be negligible compared to $(k_1^2 + D_1 k_{As}(As(OH)_2O^-))$, so that

$$\eta = (k_1^2 + D_1 k_{OH}(\dot{OH}^-) + D_1 k_{As}(As(OH)_2O^-)^{1/2}$$

$$\eta \cong (k_1^2 + D_1 k_{As} As(\dot{OH})_2O^-)^{1/2} \quad .$$

The height of the contactor was expressed as

$$Z = \left(1 + \frac{a\bar{H}\eta}{k_g a}\right) \frac{V_1}{\eta a} \int_{(CO_3^=)_{in}}^{(CO_3^=)_{out}} \frac{d(CO_3^=)}{HPy - C_b} \qquad (62)$$

$(CO_3^=)$ was related to y, the bulk concentration of CO_2 in the gas stream, and to (HCO_3^-) by mass balances; H, C_b and other relevant constants were calculated as shown in Section II-C; and the height was determined numerically by a Simpson's Rule integration technique. The mass balances and integration procedure are described in Appendix XI.

d. Observations. The results of the calculation, together with many of the relevant parameters, are summarized in Table 4. The values of interfacial area calculated using the energy-dissipation model were from 2 to 20 times greater than the dry packing area, a_o. The effect of increased column diameter in decreasing the superficial gas and liquid velocities had the result of decreasing the two-phase pressure

Table 4. CO_2 absorption in co-current packed columns.

	Single column		High-CO_2-partial-pressure column		Low-CO_2-partial-pressure column	
	D = 1.333 ft	D = 2.666 ft	D = 1.333 ft	D = 2.666 ft	D = 1.333 ft	D = 2.666 ft
$\bar{L}$	618,000 lb/hr	618,000 lb/hr	183,430 lb/hr	183,430 lb/hr	183,430 lb/hr	183,430 lb/hr
$\bar{G}$	5445 lb/hr	5445 lb/hr	6583 lb/hr	6583 lb/hr	3015 lb/hr	3015 lb/hr
$\bar{V}_l$	1.64 ft/sec	0.41 ft/sec	0.49 ft/sec	0.12 ft/sec	0.49 ft/sec	0.12 ft/sec
$\bar{V}_g$	7.71 ft/sec	1.93 ft/sec	7.16 ft/sec	1.79 ft/sec	6.10 ft/sec	1.53 ft/sec
$k_c a$	32.08 sec^{-1}	2.21 sec^{-1}	12.13 sec^{-1}	0.97 sec^{-1}	7.41 sec^{-1}	0.64 sec^{-1}
$k_l a$	5.82 sec^{-1}	0.60 sec^{-1}	1.51 sec^{-1}	0.19 sec^{-1}	1.24 sec^{-1}	0.16 sec^{-1}
R_l	0.34	0.34	0.20	0.20	0.25	0.25
$\Delta P/\Delta L$	6.71 psi/ft	0.43 psi/ft	1.53 psi/ft	0.10 psi/ft	1.02 psi/ft	0.07 psi/ft
(1)						
a	1.57 cm^{-1}	1.57 cm^{-1}	1.57 cm^{-1}	1.57 cm^{-1}	1.57 cm^{-1}	1.57 cm^{-1}
Height	32.3 ft	51.3 ft	47.4 ft	31.0 ft	94.9 ft	58.3 ft
ΔP	216.6 psi	22.0 psi	72.7 psi	3.1 psi	96.8 psi	3.9 psi
(2)						
a	39.9 cm^{-1}	6.4 cm^{-1}	22.7 cm^{-1}	4.3 cm^{-1}	14.6 cm^{-1}	3.2 cm^{-1}
Height	12.1 ft	21.0 ft	9.0 ft	13.7 ft	24.9 ft	32.7 ft
ΔP	81.0 psi	9.0 psi	13.8 psi	1.4 psi	25.4 psi	2.2 psi

(1) Height calculated assuming effective interfacial area = a_o, the dry packing area.

(2) Height calculated using effective interfacial area obtained from energy-dissipation model.

drop per unit length and the transport coefficients, $k_c a$ and $k_l a$. When interfacial area was calculated from the energy-dissipation model, the effect of increasing diameter was also to decrease the effective interfacial area. The net effect was an increase in the necessary column height, to a degree similar to that observed for the HCl absorption cases. However, in the case where the interfacial area was considered equal to the fixed a_o, both increases and decreases in tower height with increasing diameter were observed. The energy-dissipation model is probably the more reasonable approach to the problem of determining interfacial area, because of the account this model takes of what is physically occuring within the column. More confidence in the results can only be obtained through experimentation.

For the case of HCl absorption in a co-current packed column, it was observed (Section IV-A-2-c) that using two stages, at constant diameter, had little effect on the total column height required. The results for the CO_2 system contrast with this conclusion, and indicate a marked increase in the total column height required for the two-stage case. The primary reason for this is an increase in the number of liquid phase transfer units, defined by the integral in Eq. (62). In the single-contactor absorption case, the value of this integral was 112, whereas for the high-and low-CO_2-partial-pressure contactors, the values were 146 and 261, respectively. The increase in the number of transfer units in the two-contactor case results both from an increased change in reactant concentration and a reduced physical solubility driving force. This latter effect is indicated by the observation

that although the change in reactant concentration in the single and low-CO_2-partial-pressure contactors is approximately the same, the number of transfer units in the low-CO_2-partial-pressure contactor is more than twice the number in the single contactor.

The magnitude of the term $1 + \frac{aH\eta}{k_g a}$ ranged from 1.07 to 1.28, indicating that the extend of gas-phase resistance to mass transfer was limited.

B. Open Pipe Contactors

1. General Consideration

Co-current gas-liquid flow in open pipes has been suggested as a means of obtaining good gas-liquid contacting efficiency. As with co-current packed columns, such a contacting scheme for absorption is limited to a maximum separation performance of one equilibrium stage per unit.

Excellent general discussions of the two-phase-flow literature have been presented by Dukler and Wicks[40] and Scott,[41] and a comprehensive index to the two-phase-flow literature has been compiled by Gouse.[42]

Mass transfer in two-phase flow is related to:

(1) Phase distribution, including flow patterns, liquid holdup, film thickness and entrainment.

(2) Pressure drop.

(3) Interfacial structure, including factors giving rise to entrainment, the rate of circulation between the fluid body and the interface and interfacial shear--all of which affect the local rates of mass transfer.

a. Phase distribution. The flow patterns encountered in co-current gas-liquid flow are depicted in Fig. 8. A useful empirical correlation for predicting the flow patterns as a function of gas and liquid flow rates and physical properties has been developed in the form of a diagram by Baker,[43] presented in Fig. 9. This correlation has proved quite successful in predicting flow patterns for ranges of pipe sizes, physical properties and pressures, although some discrepancies have been reported.[40]

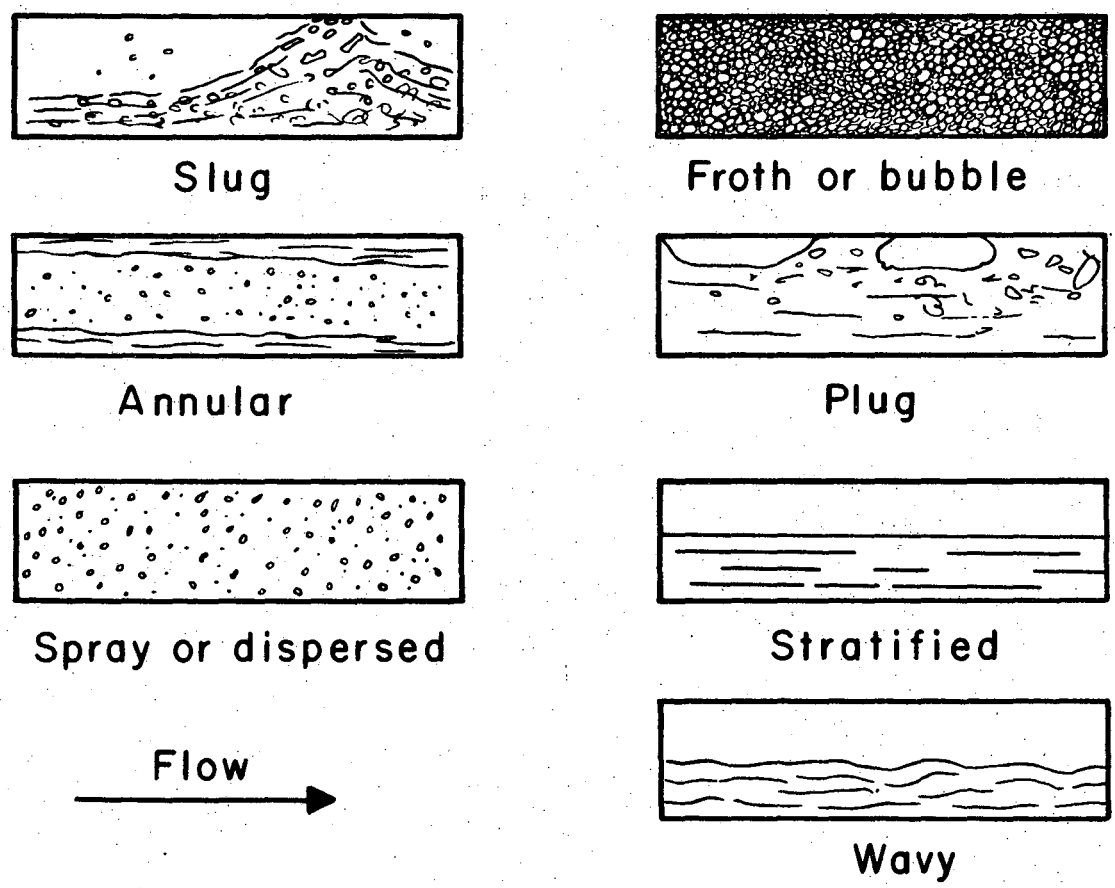

Fig. 8. Flow patterns in two-phase gas-liquid horizontal flow.

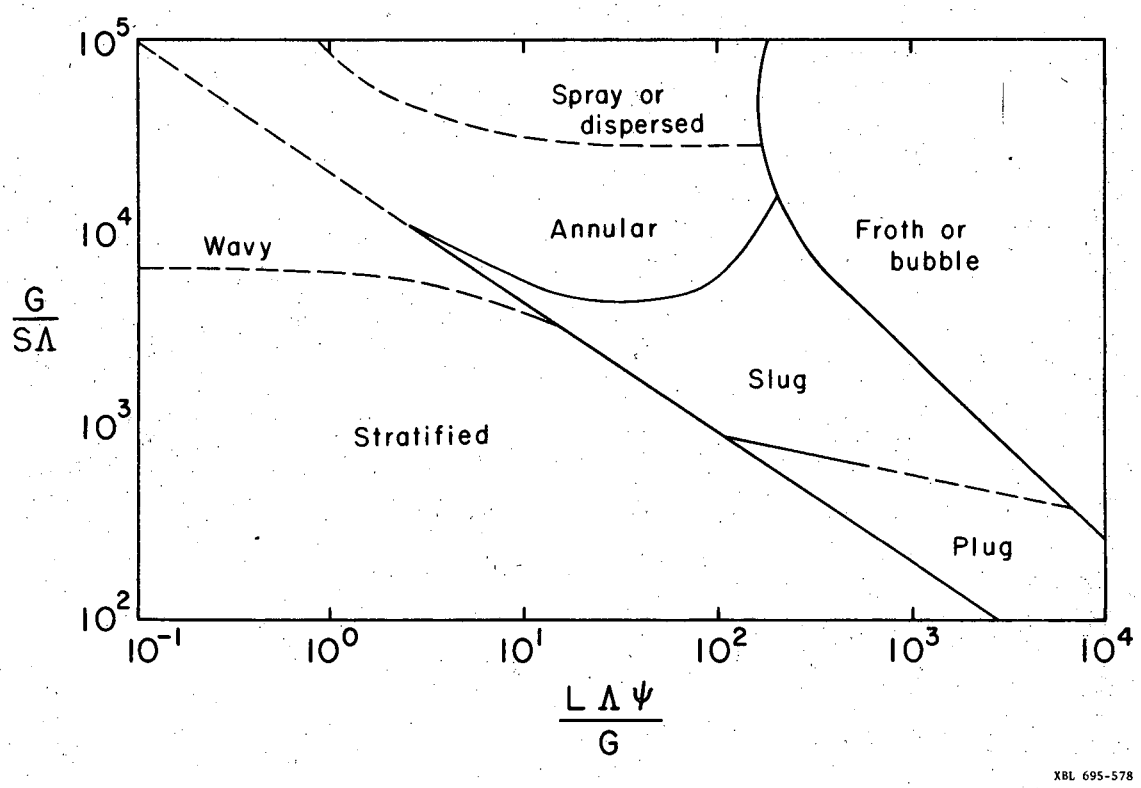

$$\Lambda = \left[\left(\frac{\rho_g}{0.075}\right)\left(\frac{62.3}{\rho_l}\right)\right]^{1/2}$$

$$\Psi = \frac{73}{\sigma}\left[\mu_l \left(\frac{62.3}{\rho_l}\right)^2\right]^{1/3}$$

Fig. 9. Baker correlation of flow patterns in gas-liquid horizontal flow (ρ = lb/ft^3; σ = dynes/cm; μ_l = lb/ft hr; G/S = lb/ft^{2}hr).

Lockhart and Martinelli[23] have correlated liquid holdup, defined as the fraction of the pipe volume occupied by liquid at any point and instant in time, as a function of the dimensionless parameter χ, defined by Eq. (69) below. This correlation is claimed valid for all flow conditions fulfilling the requirements that the static pressure drop for each phase be the same and that the combined volumes of the liquid and gas phases at any instant must equal the pipe volume. These assumptions imply a uniform axial flow distribution, and preclude such regimes as segregated slug flow.

The Lockhart and Martinelli derivation is based on an assumption of fully segregated flow. Hughmark[44] derived a holdup relation based on a homogeneous model proposed by Bankoff[45] to account for some of the complexities in bubble flow. The Hughmark correlation defined:

$$R_g = K\, y_G \tag{63}$$

where: R_g = gas holdup = $1 - R_l$

$$y_G = \frac{\frac{G}{\rho_g}}{G/\rho_g + L/\rho_l} \tag{64}$$

K = constant characteristic of the distribution studied

K is correlated graphically as a function of:

$$Z = \frac{(Re)^{1/6}(Fr)^{1/8}}{(1 - y_G)^{1/4}} \tag{65}$$

where:

$$Re = \frac{D\left[\frac{G + L}{S}\right]}{\mu_l R_l + \mu_g R_g} \tag{66}$$

$$Fr = \frac{\left[\frac{\frac{L}{\rho_l} + \frac{G}{\rho_g}}{S}\right]^2}{Dg_c} \quad . \tag{67}$$

Dukler, Wicks and Cleveland[46] have reported the Hughmark correlation to be the most generally satisfactory, although the Martinelli correlation is better for predicting holdup in annular flow, as would be expected from its derivation.

b. Pressure drop. A number of correlations for predicting the pressure drop in horizontal co-current gas-liquid flow are available.

For moderate pressures and small pipe diameters (less than six inches), Wicks and Dukler[46] report the Lockhart and Martinelli[23] correlation to be the most successful at predicting two-phase pressure drops. The two-phase pressure drop is predicted as

$$(\Delta P/\Delta L)_{tp} = \phi_g^2 (\Delta P/\Delta L)_g \tag{68}$$

where ϕ_g is a parameter correlated against the dimensionless variable

$$\chi = [(\Delta P/\Delta L)_l/(\Delta P/\Delta L)_g]^{1/2} \tag{69}$$

$(\Delta P/\Delta L)_l$ and $(\Delta P/\Delta L)_g$ are the pressure drops per unit length calculated by assuming that the liquid or gas flowed alone in the pipe. The value

of ϕ_g is dependent on whether the phases are in laminar or turbulent flow, and four ϕ_g's are defined, corresponding to turbulent-turbulent, turbulent-viscous, viscous-turbulent and viscous-viscous conditions in the individual phases.

Hughmark[47] has pointed out that the Lockhart and Martinelli correlation does not extrapolate well to high pressures or large pipe diameters. The pressure drop in horizontal pipes is due both to the frictional pressure drop and the pressure drop due to the acceleration of both phases that results when the gas expands with decreasing total pressure in the pipe. As the pipe diameter decreases, at constant L and G, the pressure gradient becomes greater, resulting in a greater expansion of the gas than would occur in pipes of larger diameter. This acceleration effect may not be important at high pressures, when the pressure drop is small relative to the total pressure. Since the Lockhart and Martinelli correlation was derived using data from small pipes at low system pressures, it becomes increasingly less satisfactory for high pressures and larger diameters, and tends to overestimate the pressure drop.

Hughmark[47] has developed a correlation which is claimed to correct for this error, based on a two-phase friction factor:

$$f_{tp} = \frac{2g_c D \, \Delta P}{V^2 \rho_{tp} \Delta L} \tag{70}$$

where $$V = V_l + V_g \tag{71}$$

$$\rho_{tp} = \rho_l R_l + \rho_g R_g \quad . \tag{72}$$

The quantity f_{tp}/f_l, where f_l is the friction factor calculated by assuming than only liquid flows through the pipe, is presented as a function of $(1 - y_G)$, with $(Re_{tp})(\rho_g/\rho_l)(0.085/D)$ as a parameter. Re_{tp} and y_G are as defined in Eqs. (66) and (64).

Another correlation which has been proposed to account for the effects of larger pipe diameters and higher pressures has been presented by Chenoweth and Martin.[48] $(\Delta P/\Delta L)_{tp}/(\Delta P/\Delta L)_l^*$ was plotted against $(1 - y_G)$, with $(\Delta P/\Delta L)_g^*/(\Delta P/\Delta L)_l^*$ as a parameter, where:

$(\Delta P/\Delta L)_{l,g}^*$ = pressure drop calculated from friction factors based on the liquid or gas properties, but using a combined flow rate, $V = V_l + V_g$.

McManus[49] has claimed that the Chenoweth-Martin correlation is superior to other correlations for predicting the pressure drop in annular flow.

c. Entrainment. The net amount of entrainment of a liquid in a gas stream represents an equilibrium between liquid being torn off a liquid surface due to the shearing forces of a gas stream and the re-entry of the entrained drops into the bulk liquid. In evaluating the importance of entrainment in a mass transfer process, both the net amount of entrainment and the rate of "interchange" of droplets between the liquid and the gas stream must be considered. The comments in this section pertain chiefly to the annular-flow regime.

Wicks and Dukler[50] have proposed a correlation to determine the net amount of entrainment based on the Lockhart and Martinelli parameter, χ. A parameter R_{en} is determined from a graphical correlation of

R_{en} vs. χ, and the amount of entrainment is calculated as

$$E_n = \frac{(\Delta P/\Delta L)_g R_{en}}{Q_l/Q_g \; We_c} \tag{73}$$

where: R_{en} = entrainment parameter ($lb_m ft^3/lb_f hr$)

E_n = entrainment, lb_m/hr

Q_g = volumetric gas flow rate, ft^3/hr

Q_l = volumetric liquid flow rate, ft^3/hr

We_c = critical Weber number--13 for sudden shock exposure of liquid to gas; 22 for gradual acceleration .

Cousins, Denton and Hewitt[51] have studied the mechanism of droplet interchange in vertical annular flow. The motion of droplets to the annular liquid may be characterized by a mass-transfer equation

$$m_i = k\Delta c_m \tag{74}$$

where: m_i = mass transfer rate, lb_m/ft^2hr

k = mass transfer coefficient, ft/hr

Δc_m = difference between the bulk mean concentration of water droplets and the concentration at the liquid surface, lb/ft^3.

If the concentration of droplets at the liquid surface is assumed to be zero,

$$\Delta c_m = \frac{E_n}{E_n/\rho_l + G/\rho_g} \tag{75}$$

where G is the gas flow rate, lb/hr. If the interchange process has reached steady state, the rate of mass transfer of droplets to the liquid

surface equals the rate of removal of these droplets from the surface. If $E_n/\rho_L << G/\rho_G$, and the mass-transfer rate is redefined as I'_n, the steady-state interchange rate, Eq. (74), may be re-written as

$$I'_n = \frac{k_i E_n \rho_g}{G} \tag{76}$$

where: I'_n = interchange rate, lb/hr ft^2

k_i = mass transfer coefficient for steady state interchange, ft/hr.

Cousins, et al., proposed that k_i could be related to physical conditions by an equation of the form

$$\frac{k_i d}{D_g} = A(Re_g)^s(Sch_g)^q \tag{77}$$

based on an analogy to the mass transfer of trace components in a gas.

Measurements of I'_n were made by Cousins, et al., by a dye injection technique in a vertical 3/8-inch pipe. The results obtained are valuable only in giving an order of magnitude estimate of I'_n, and no test of Eq. (77) for different physical properties or pipe diameters was made. Using a somewhat different technique, involving the absorption of a highly soluble gas, Anderson, Bollinger and Lamb[52] measured interchange in a horizontal one-inch pipe, and showed that beyond a certain value of the liquid Reynolds number, the amount of interchange becomes a relatively constant fraction of the liquid flow rate (% of liquid flow rate per foot) and independent of the gas rate. The results of the two experimenters were qualitatively similar, yielding values of interchange in the range of 4 to 15% of the liquid flow rate per foot.

d. Mass transfer. The easiest flow patterns to characterize hydrodynamically are the annular and froth regimes, being near the extremes of fully segregated and fully homogenous flow. This characterization is essential to predicting mass-transfer behavior, especially when absorption involves a first-order chemical reaction. The annular and froth-flow regimes each exhibit properties conducive to efficient mass transfer, and are discussed separately.

The available studies of mass transfer in co-current flow in pipes were limited to the consideration of horizontal flow, and this was the configuration evaluated, despite the possible process inconveniences of horizontal, as opposed to vertical, flow.

2. Annular Flow

For both the $HCl-H_2O$ and $CO_2-K_2CO_3$ systems, the Baker parameter $L/G\Lambda\psi$ indicated that for a proper choice of pipe diameter, the annular-flow regime could be expected.

At low values of the gas and liquid rates, annular flow may be characterized by an almost complete segregation of gas and liquid, with the liquid in a layer along the pipe wall. As the gas and liquid rates increase, a considerable amount of shear will occur between the liquid and the gas, resulting in the occurence of waves in the liquid. As these waves break off, liquid droplets will become entrained in the gas phase. The potential utility of annular flow as a mass-transfer scheme lies in the high liquid-phase mass-transfer coefficients which may result because of an absence of a laminar boundary layer in the turbulent annular liquid phase and the high interfacial area which may result from liquid droplets becoming entrained in the gas.

Bollinger[53] measured k_1 for a liquid-phase controlled absorption as a function of liquid rate, assuming the effective interfacial area to be the cylindrical area per unit volume defined by using a radius equal to the pipe radius minus half the liquid-film thickness.

Wales[54] studied liquid-phase controlled mass transfer in annular and dispersed regimes. The addition-of-resistances concept was used to determine the gas-phase mass-transfer coefficient and interfacial area from the measured value of the over-all mass-transfer coefficient. For the pseudo first-order system studied by Wales (the absorption of CO_2 into NaOH), it was assumed that $D_1 k_2 C_o >> k_1^2$, and the resistances to mass transfer were related as:

$$\frac{1}{K_g a} = \frac{H}{a(D_1 k_2 C_o)^{1/2}} + \frac{1}{k_g a} \tag{78}$$

where: $K_g a$ = over-all (chemical) mass-transfer coefficient, lb moles/ft^3 hr atm

$a(D_1 k_2 C_o)^{1/2}$ = hr^{-1}

H = solubility constant, atm ft^3/lb mole

$k_g a$ = lb moles/ft^3 hr atm .

By plotting the reciprocal of the experimentally determined value of $K_g a$ against the known value of $H/(D_1 k_2 C_o)^{1/2}$, lines were drawn with a slope equal to "a" and an intercept $1/k_g a$. The values for the interfacial area so determined ranged from 100 to over 700 ft^2/ft^3, with liquid and gas rates of 500 to 2500 and 150 to 300 pounds per hour respectively. The area per unit volume of a one-inch pipe, as was

used for Wales' experiments is, neglecting film thickness, about 24 ft^2/ft^3. The excess interfacial area can only be explained by liquid becoming dispersed or entrained in the gas phase. This suggests that unless the liquid and gas rates are so low that little entrainment in the gas will occur, the assumption of effective interfacial area made by Bollinger[53] is inadequate.

Anderson, Bollinger and Lamb[52] analyzed mass transfer in a gas-phase-controlled absorption system by developing a model in conformance with the observed hydrodynamics of annular flow. The mechanisms of mass transfer were delineated as:

(1) Molecular diffusion at the interface between the gas the the annular liquid. Coefficients for this mechanism could be derived from extrapolation of wetted-wall-column data.

(2) Diffusion of solute between entrained liquid drops and the gas carrying the entrained liquid.

(3) Interchange between entrained liquid droplets and the annular liquid. These droplets will be closer to equilibrium than the bulk liquid into which they return, thereby enhancing the rate of mass transfer.

A means was presented to predict interchange from over-all mass-transfer coefficients. Because of the finding that interchange becomes a relatively constant fraction of total liquid flow rate at high liquid Reynold's numbers, the model offers an approach for design calculations which, if the approach to equilibrium of the entrained droplets is known, obviates the necessity of knowning the total effective interfacial area explicitely.

Jepsen[55] measured values of k_1a for physical absorption in the annular- and mist-annular flow regimes and presented an empirical correlation relating k_1a to energy dissipation and physical properties of the system. An evaluation of the data of other experimenters was made.

Hughmark[56] has proposed an analogy between momentum and mass transfer for annular flow, which is claimed to fit the data of Bollinger[53] and Anderson, Bollinger and Lamb.[52]

a. Annular contactor--HCl absorption. i. Design considerations. Based on the mass flow rates of gas and liquid determined from the overall mass balance (Section III-B-2) and the physical properties of the system, it was found that by choosing a pipe diameter of 5 inches, the Baker correlation predicts that annular flow will exist for the $HCl-H_2O$ system in the single and multiple contactors. The region on the flow map to which the flow rates corresponded is shown on Fig. 14.

Because of the nature of the flow, the low pressure of the system and the relatively small pipe diameter, the Lockhart and Martinelli[23] correlation was used to calculate the pressure drop and liquid holdup.

To analyze the mass-transfer behavior of the system, the model developed by Anderson, et al.,[52] was used. The solute mass balance for symmetrical annular liquid flow can be written in a form which accounts both for diffusional mass transfer between the gas and the annular liquid and the interchange of entrained liquid between the annular liquid and the gas stream.

$$\frac{d(L_a x_a)}{dz} = I_n(x_e - x_a) + K'_g M_{HCl} P(y_{HCl} - y^*_{HCl})2\pi r \qquad (79)$$

where: L_a = flow rate of liquid in annular film, gms/hr

I_n = interchange of liquid between annular film and gas core, gms/ft hr

K'_g = mass-transfer coefficient characterizing diffusional mass transfer to the annular liquid, gm moles/atm ft^2hr

P = total pressure, atm

M_{HCl} = molecular weight of HCl, gms/gm mole

$2\pi r$ = annular area per length of contactor, ft

x_e = wt fraction of solute in entrained liquid

x_a = wt fraction of solute in annular liquid

y_{HCl} = mole fraction of solute in bulk gas stream

y^*_{HCl} = mole fraction of solute in equilibrium with liquid of composition x_a .

This equation does not account for the mass transfer between the solute gas and the entrained liquid. This may be accounted for by making an assumption regarding x_e. For the gas-phase controlled system studied by Anderson, et al., (NH_3-H_2O) it was shown that the entrained droplets were in equilibrium with the bulk gas. This result was assumed to be applicable to the HCl absorption system, and x_e was specified to be in equilibrium with the gas of composition y_{HCl}.

For the adiabatic absorption of HCl, a mass balance must also be written to account for the rate of vaporization of water. In general, this mass balance is represented by Eq. (26). Although vaporization

occurs both from the annular liquid and the entrained liquid droplets, it is not possible to characterize the mechanism by an equation analogous to Eq. (79). This is because the quantities x_{eHCl} and x_{eH_2O} cannot be specified independently as being in equilibrium with the gas, since $x_{eH_2O} = 1 - x_{eHCl}$. To account for the vaporization of the water, it was assumed that the gas was saturated with water vapor down the entire length of the contactor. This was shown to be nearly the case in the co-current packed column, where this assumption was not made, as shown in Fig. 7. The partial pressure of H_2O in the gas phase was assumed to be in equilibrium with the entrained liquid droplets, which were assumed to account for most of the evaporation. (Note that with this specification of the problem, the flow rates and composition obtained by a solution of the design equation are identical to those determined by the "black box" material and heat balance.)

K'_g was calculated, using the assumption of Anderson, et al., that it may be obtained by extrapolating correlations developed for wetted-wall mass-transfer data, by the analogy:

$$j'_D = \frac{K'_g P_{BM}}{G_m} (Sch_g)^{2/3} = 0.0395 \, (Re_g)^{-1/4} \tag{80}$$

where:

$$P_{BM} = \frac{(P2 - p2^*) - (P1 - p1^*)}{\ln \dfrac{(P2 - p2^*)}{(P1 - p1^*)}} \text{ atm} \tag{81}$$

P_i = Total pressure at point i in reactor

p_i^* = partial pressure of solute in equilibrium with x_e at point i in reactor

G_m = molar gas flow rate, gm moles/hr

K'_g = gm moles/hr ft^2 atm .

In the range of liquid- and gas-phase Reynold's numbers studied by Anderson et al., interchange was found to be independent of gas rate and equal to between 3 and 5% of the liquid flow rate per foot of contactor. Although the physical properties of the $HCl-H_2O$ system are comparable to those of the system studied by Anderson, et al., and the Reynolds numbers are similar, the data of Anderson, et al., were taken in a one-inch pipe. The effect of pipe diameter has not been determined. However, a comparison of Anderson's results with those of Cousins, et al., in a 3/8" pipe suggests, qualitatively, a decrease in interchange with increasing pipe diameter. This may be consistent with the observation that as the pipe diameter increases, the "acceleration" component of the two-phase pressure drop becomes relatively less important than the frictional component. The action of a gas expanding against a liquid, with the resultant acceleration of each phase would be expected to contribute substantially to the net entrainment and, hence, to the interchange. Since a quantitative estimate of this effect was impossible, interchange was assumed equal to 4% of the liquid flow rate per foot of contactor, in conformance with the range determined by Anderson, et al.

ii. Calculation. The lengths of the contactors were calculated by numerically integrating Eq. (79), using a fourth-order Runge-Kutta technique, similar to that described for the co-current packed-column calculation (Appendix X). A pressure drop per unit length based on average flow rates and physical properties was used, but the coefficient K'_g and the interchange, I_n, were calculated at each stage of the iteration. L_a was assumed equal to L, the total liquid flow rate. The performance of the Runge-Kutta procedure was tested by varying the step size. Halving the initial step size of 0.4 feet resulted in a change of less than 1% in the calculated contactor lengths.

iii. Observations. The results of the calculation are shown in Table 5, and a graph of gas- and liquid-phase compositions and temperature as a function of pipe length for the single-contactor case is shown in Fig. 10. A rough evaluation of the relative importance of the interchange and diffusional mass-transfer mechanisms may be made by comparing the magnitudes of the terms I_n and $K'_g M_{HCl} P 2\pi r$. At the entrance to the single contactor, the magnitudes of these terms are 230.3 and 131.6 lb/ft hr, respectively. Because the driving force $x_e - x_a$ is everywhere larger than the concentration difference $y_{HCl} - y^*_{HCl}$, as seen in Fig. 10, the interchange mechanism is more important than the diffusional mechanism, although the contribution of the latter is definitely not negligible.

The importance of interchange explains why the change in concentration variables and temperature are more uniform over the entire length of the contactor than was observed with the co-current packed

Table 5. Annular flow contactor--HCl absorption.

	Single Contactor		High-HCl-partial-pressure contactor		Low-HCl-partial-pressure contactor	
	Diameter = 5 inches		Diameter = 5 inches		Diameter = 5 inches	
	Inlet	Outlet	Inlet	Outlet	Inlet	Outlet
†L(lb/hr)	7008.0	7667.9	4086.8	4390.7	3879.7	4086.8
†G(lb/hr)	4406.2	3746.3	4406.9	4103.1	3989.4	3629.3
V_l(ft/sec)	0.219	0.241	0.128	0.137	0.122	0.128
V_g(ft/sec)	135.4	115.1	129.0	120.1	116.7	111.1
‡K'_g	2.76	2.28	2.70	2.55	2.35	2.14
I_n(lb/ft hr)	280.3	306.7	163.5	175.6	155.9	163.5
ΔP/ΔL(psi/ft)	0.0118		0.0101		0.0084	
Height (ft)	22.7		15.3		28.8	
ΔP (psi)	0.27		0.15		0.24	

Exchanger Duties: Interstage cooler: 34,675,000 cal/hr
Liquid cooler: 23,732,000 cal/hr

†Gas and liquid compositions are identical to those shown in Table 2B.

‡lb moles/hr atm ft^2.

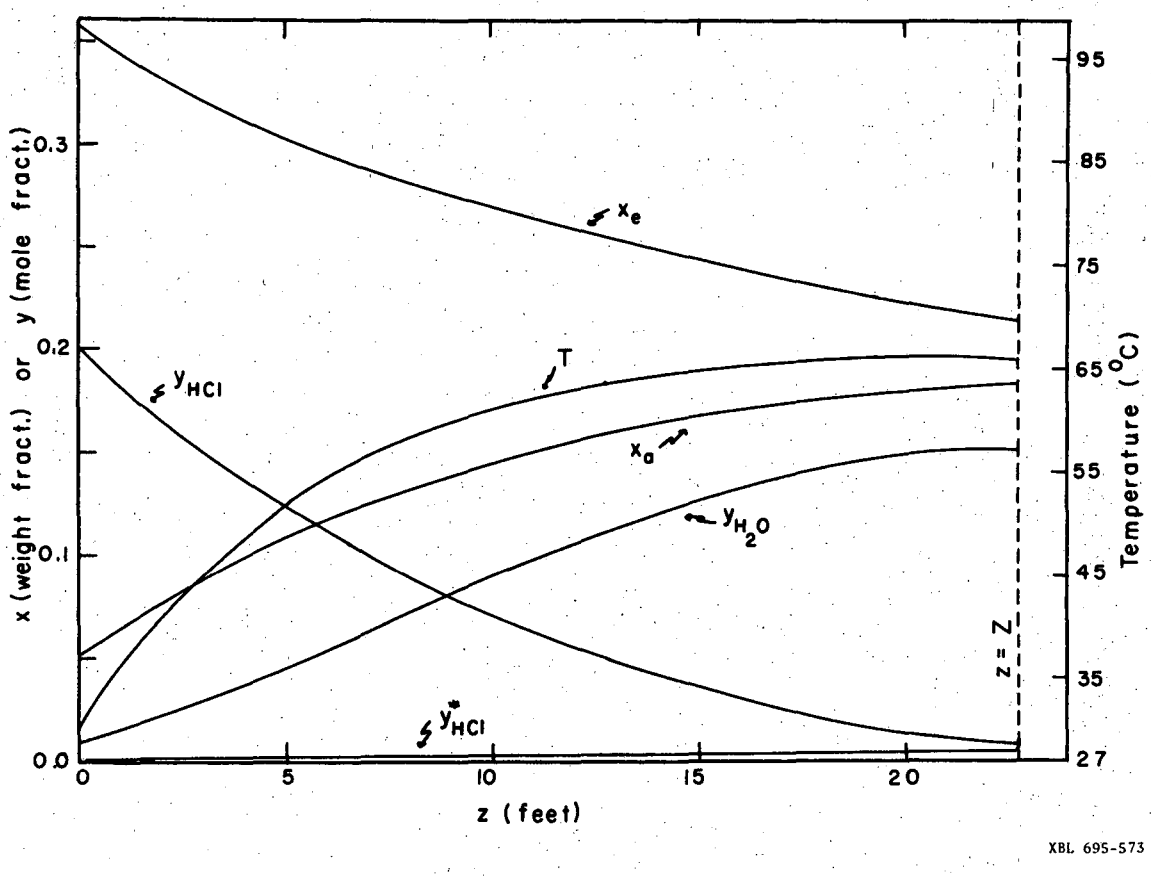

Fig. 10. Concentration and temperature profiles in a single annular-flow contactor for HCl absorption.

column. The rapid decrease in magnitude of the quantity $y_{HCl} - y^*_{HCl}$ is compensated by the less rapidly decreasing, and larger, $x_e - x_a$. As a consequence of this, the ratio of the heights of the low-HCl-partial-pressure contactor to the high-HCl-partial-pressure contactor in the two-contactor case is not as great as was observed for the analogous case with the co-current packed columns. The combined lengths of the multiple contactors is significantly larger than the single-contactor length. This results from a decrease in the over-all concentration-driving force, $x_e - x_a$, in the two-contactor case.

b. Annular contactor--CO_2 absorption. i. Design considerations.

Based on the gas and liquid flow rates determined from the over-all mass balance and the physical properties of the system, the Baker correlation predicts that annular flow will be obtainable in the multiple CO_2 contactor case by choosing diameters of the high-CO_2-partial-pressure and low-CO_2-partial-pressure contactors to be six and four inches, respectively. For the single contactor, the flow and physical properties predict the existence of froth flow. The region of the Baker correlation to which the flows and choices of diameters correspond is depicted on Fig. 14.

Because of the high pressure encountered in the system, the Chenoweth-Martin[48] correlation was used to predict the two-phase pressure drops.

Extending the model of Anderson, et al., to the liquid-phase-controlled system studied, the mass balance is written as

$$\frac{-L_a d(CO_3^{=})}{\rho_1 dz} = \frac{I_n(C_e - C_a)}{\rho_1} + \frac{S(HPy - C_b)a\eta}{1 + \frac{aH\eta}{k_g a}} \tag{82}$$

where: L_a = liquid flow rate in annular film, lb/sec

I_n = interchange, lb/ft sec

a = cylindrical area per unit volume defined by the annular liquid, cm^{-1}

$(CO_3^{=})$ = reactant concentration, gm moles/liter

$^{\dagger}C_e$ = equivalent concentration of CO_2 in entrained liquid, gm moles/liter

$^{\dagger}C_a$ = equivalent concentration of CO_2 in annular liquid, gm moles/liter

y = mole fraction of CO_2 in bulk gas

C_b = concentration of dissolved, but unreacted, CO_2 in solution, gm moles/liter

η = rate term, cm/sec

$k_g a$ = gm moles/sec atm liter

H = gm moles/atm liter

z = length coordinate, feet

S = cross sectional pipe area, ft^2

ρ_1 = liquid density, lb/ft^3 .

Although the assumption that the entrained liquid was in equilibrium with the bulk gas was reasonable for the $HCl-H_2O$ system,

---

†Based on the amount of CO_2 consumed by reaction; $Ca \neq (CO_3^{=})$, but $dC_a = -d(CO_3^{=})$.

the decreased physical solubility of CO_2 and a comparison between the solubility driving force and the amount of CO_2 which must be absorbed to reach chemical equilibrium may make this assumption less acceptable for the Vetrocoke absorption system.

Two extremes are conceivable with the interchange mechanism of mass transfer. If the droplets become equilibrated with the gas during their holding time in the gas phase, the solute concentration in the droplets will differ considerably from that in the annular liquid to which they return. At the other extreme, if the droplets returning to the annular liquid are negligibly closer to equilibrium than the liquid into which they return, the radial concentration profile will be nearly homogeneous. This would be the case if the droplets were very large and/or their lifetimes very short. The rate of absorption would still be larger than if there were no entrainment, but the increase would be due to a greater interfacial area and not, substantially, due to interchange.

Theoretically, the approach to either extreme may be estimated by considering the mass transfer in a single droplet. The transient mass balance for a single entrained droplet, assuming negligible gas-phase resistance, may be written as

$$\frac{d(V_d C_e)}{dt} = \frac{-d(V_d(CO_3^{=}))}{dt} = (HPy - C_b)\eta\, S_d \qquad (83)$$

where: V_d = droplet volume, cm^3

S_d = surface area of droplet, cm^2

t = time, sec .

This equation must be integrated from the time of inception of the drop, $t = 0$, to the time the drop re-enters the annular liquid, $t = \theta$, in order to determine the change in composition C_{eo} to $C_{e\theta}$. To obtain an approximate solution to this equation, it was assumed that η and the drop size were independent of time and that the solubility driving force remained constant during the holding time of the drop. The result is

$$\frac{C_{e\theta} - C_{eo}}{HPy - C_b} = \eta \frac{S_d}{V_d} \theta \quad . \tag{84}$$

An estimate of the holding time of a droplet may be obtained from a knowledge of the net amount of entrainment, the rate of droplet interchange and the superficial gas velocity, at which the entrained droplet is assumed to travel, yielding

$$\theta = \frac{E_n}{I_n V_g} \tag{85}$$

S_d/V_d may be estimated if a mean surface-diameter droplet size is known. An approximation, which is often nearly correct for typical mass-transfer situations, is that

$$\eta = (k_1^2 + D_1 k_2 C_o)^{1/2} \cong (D_1 k_2 C_o)^{1/2} \quad .$$

Equation (84) was evaluated by using an estimate of the net entrainment from the Wicks and Dukler correlation,[50] a mean drop size of 75 microns reported by Cousins, et al.,[51] and assuming that interchange was equal to 4% of the liquid flow rate, in accord with the

results of Anderson, et al.[52] If the entrained droplets were to equilibrate with the gas, the value of the ratio of change in reactant concentration to the solubility concentration difference should be of the order of 100:1. Evaluation of the right hand side of Eq. (84) failed to yield a value approaching this magnitude, and indicated a ratio of the order of 1:1 to 10:1. The apparent reason for this is that the magnitude of the net entrainment calculated with the Wicks and Dukler correlation was quite small, due to the low gas-phase pressure drop calculated from the Chenoweth-Martin correlation. This results in a low value of $\theta(\sim 10^{-4}$ sec) which, as discussed above, will tend to make the contribution to mass transfer due to interchange minimal. Because of the uncertainties involved in the estimates of I_n, E and the droplet diameter, a completely reliable evaluation of Eq. (84) is not possible. The indication is, however, that it is unrealistic to assume full chemical equilibrium between the droplets and the surrounding gas in this case.

Several calculations were made to determine the size of the contactors, based on the assumptions that:

(1) The entrained droplet concentration was in equilibrium with the gas.

(2) The driving force for interchange mass transfer was 10% and 50% of that predicted by assuming the drop to be in equilibrium with the gas.

(3) A homogeneous radial concentration profile existed, with the interfacial area equal to the annular area plus the interfacial area associated with the entrained liquid, calculated using the Wicks and

Dukler entrainment correlation and a droplet size equal to that reported by Cousins, et al.

The correlation of Jepsen[55] was used to determine the value of k_1a. For energy dissipations greater than 0.05 atm/sec, as were found in this system, Jepsen's result is

$$k_1 a D_1^{0.5} \sigma^{-0.5} \mu_1^{-0.05} = 18.75\ E^{0.79} \tag{86}$$

where: $E = (\Delta P/\Delta L)_{tp}(V_1 + V_g)$ atm/sec

μ_1 = centipoise

D_1 = cm^2/sec

σ = dynes/cm

k_1a = ft/sec .

The value of k_1 was determined by dividing k_1a by the annular area per unit volume, corrected for liquid film thickness, or by the total area per unit volume, as used in the calculation based on assumption (3). Dividing k_1a by the annular area to determine k_1 may not be totally consistant with the situation in the slug-annular flow regime studied by Jepsen, but was assumed to give an adequate approximation of the magnitude of this term. It is further justified by the fact that, in the calculations based on assumptions (1) and (2), the importance of the diffusional mechanism was shown to be much less than that of interchange.

The gas-phase resistance to mass transfer was neglected in the calculations. This is justified, in the calculations based on assumptions (1) and (2), by the lack of importance of diffusional mass transfer.

Interchange was assumed equal to 4% of the liquid flow rate per foot of contactor and, because of the small values of E_n calculated, L_a was taken equal to the total liquid flow rate.

ii. Calculation. Values of the mass-transfer coefficients, pressure drop and interchange were calculated based on average flow rates and physical properties in the contactors. Equation (82) was integrated numerically, using Simpson's rule.

iii. Observations. The results of the calculation are shown in Table 6. The relative importance of interchange and diffusional mass transfer, in the cases where both mechanisms were assumed, may be evaluated by comparing the terms $(I_n/\rho_l)(C_e - C_a)$ and $\eta aS(HPy - C_b)$ in Eq. (82), since the gas-phase resistance to mass transfer was neglected. I_n/ρ_l is equal to 97.2 ft^2/hr in each of the two contactors. The term ηaS has a value of 193.7 ft^2/hr in the high-CO_2-partial-pressure contactor and 344 ft^2/hr in the low-CO_2-partial-pressure contactor. However, the magnitude of the concentration difference $C_e - C_a$ is of the order of 100 times greater than the physical solubility driving force, $HPy - C_b$. Because of this fact, the interchange mass-transfer mechanism dominates in the rate equation, and the diffusional term in Eq. (82) is effectively negligible.

It may be observed that, when the interchange mechanism is assumed, the length of the low-CO_2-partial-pressure contactor is substantially less than that of the high-CO_2-partial-pressure contactor. This result is in contrast to the situation observed in other multiple-contactor cases, and is due to the dominance of the interchange-mechanism

Table 6. Annular flow contactor--CO_2 absorption.

	High-CO_2-partial-pressure contactor	Low-CO_2-partial-pressure contactor
Diameter	6 inches	4 inches
$\overline{L}$	6 inches	4 inches
$\overline{G}$	183,430 lb/hr	183,430 lb/hr
$\overline{V}_l$	3.42 ft/sec	7.77 ft/sec
$\overline{V}_g$	50.93 ft/sec	97.70 ft/sec
$k_l a$	0.254 sec^{-1}	1.116 sec^{-1}
$\Delta P/\Delta L$	0.069 psi/ft	0.231 psi/ft
R_l	0.15	0.14
E_n	120 lb/hr	850 lb/hr
I_n	7337.2 lb/ft hr	7337.2 lb/ft hr
(1) a	0.260 cm^{-1}	0.391 cm^{-1}
Height	28.0 ft	8.3 ft
ΔP	1.9 psi	1.9 psi
(2) a	0.260 cm^{-1}	0.391 cm^{-1}
Height	55.2 ft	16.5 ft
ΔP	3.8 psi	3.8 spi
(3) a	0.260 cm^{-1}	0.391 cm^{-1}
Height	244.7 ft	78.7 ft
ΔP	16.9 psi	18.2 spi
(4) a	0.295 cm^{-1}	0.686 cm^{-1}
Height	2069.9 ft	1767.6 ft
ΔP	---	---

(1) Droplets assumed to be in equilibrium with the gas

(2) 50% of driving force corresponding to droplet equilibrium assumed

(3) 10% of driving force corresponding to droplet equilibrium assumed

(4) Interchange neglected; interfacial area based on droplet size data and calculated net entrainment

term in Eq. (82). The log-mean average driving force, $(C_e - C_a)_{lm}$ was calculated in the high- and low-CO_2-partial-pressure contactors. The result was that the average driving forces in the two contactors were nearly identical. If this is the case, and the term accounting for diffusional mass transfer is negligible, the height of the contactors should be proportional to the change in reactant concentration in the specific contactors. Referring to Table 1, the ratio of the change in reactant concentration in the high-CO_2-partial-pressure contactor to that in the low-CO_2-partial-pressure contactor is about 3.38:1. The ratio in column heights varies from 3.38:1 to 3.1:1, with the decreasing ratio associated with calculations assuming a driving force $C_e - C_a$ less than the driving force calculated assuming total equilibrium of the droplets with the gas. With the interchange mechanism neglected, the ratio in contactor lengths is in accord with the more conventional pattern.

Which of the assumptions regarding the approach of the droplets to equilibrium with the gas phase is best can only be determined through experiment. It appears, on comparing the contactor lengths, that unless the droplets are near to equilibrium, the annular flow contactor will not be a competitive device for this absorption system. To make more accurate estimates in this regard, more information concerning interchange rates, net amounts of entrainment and droplet distribution data would be valuable.

3. Froth Flow

At sufficiently high values of L/G and G/S, the Baker correlation, Fig. 9, indicates that a froth, or bubble, flow regime will be established. This pattern is characterized by a relatively homogeneous dispersion of small bubbles in the liquid phase. Some disagreement exists in the literature concerning the accuracy with which the Baker correlation adequately predicts the onset of froth flow. Data of Hoogendoorn[40] failed to confirm the existence of froth flow over much of the froth flow regime depicted by the Baker correlation. Heuss, et al.[31] and James, et al.,[37] have found froth flow to exist quite near the boundary predicted by the Baker correlation between froth and dispersed, annular and slug flow. However, Jepsen[55] has commented that, in the case of the data of Heuss, et al., the froth-flow pattern observed may be due to entrance effects, and that the steady-state regime would be slug-annular. The validity of Jepsen's observation is somewhat questionable in view of the large values of z/D for which the froth regime was actually observed in the work of Heuss, et al.[74]

The potential advantage of froth flow for mass transfer lies in the great amount of interfacial area associated with the froth. The high L/G's, with the consequent high levels of turbulence, may also result in high values of gas- and liquid-phase mass-transfer coefficients.

Heuss, et al.,[37,57] have made the only available study of mass transfer in fully developed froth flow. The "bubble" and plug flow regimes discussed in a mass-transfer study made by Scott and Hayduk[58] were characterized by a discrete gas phase travelling along the top of

their horizontal pipe. Their results, which showed $k_l a$ to be nearly independent of the bubble area, agreed closely with the results of Jepsen for slug-annular flow, and would not be expected to predict mass-transfer coefficients in the hydrodynamically distinct region of fully developed froth flow.

Heuss, et al., have developed correlations to predict $k_l a$, $k_g a$ and the effective interfacial area, based on oxygen and ammonia absorption experiments. From oxygen absorption data at 25°C, k_l was correlated as:

$$\frac{k_l d_{ds}}{D_l} = 0.0316 \left[\frac{DU_{hom}\rho_l}{\mu_l}\right]^{0.9} \left[\frac{1}{R_g}\right]^3 \tag{87}$$

where $k_l d_{ds}/D_l$ and $DU_{hom}\rho_l/\mu_l$ are the dimensionless Sherwood and Reynolds numbers and:

$$d_{ds} = \text{mean "diameter-surface" drop diameter}$$
$$= \frac{\Sigma N_i d_i^2}{\Sigma N_i d_i} \text{ , for a system of Ni dispersed particles} \tag{88}$$

$$U_{hom} = \frac{\frac{L + G}{S}}{\rho_l(1-R_g) + \rho_g R_g} \tag{89}$$

R_g = gas phase holdup (void fraction)

D = pipe diameter .

From ammonia absorption data at 25°C, $k_g a$ was calculated as:

$$k_g a = 0.016\ R_g^2\ U_{hom}^{3.2} \tag{90}$$

where: $k_g a$ = lb moles/hr ft^3 atm .

Interfacial area for a system of dispersed gas bubbles may be expressed as:

$$a = \frac{6R_g}{d_{sv}} \tag{91}$$

where d_{sv} is the mean surface-volume diameter defined by Eq. (53).

James and Silberman[37] have made extensive measurements of bubble sizes and distributions in bubble flow. Based on calculations made with these data, Heuss, et al., concluded that d_{sv} was equal to a bubble diameter exceeded by only 5% or 10% of the bubbles, and was taken to equal d_{95}. d_{ds}, which was found to be equivalent to d_{80} or d_{85}, was taken by Heuss, et al., to be $0.8d_{sv}$. Bubble diameters, corrected for atmospheric conditions (14.7 psia, 70°F) were correlated by James and Silberman for data in 2-1/2-inch and 4 inch pipes using a dimensionless bubble diameter, d', to yield

$$d' = V_1 \, d_{atm}(\rho_1/\sigma D)^{1/2} \quad . \tag{92}$$

A plot of d_{atm} vs. $D^{1/2}/V_1$ is shown in Fig. 11 for d_{50} and d_{95}.

The value of d_{sv} has been found to be a function of the void fraction in the system. For a case of small relative velocities between phases, Vermeulen, Williams and Langlois[59] found d_{sv} proportional to $R_g^{1/3}$. d_{sv} may also have to be corrected for slugging and wall effects.

The temperature dependence of $k_g a$ and $k_l a$ were measured by Heuss, et al., with the result

$$k_g a \sim e^{-(0.01 \pm 0.008)T} \quad \text{For } T = 17.7 \text{ to } 28.4°C \qquad (93)$$

$$k_l a \sim e^{+(0.042 \pm 0.008)T} \quad \text{For } T = 19 - 34°C \qquad (94)$$

(T = °C) .

a. Froth flow contactor--CO_2 absorption. i. Design considerations. As noted in Section IV-B-2-b, the flow rates present in the single-contactor absorption of CO_2, together with the physical properties of the system, predict the existence of froth flow. Because of the lower L/G's obtained by using multiple contactors, froth flow cannot be obtained in this case unless the absorbent is recycled. The flow diagram for this recycle system, together with the recycle rates necessary to produce froth flow in each of the multiple reactors and the resultant liquid composition, is shown in Fig. 12. The recycle ratios indicated by this configuration are on the order of 10:1. To insure a sufficient gas mass velocity per unit area, diameters of 0.502 feet, 0.9441 feet and 0.7131 feet were selected for the single, high- and low-CO_2-partial-pressure contactors respectively. These diameters were near the maximum possible, while still maintaining froth flow, in order to keep the two-phase pressure drop to a minimum. The region of the Baker correlation to which these flow rates and diameters correspond is shown in Fig. 14.

Pressure drop and void fraction were calculated by the Hughmark methods.[44,47]

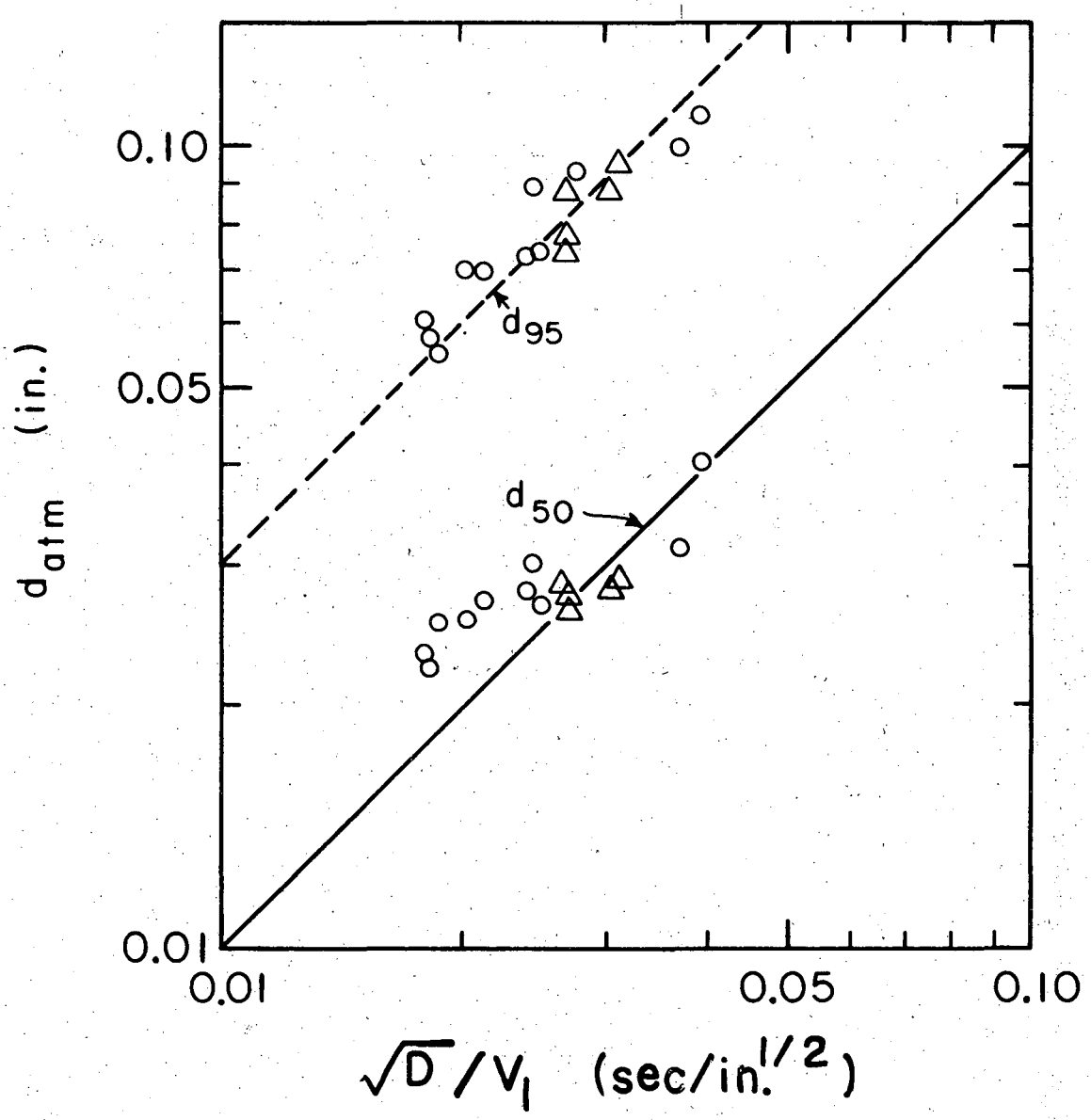

XBL 695-591

Fig. 11. Bubble diameter vs. $(D)^{1/2}/V_1$; James and Silberman data; 0, 2-1/2 in. pipe; Δ, 4 in. pipe.

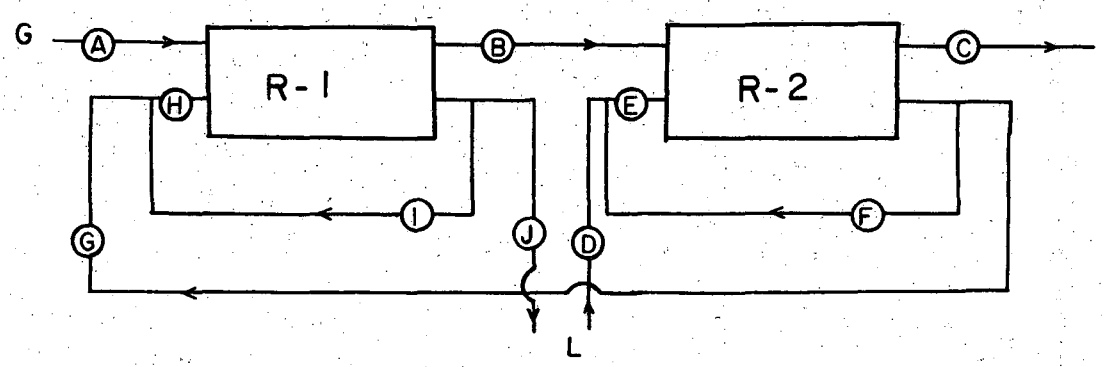

XBL 695-566

Gas Flows and Compositions (A,B,C): See Table 1.B.

Liquid Flows and Compositions

Stream	Flow Rate (lb/hr)	Composition (standard Cubic Feet CO_2/gallon)
D	183,430	2.00
E	1,090,400	2.81
F	906,980	2.97
G	183,430	2.97
H	1,817,300	5.13
I	1,633,900	5.37
J	183,430	5.37

Fig. 12. Flow diagram for absorption of CO_2 in two froth-flow contactors.

The rate equation for the froth-flow system was identical to that used for the CO_2 co-current packed column, Eq. (52).

The mass-transfer coefficients were calculated using the correlations of Heuss, et al. The value of d_{95}, corrected for atmospheric conditions, was obtained using Fig. 11. This value of d_{95} corresponded to data obtained by James and Silberman for void fractions less than 0.1. Assuming d_{sv} to be proportional to $R_g^{1/3}$, d_{sv} was calculated from d_{95} by

$$d_{sv} = (R_g/0.1)^{1/3}\, d_{95} \tag{95}$$

d_{ds} was taken equal to 0.8 d_{sv}. Using physical properties for the CO_2 system corrected for atmospheric conditions, k_1 was calculated using Eq. (87), and was corrected for the system temperature by Eq. (94), with the assumption made that this temperature correction was valid beyond the range of the work of Heuss, et al.

$k_g a$ was calculated from Eq. (90), based on a void fraction corresponding to process conditions. This correlation does not include the effects of physical properties or pressure. It was assumed that Eq. (46), used to correct for gas properties in a packed column, might represent an adequate correction and was used, along with Eq. (93), to correct for system properties at constant temperature and pressure.

Interfacial areas were calculated from Eq. (91), based on the void fraction corresponding to process conditions and values of d_{sv} corresponding to atmospheric conditions. Because the values of k_1 calculated were so large that $\eta = (k_1^2 + D_1 k_2 C_o)^{1/2} \cong k_1$, Eq. (94),

applied to k_1, was assumed to account for the effects of temperature on both k_1 and a. Although pressure would be expected to effect interfacial area, because of its effects on R_g and d_{sv}, the nature of this effect was unknown and, hence, neglected.

ii. Calculation. The design equation was numerically integrated, using Simpson's rule. Average flow rates and values of the transport coefficients were used. The method of solution is similar to that discussed for the co-current packed column for CO_2 absorption, discussed in Appendix XI.

iii. Observations. The results of the calculation are shown in Table 7. The values of the physical mass transfer coefficients, k_1, were so large that $k_1^2 >> D_1 k_2 C_o$, so that $\eta = (k_1^2 + D_1 k_2 C_o)^{1/2} \cong k_1$. As a result of this decreased resistance to mass transfer in the liquid phase, the extent of gas phase control, related to the magnitude of the term $1 + aH\eta/k_g a$ in Eq. (52), was substantial. The value of the term ranged from 1.57 in the single contactor to 7.91 and 4.93 in the high- and low-CO_2-partial-pressure contactors. These values may be compared to the range of 1.07 to 1.28 calculated for the co-current packed column cases, where the values of k_1 calculated were small.

b. Froth-flow contactor--HCl absorption. i. Design considerations. Because of the relatively low L/G's encountered in HCl absorption, froth flow is not possible without a high recycle of absorbent. Operating an HCl-absorption system with an externally cooled recycle stream will have the effect of making the process more nearly isothermal than was possible without this recycle, because of the larger liquid rate and the

Table 7. Froth flow contactor--CO_2 absorption.

	Single contactor	High-CO_2-partial-pressure contactor	Low-CO_2-partial-pressure contactor
Diameter	0.502 ft	0.944 ft	0.713 ft
Total $\overline{L}$	618,000 lb/hr	1,817,300 lb/hr	1,090,400 lb/hr
$\overline{G}$	5445 lb/hr	6583 lb/hr	3015 lb/hr
U_{hom}	41.0 ft/sec	19.5 ft/sec	24.2 ft/sec
k_l	5.97 cm/sec	8.55 cm/sec	7.46 cm/sec
†$k_g a \times 10^4$	9.84	0.51	1.09
a	17.95 cm^{-1}	7.29 cm^{-1}	10.95 cm^{-1}
R_l	0.28	0.49	0.58
$\Delta P/\Delta L$	0.100 psi/ft	0.017 psi/ft	0.025 psi/ft
Height	11.9 feet	2.6 feet	5.5 feet
ΔP	1.19 psi	0.045 psi	0.137 psi

†gm moles/sec cm^3 atm

consequently smaller change in liquid composition through the contactor. As the process becomes more isothermal, the outlet liquid concentration of HCl will be higher, possibly obviating the necessity of multiple staging to produce HCl of commercially valuable strength.

Because the recycle ratios required to produce froth flow are of the order of 100, the process was considered to be isothermal for the purpose of calculation. It was also assumed that the amount of water vaporized would be negligible. Calculation was limited to the single absorber. The gas and liquid flow rates and compositions consistent with the above assumptions, together with the recycle flow rate necessary to insure froth flow, are shown in Fig. 13. A diameter of 0.874 feet was chosen to insure froth flow.

The pressure drop and void fraction were calculated by the Hughmark[44,47] methods.

The form of the rate equation is identical to Eq. (24) for HCl absorption in a co-current packed column.

The value of $k_g a$ was calculated using Eq. (90) and was corrected for physical properties, temperature and pressure by Eqs. (46) and (93). The liquid-phase resistance to mass transfer was neglected.

ii. Calculation. An value of $K_g a_{HCl}$ based on average flow conditions and void fraction was used to calculate the length of the contactor. Since only the concentration of HCl was assumed to be changing in the gas phase, the design equation was re-written as

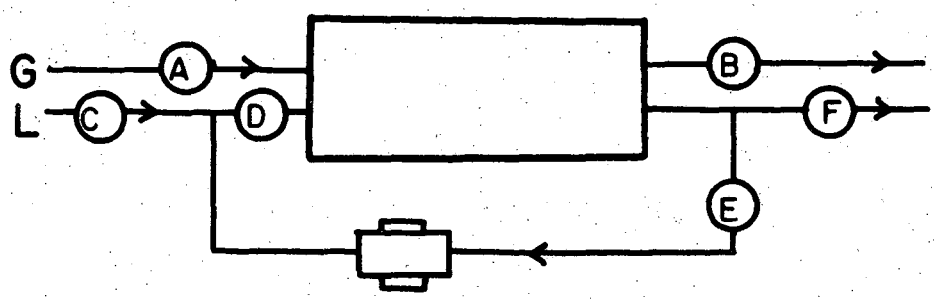

XBL 695-565

Gas Flow Rates and Compositions (A,B): See Table 8.

Liquid Flow Rates and Compositions

Stream	Flow Rate (lb/hr)	Composition (wt. frac. HCl)
C	3826	0.050
D	1,839,000	0.2545
E	1,834,000	0.2550
F	4879	0.2550

Fig. 13. Flow diagram for HCl absorption in froth-flow contactor.

$$Z = \int_{y_{HCl,1}}^{y_{HCl,2}} \frac{d(G_m y_{HCl})}{K_g a_{HCl} SP(y_{HCl} - y^*_{HCl})} = \frac{GI}{K_g a_{HCl} SP} \int_{y_{HCl,1}}^{y_{HCl,2}} \frac{d\left[\frac{y_{HCl}}{(1 - y_{HCl})}\right]}{(y_{HCl} - y^*_{HCl})} \tag{96}$$

where: GI = molar flow rate of gaseous inerts, lb moles/hr

G_m = total molar gas flow rate, lb moles/hr

$K_g a$ = lb moles/ft^3 atm hr

S = ft^2

P = atm

Z = ft .

Because, as seen in Fig. 13, the concentration of HCl in the liquid does not change appreciably in the contactor, y^*_{HCl} may be considered effectively constant, and equal to the gas composition in equilibrium with the outlet liquid. Given this assumption, Eq. (96) may be integrated analytically, with the result

$$Z = \frac{GI}{K_g a_{HCl} SP} \left[\frac{1}{1 - y^*}\right]^2 \left[\frac{1 - y^*}{1 - y_2} - \frac{1 - y^*}{1 - y_1} + \ln \frac{(y_2 - y^*)(1 - y_1)}{(y_1 - y^*)(1 - y_2)}\right] . \tag{97}$$

The value of the integral in the last term of Eq. (96), with $y_1 = 0.20$, $y_2 = 0.01$ and $y^* = 0.005$ is 4.16.

iii. Observations. As shown in Fig. 13 and Table 8, the outlet absorbent concentration produced in the HCl froth-flow device is about 25.5% by weight. This concentration compares favorably with the outlet concentration of about 28% obtained in the multiple-contactor schemes, such as were discussed in conjunction with absorption in co-current packed columns and annular-flow contactors, and is considerably greater than the concentration of 18.4% which may be produced in a single contactor without recycle. This results from the effect of the large recycle rate in keeping the process nearly isothermal. This scheme may represent an approach, simpler than multi-staging, to the problem of producing an absorbent of commercially valuable strength, if the recycle pumping costs are not prohibitive.

C. Dispersed Phase Systems

1. General Considerations

In the packed column and two-phase flow contactors, mass transfer is greatly enhanced by the dispersion of gas-in-liquid or liquid-in-gas which results because of the hydrodynamic conditions or mechanical features, such as packing, inherent to the specific device and/or pattern of flow. A number of contacting devices have mechanical features specifically designed to create gas-in-liquid or liquid-in-gas dispersions, with consequent high interfacial areas.

Various types of spray absorbers are in limited commercial use. The principle types of these absorbers are spray columns, cyclonic (or centrifugal) spray devices and venturi devices. Each of these devices is characterized by a relatively high liquid pumping or gas compressor

Table 8. Froth flow contactor--HCl absorption.

Diameter = 0.874 feet

		Inlet				Outlet		
		lb/moles/hr	lb/hr	Mole %		lb moles/hr	lb/hr	Mole %
	HCl	30.08	1097.2	20.0	HCl	1.22	44.3	1.0
	H_2O	1.28	23.1	0.8	H_2O	1.28	23.1	1.0
Gas Flow	H_2	6.02	12.2	4.0	H_2	6.02	12.2	5.0
	Air	113.00	3273.7	75.1	Air	113.00	3273.7	93.0
	Total	150.38	4406.2	99.9	Total	121.52	3353.3	100.0

	Inlet	Outlet
Temperature	30.0°C	30.0^{+}°C
Net liquid flow	3826.4 lb/hr	4879.3 lb/hr
Net liquid composition	5.0 w/o HCl	25.5 w/o HCl
†Total liquid flow	1,839,000 lb/hr	1,840,000 lb/hr
†Total liquid composition	25.45 w/o HCl	25.50 w/o HCl

R_1	0.407
$\Delta P/\Delta L$	0.057 psi/ft
$K_g a_{HCl}$	145.8 lb moles/hr ft^3 atm
Height	5.7 ft
ΔP	0.33 psi

†Flow and composition in contactor.

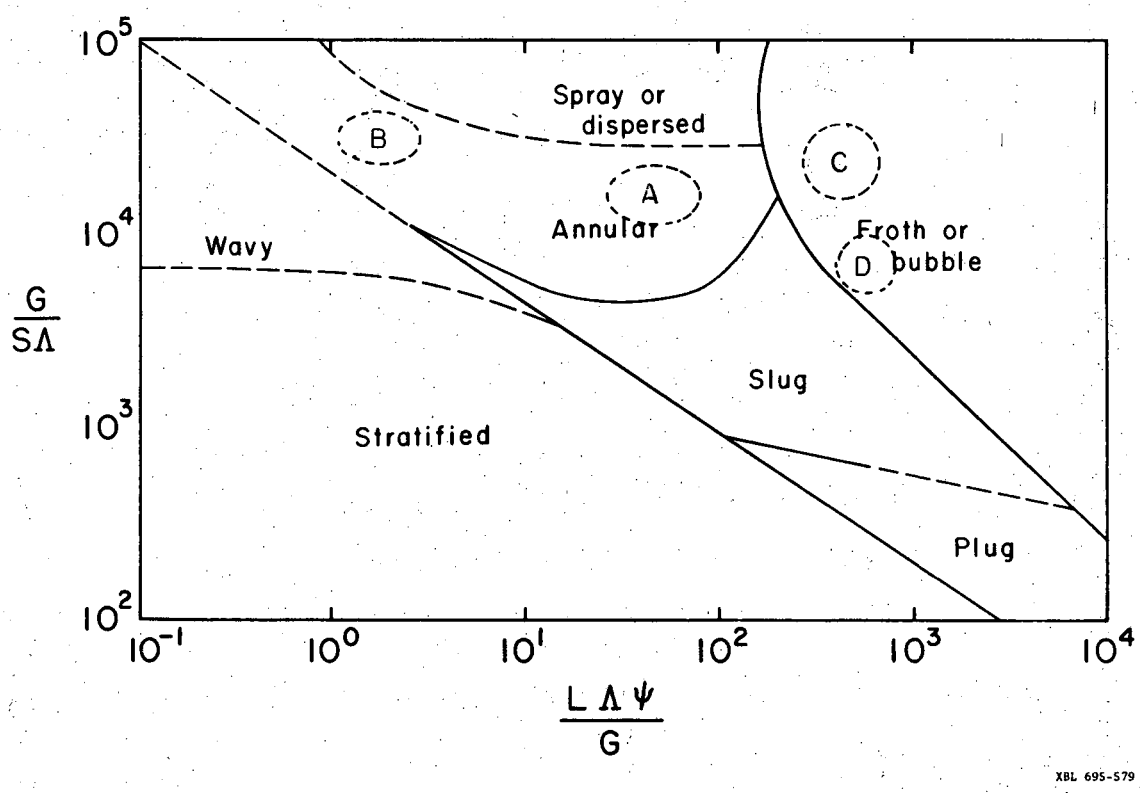

A: Annular flow, CO_2 absorption

B: Annular flow, HCl absorption

C: Froth flow, CO_2 absorption

D: Froth flow, HCl absorption

Fig. 14. Regions of Baker correlation to which open pipe contactor designs correspond.

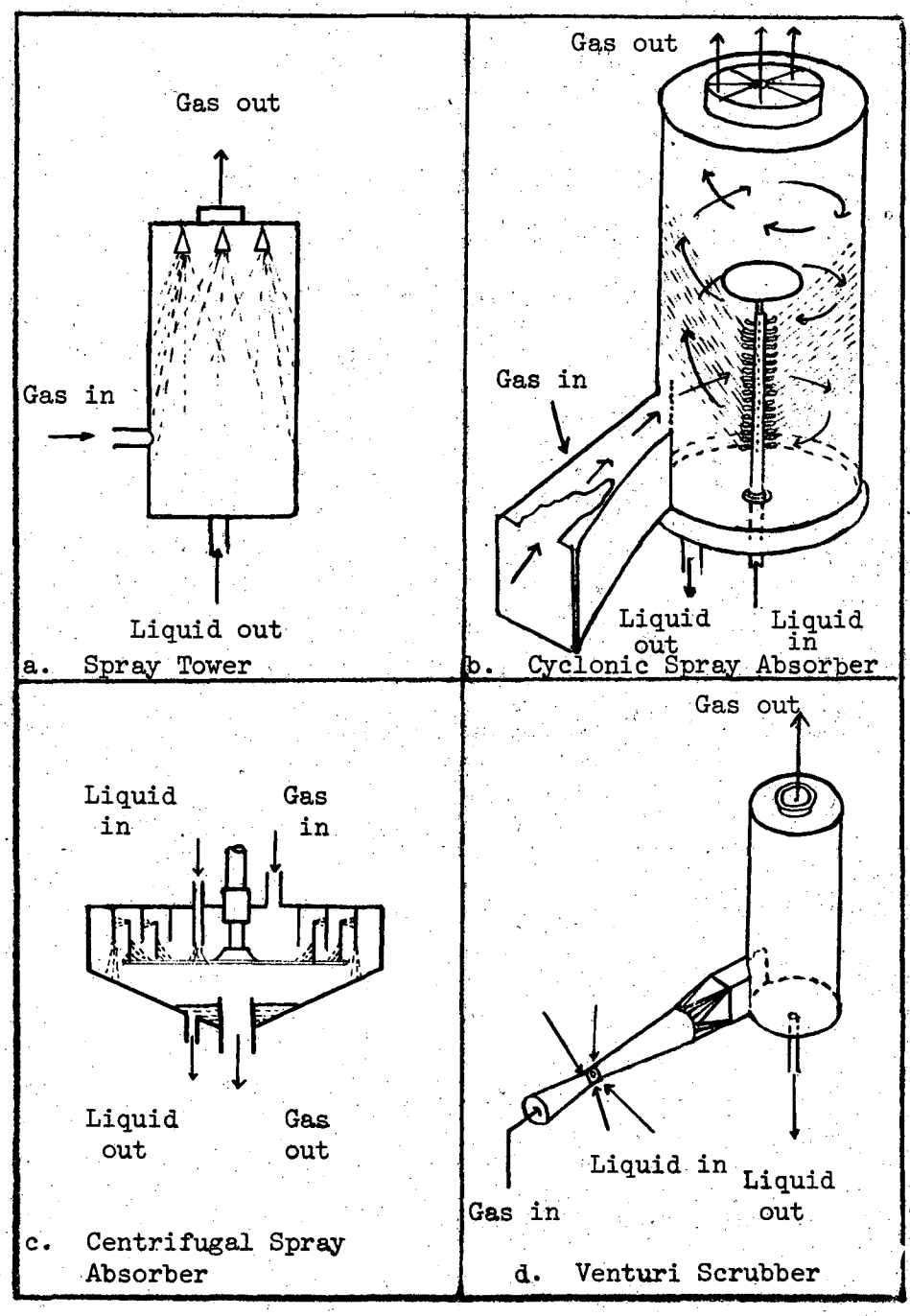

XBL 695-569

Fig. 15. Dispersed-phase contacting devices.

requirement, a great possibility of entrainment of liquid droplets in the process gas stream and a limited number of equilibrium stages per device, resulting either from the configuration of the equipment or a high degree of mixing in the gas phase. General discussions of spray absorption systems have been presented by Perry,[28] Sherwood and Pigford[61] and Strauss,[62] and a summary of literature relevant to specific devices has been compiled by King.[60]

A typical spray-tower configuration is shown in Fig. 15a. Variations of this configuration have been proposed in line with the observation that the rate of absorption at the drop surface is most rapid immediately after the droplets are formed.[61] The mass-transfer characteristics of the spray tower are discussed more fully in the following section.

Two basic types of centrifugal absorbers are shown in Fig. 15 b,c, which represent schematically apparatus used by Johnstone and Kleinschmidt[63] and discussed by Nonhebel.[64] The gas rates used in such absorbers can be greatly increased over the maximum in a spray tower because the liquid is forced to impinge either on the wall or on the vanes of the apparatus and descend, thereby greatly decreasing the amount of entrainment. A further advantage, particularly of the device depicted in Fig. 15c, is that a secondary impact spray may result as the primary spray hits the vanes of the rotor. This secondary impact spray is finer than the primary spray, and the continuous regeneration of fine spray greatly enhances the rate of mass transfer.

In a venturi device, Fig. 15d, the dispersion of droplets may be accomplished either by injecting a liquid stream at a point preceding the throat or by taking advantage of the reduced pressure and high level of turbulence in the venturi throat to provide both the pumping power and the dispersing mechanism. In either case, the primary pressure drop occurs in the gas phase, as contrasted to the spray tower and centrifugal absorber, in which the major pressure drop is associated with the liquid phase. The venturi is limited to applications characterized by low liquid-to-gas ratios.

Another form of the venturi device, sometimes called a jet scrubber, has been used to produce gas-in-liquid dispersion, and is identical to the venturi depicted in Fig. 15d, except that the gas and liquid streams are interchanged. An apparatus of this type has been studied by Bauer, Fredrickson and Tsuchiya.[65] The low pressure at the throat may be used to pump the gas, which is dispersed by the high shearing forces present in the venturi throat. The majority of the mass transfer was found to occur in or near the venturi throat. This apparatus is limited to applications with very low gas to liquid ratios, such as reducing the anaerobic bacteria content in a liquid stream by the introduction of oxygen.

2. Spray Towers

The potential attractiveness of spray towers as absorption devices lies in the great amount of surface area associated with the sprayed droplets, the high degree of turbulence which may exist within these droplets and the low gas-phase pressure drop.

The most comprehensive study of mass transfer in a spray tower has been presented by Pigford and Pyle.[66] Data were obtained for ammonia absorption, oxygen desorption and air dehumidification with several types of spray nozzles in counter-current spray towers of different heights and diameters. The number of transfer units, for the liquid- and gas-phase-controlled mass-transfer systems, was measured as a function of the liquid and gas rates in the columns. The lengths of the transfer unit, LTU_l or LTU_g, may be determined from the reported values of NTU_l and NTU_g by

$$LTU_l = (\text{tower height})/NTU_l \tag{98}$$

$$LTU_g = (\text{tower height})/NTU_g \tag{99}$$

where

$$LTU_l = L/k_l aS\rho_l \tag{100}$$

$$LTU_g = G/k_g aMSP \tag{101}$$

$$NTU_l = \int \frac{dC}{C^* - C} \tag{102}$$

$$NTU_g = \int \frac{dy}{y - y_i} \tag{103}$$

and L and G are the liquid and gas mass flow rates, S is the tower cross sectional area and M is the molecular weight of the transferred species.

Based on the measured drop size distributions from specific nozzles reported by Pigford and Pyle, it is possible to predict the interfacial area.

Certain cautions must be exercised in using the data of Pigford and Pyle. The degree of droplet turbulence is greatest immediately after their formation, and the rate of interfacial mass transfer is consequently greatest in the vicinity of the nozzles. Hence, the number of transfer units is not directly proportional to the tower height. This is especially true in a situation with liquid-phase-controlled mass-transfer, where the rate of circulation is an important mass-transfer consideration. A substantial amount of liquid was found to hit the walls of the tower before reaching its base. This implies that the actual effective area for mass transfer may be considerably less than that predicted using drop-size distribution data. Lastly, although the flow pattern of Pigford and Pyle's experiments was counter-current, a considerable amount of mixing of the gas in the axial direction would have occurred, resulting in a situation far removed from true, counter-current performance in terms of the mass-transfer driving forces provided. Pigford and Pyle evaluated NTU's corresponding to the assumption of no axial mixing in either phase, and their data must be interpreted accordingly.

The computational study of the attractiveness of spray towers was limited to a consideration of the spray tower for CO_2 absorption. The spray tower has been suggested as a promising device for the absorption of HCl,[66] but because of the complex heat-transfer effects which need to be considered, the calculation was not made.

3. Spray Tower--CO_2 Absorption

a. Design considerations. Spray columns for the Vetrocoke absorption process were designed assuming plug co-current and counter-current flow and co-current flow with a completely axially-mixed gas phase. Only the multiple-contactor system was considered.

To operate a spray column counter-currently, the gas rate must be low enough to prevent excessive entrainment of liquid and the liquid rate must be low enough to prevent excessive formation of turbulent eddies in the gas phase which would prevent the upward flow of gas. Based on the data of Pigford and Pyle, the limiting gas rate is apparently of the order of 800 lb/hr ft^2 at atmospheric pressure. The limiting liquid rate may be estimated qualitatively using a procedure discussed by Foust, et al.,[35] based on a model of an infinite system of equal-sized spheres and a slip velocity based on the minimum free cross section at the stream section containing the particle. Using this analysis, with the gas and liquid flow rates determined for the multiple CO_2 reactors, it was concluded that counter-current flow was feasible for this situation.

To calculate the interfacial area associated with a stream of falling droplets, the relative, or slip, velocity between phases must be known. Liquid droplets will reach a terminal velocity, V_t, which is related to the droplet dimensions and the physical properties of the surrounding gas. For spherical droplets, the terminal velocity may be written as

$$V_t = \sqrt{\frac{4(\rho_l - \rho_g)g_c D_p}{3C_D \rho_g}} \tag{104}$$

where C_D is the drag coefficient. The drag coefficient, C_D, has been plotted as a function of the Reynolds number, $D_p V\rho/\mu$, with the sphericity of the particles as a parameter.[35] The slip velocity for counter-current flow is defined, with reference to the dispersed component, as

$$V_{sl} = V_t - V_g \quad . \tag{105}$$

For co-current flow, the definition is

$$V_{sl} = V_t + V_g \quad . \tag{106}$$

It was assumed that the nozzles were Sprayco-5B nozzles, as used in many of Pigford and Pyle's experiments. Based on the mean surface-diameter drop diameter from these nozzles reported by Pigford and Pyle, the volumetric flow rate of the liquid and the slip velocity, the drop surface area per unit tower volume can be calculated.

Column diameters were chosen to make the gas mass velocity 300 lb/ft^{2}hr, corresponding to diameters of 5.287 feet and 3.566 feet for the high and low CO_2 partial-pressure contactors respectively. At these diameters, the liquid flow rate was beyond the range of liquid flow rates covered by the Pigford and Pyle data, making it impossible to predict LTU directly. However, values of LTU were calculated from NTU data obtained in a 52-inch tall, 31.5-inch diameter column using Eq. (98) for a gas rate of 300 lb/hr ft^2 and several liquid rates. The

value of k_1a was calculated as $L/(LTU)S\rho_L$, and k_1 was extracted from the values of k_1a obtained using values of interfacial area calculated on the basis of a slip velocity, liquid flow rate and column diameter of the Pigford and Pyle experiments. A weighted area was used based on the fact that at this gas velocity, about two-thirds of the liquid collected at the bottom of the column was taken off the wall. In the range studied by Pigford and Pyle, a plot of k_1 against log L was linear. Extrapolating this plot to the value of L in the CO_2 absorption process, a value of k_1 was obtained. It was found that $k_1^2 << D_1k_2C_o$, so that for this pseudo first-order chemical absorption process, an accurate knowledge of the value of k_1 was unnecessary, as long as the order of magnitude of the value obtained by the above procedure is correct.

For the Vetrocoke design problem, it was desired to correct the interfacial areas estimated on the basis of the slip velocities for inpingement of droplets on the wall. This effect is a complex function of the arrangement of the nozzle, the nozzle characteristics and the column diameter. Pigford and Pyle found that the number of transfer units measured in a 31.5-inch versus a 12-inch column increased by a factor of about 1.33, or approximately as $(\text{diameter})^{0.3}$. Since in a 31.5-inch column approximately two-thirds of the liquid was collected off the wall, it was assumed that

$$a = \frac{a'(D/31.5)^{0.3}}{3} + a_w \qquad (107)$$

where: a' = predicted area, based on slip velocity and droplet size distribution data

a = corrected effective interfacial area

a_w = column wall area/unit volume

D = tower diameter, inches.

The effect of gas-phase resistance to mass transfer was ignored.

b. Calculation. The mass balance for the Vetrocoke absorption process--Eq. (52) with the gas-phase resistance to mass transfer considered negligible--was numerically integrated, using Simpson's rule. Average values of the flow rates were used for the calculation. The liquid flow rate and, hence, change in composition for the counter-current case were taken to be the same as for the co-current case. For the co-current case in which the gas phase was axially well-mixed, it was assumed that the gas composition was everywhere equal to the outlet composition.

c. Observations. The results of the calculation are shown in Table 9. Although the lowest tower heights were those calculated assuming counter-current plug flow, this result is probably over-optimistic, because of the axial-gas-phase-mixing problems which would be met in a counter-current spray tower--especially with liquid rates of the magnitude of those considered in this study. The effect of assuming an axially well-mixed gas phase is to increase the necessary tower heights severely, especially in the low-CO_2-partial-pressure tower. Since the problem of axial mixing would not be expected to be as great in a co-current spray tower, the sizes calculated assuming

co-current plug flow probably represent the most reasonable estimate of the necessary spray tower size for this process.

Table 9. Spray tower--CO_2 absorption.

	High-CO_2-partial-pressure tower	Low-CO_2-partial-pressure tower
Diameter	5.29 ft	3.57 ft
$\overline{L}$	183,430 lb/hr	183,430 lb/hr
$\overline{G}$	6583 lb/hr	3015 lb/hr
V_l	0.031 ft/sec	0.067 ft/sec
V_g	0.453 ft/sec	0.848 ft/sec
V_t	2.053 ft/sec	6.082 ft/sec
(1) a	3.07 cm^{-1}	1.78 cm^{-1}
Height	3.3 ft	22.8 ft
(2) a	1.96 cm^{-1}	1.35 cm^{-1}
Height	6.0 ft	34.1 ft
(3) a	1.96 cm^{-1}	1.35 cm^{-1}
Height	13.9 ft	199.2 ft

(1) counter-current plug flow

(2) co-current plug flow

(3) co-current flow; gas phase perfectly well-mixed axially

V. EVALUATION AND CONCLUSIONS

A. General Considerations

An accurate analysis of the attractiveness of a device for absorption is a complex task, intimately related to the specific process being considered. The primary investment costs associated with a typical absorption system, including the regenerator, may be itemized as

(1) The cost of the absorber shell.

(2) The cost of the regenerator shell.

(3) The costs of absorber and regenerator internals, such as packing or plates, and external devices, such as entrainment separators and nozzles, necessary for the practical utility of the devices.

(4) The costs of liquid pumps, gas compressors, external heat exchangers and piping.

(5) Initial absorbent and catalyst (when used) costs.

Typical operating costs may be listed as:

(1) Costs of power for running the pumps and compressors.

(2) Costs associated with steam which may be required for regeneration purposes.

(3) Costs of coolants used in heat exchangers.

(4) Make-up absorbent and catalyst costs.

The task of comparing various absorption devices may be simplified if some of the operating or investment costs may be assumed constant--i.e., independent of the specific device used--or of negligible importance in the over-all economics of the operation. It may be complicated if, as in the case of HCl absorption, the product absorbent may have commercial value.

An approach to the general comparison of absorption devices has been proposed by Lunde.[69] By investigating the relation between the over-all mass-transfer coefficient and the variables of gas and liquid flow rate and pressure drop, the number of transfer units, defined by Eqs. (102) and (103), may be related to the power consumptions associated with the gas and liquid phases and the size of the device. This analysis was carried out by Lunde for packed columns, spray towers, venturi-devices and cyclonic scrubbers for systems in which the majority of resistance to mass transfer was in the gas phase. A comparison was made between devices on the basis of the number of transfer units obtainable per unit of power consumed in the gas or liquid phase.

A greatly simplified approach was used in this investigation to compare the contactors studied with each other, and, where possible, with devices currently used to carry out the absorption processes. After eliminating from consideration items that would be constant for all devices or would be expected to have small influence on the over-all economics of the process, quantities characteristic of investment and operating costs were assigned to each device. These cost functions may be displayed on graphs, with axes representative of the ranges of operating and investment variables encountered. Graphs of this nature are shown in Figs. 16 and 17.

Generally, points nearest the origin represent the lowest capital and operating costs, and would be associated with the most attractive devices. In economic optimization studies, there is frequently a trade-off between operating and capital costs for a

given device associated with the variation of a parameter such as column diameter. If sufficient data of this nature were available, a family of hyperbola-like curves--each characteristic of a specific device--convex to the origin, might be expected. The curves closest to the origin would represent the best devices. In this study, results sufficient to evaluate the trade-off between operating and capital costs were limited to the studies of co-current packed columns. For other devices, such studies were difficult to make. For example, the variation of pipe diameter in co-current pipe flow might result in changing the flow regime to one not applicably treated by the mass-transfer mechanism assumed.

Although no set of curves was obtainable, the points closest to the origin will still represent better devices. To give an indication of the relative importance of distance from the origin in the x and y directions, an assignment of cost values to the investment and operating variables must be made. As an example, the material required in Vetrocoke absorbers is low cost carbon steel, since the catalyst tends to eliminate the corrosive characteristics of potassium carbonate. Hydrogen chloride, on the other hand, is extremely corrosive, and expensive materials, such as graphite, must be used. For a given energy requirement, the capital costs per unit shell volume of a Vetrocoke absorber would be less important than the corresponding costs for an HCl absorber.

Because the purpose of this investigation was only to give a general indication of the competitive characteristics of various devices, the problems of cost assignment were not considered.

B. CO_2 Absorbers

1. Basis of Evaluation

The results of the calculations to determine the sizes of and pressure drops through co-current packed columns, annular- and froth-flow open-pipe devices, and spray towers appear in Tables 4, 5, 7 and 9. For the cases of the co-current packed column, annular-flow contactor and spray column, results based on different mass-transfer models are shown to give an indication of the sensitivity of the calculated size requirements to the assumptions inherent in the various models. The difficulties in selecting the correct model have been outlined. However, in order to be able to compare the devices, some selection must be made, and an effort was made to select the most reasonable models as a basis of comparison. Since the model selected was generally an optimistic one, if the device based on this selection appeared favorable, consideration was made of the effects on operating and investment requirements of assuming the device was actually characterized by a less optimistic model.

The choices made were:

(1) For the co-current packed columns, the vessel sizes calculated using interfacial areas based on the energy-dissipation model were selected. This model was felt to represent a more realistic approach to the problem of defining interfacial area than merely assuming it to be constant and equal to the packing surface area.

(2) For the annular-flow contactors, a vessel size corresponding to the driving force $C_e - C_a$ being 50% of that which would exist if the

droplets were in equilibrium with the gas was selected. The case with the driving force 10% of the equilibrated driving force was also considered.

(3) For the spray tower, the size based on co-current plug flow was selected, since the size was comparable to that calculated assuming counter-current plug flow and the actual mass-transfer situation would not be expected to be as bad as the case corresponding to an axially perfectly mixed gas phase.

It was assumed that the absorber used by Phillips Petroleum to carry out the Vetrocoke absorption process was a counter-current sieve-tray column. The number of trays necessary to effect the desired purification was taken to be the same for the scaled down gas and liquid flow rate case as in the full-scale absorber. The number of trays was estimated from a known number of 25 trays in the lower section of the swaged column used and an estimated number of 7 trays in the upper portion. Based on the number of trays and an estimated tray spacing of 24 inches, the height of the column was calculated to be 66 feet. The diameters of the upper and lower sections of the column, corresponding to the scaled gas and liquid rates, was estimated by procedures outlined by Fair,[70] with the assumptions that

(1) The gas velocity to be used was 75% of the flooding velocity.

(2) The active tray area was equal to 88% of the total tray area.

The column diameters calculated were 1.5 feet in the upper (15 feet) section, where the absorbent flow rate was about 60 GPM, and 2.6 feet in the lower (51 feet) section, where the absorbent flow rate was about 360 GPM. The pressure drop through the column was assumed to be 5 psi, based on the pressure drop measured in the Phillips absorber.

The capital requirements of the absorbers were assumed to be directly proportional to the internal surface areas--excluding heads--of the devices. This assumes constant wall thickness and negligible cost of absorber internals and heads, and is consistent with a procedure used by Riess.[20] The costs of such auxilliary equipment as nozzles and entrainment separators were neglected, since they would be similar for all of the devices.

If the outlet absorbent flow rates and concentrations were in all cases the same, the costs of the regenerator could be assumed constant and neglected. Similarly, the reboiler steam requirements could be neglected. However, the effect of multi-staging is to reduce greatly the necessary absorbent flow rate and, because the amount of CO_2 scrubbed is the same, increase the concentration of the absorbent entering the regenerator. With two contactors, the necessary absorbent flow rate was similar, and, in fact, less than that used in the Phillips process (scaled). The effect of the greater flow rate in the single-contactor case would be to increase the necessary regenerator diameter but, because the absorbent concentration change would be less, might also be to decrease its height, depending on the change in the mass-transfer coefficients. Because of these compensating effects, and because consideration of the stripper is a major problem in itself, the investment costs associated with the regenerator were neglected. The effect on steam consumption and the capital and operating costs associated with the heat exchangers used to cool the absorbent stream should still be considered but because the multiple-contactor cases, in which the

regeneration and cooling requirements would be less, appeared more favorable than the single-contactor cases without consideration of these factors, the steam and exchanger costs were neglected.

The operating variables considered were those associated with pumping the liquid stream and compressing the gas. These variables were expressed as energy requirements per hour, or KWH/hr.

The pumping requirements considered were those associated with pumping the liquid from the regenerator to the absorber and with recirculating the absorbent in the froth-flow devices. For purposes of comparison, the kinetic energy and frictional losses in the external piping were assumed to be independent of the particular contactor used and were, consequently, neglected. The energy requirement was then described by

$$-W_f = \frac{\Delta P}{\rho_l} + \frac{g\Delta z}{g_c} \quad \frac{\text{ft lb}_f}{\text{lb}_m} \tag{108}$$

Δz represents the height to which the liquid must be pumped, and was assumed equal to the column height (zero for the horizontal absorbers). ΔP represents the difference in pressure between the regenerator (22.7 psia) and the absorber (140 psia) or, in the case of the froth-flow-device re-circulation pump, the pressure drop through the device. An additional pressure drop of 10 psi was assumed through the nozzles of the spray tower. The power requirement is expressed as

$$\text{Power} = \frac{(L)(-W_f)(1.3558\times10^{-3})}{3600} \text{ KWH/hr} \tag{109}$$

in which L is the mass liquid flow rate, lb/hr.

The pressure drop through the absorbers would be reflected by a gas-compressor requirement. In an actual hydrogen plant, this compression might be done at the beginning of the process, before the reformer, where the pressure is about 235 psia. The pressure drop might also be reflected in an increased compression requirement at the tail-end of the process, in conjunction with preparing the process stream for an application such as the synthesis of ammonia. The compressor requirement would be different in each case because of the differences in gas composition and percentage increase in gas pressure. In this study, it was desired to circumvent these process considerations, while still assigning an operating variable to reflect the pressure drop through the contactor. To this end, a compressor was assumed to exist immediately after the absorber, compressing the gas of outlet composition from the outlet pressure, P1 to a pressure equal to the pressure of the gas stream entering the absorber, P2. A constant value for P1 of 135 psia was assumed, and P2 was calculated as P1 plus the two-phase pressure drop in the column. The compression was assumed, for simplicity, to be isothermal, for which the power requirement may be written as[75]

$$\text{Power} = \frac{(G)(P1)}{3600\ \rho_g} \ln(P2/P1)(1.3558\times10^{-3}) \quad \text{KWH/hr} \quad . \qquad (110)$$

Perfectly efficient pumps and compressors were assumed.

2. Results

The conclusions regarding the utility of the devices studied as possible alternatives to the sieve-tray column may be made with reference to Fig. 16.

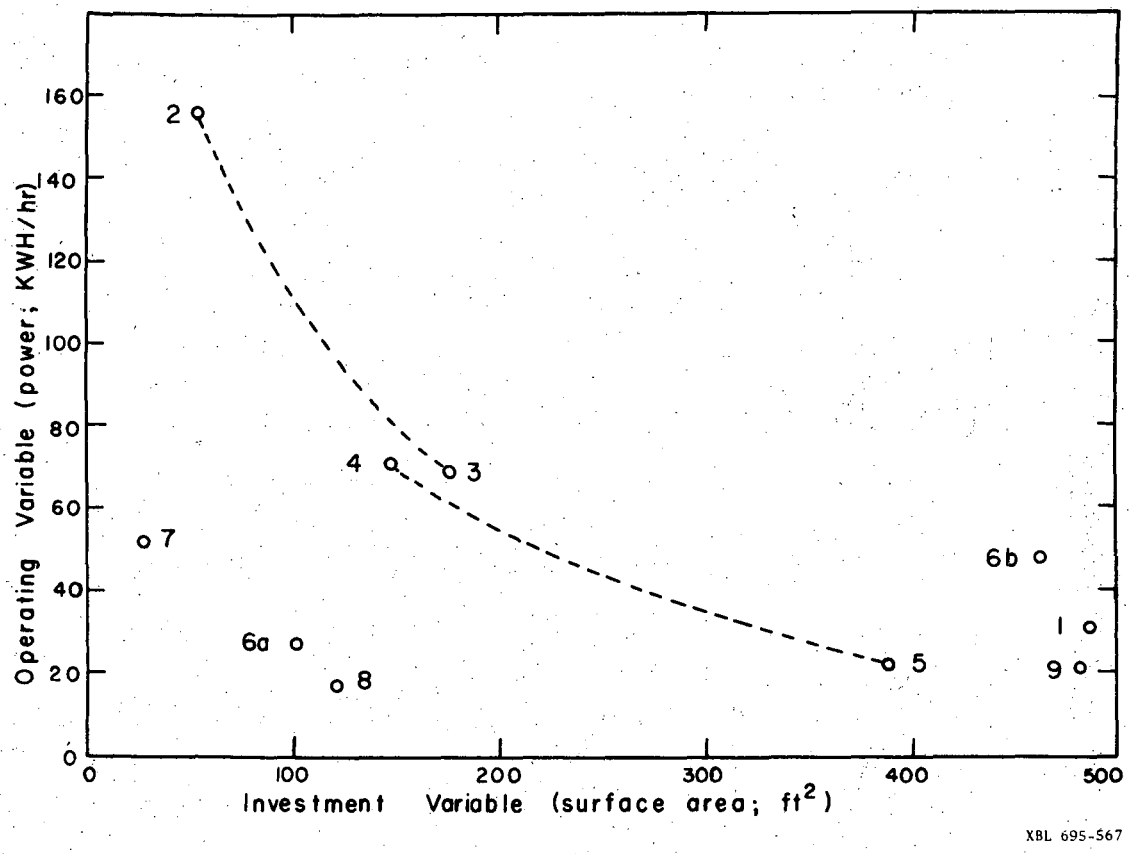

1. Sieve-tray tower.
2. Single co-current packed column; D = 1.33 ft.
3. Single co-current packed column; D = 2.66 ft.
4. Staged co-current packed columns; D = 1.33 ft.
5. Staged co-current packed columns; D = 2.66 ft.

6a. Staged annular-flow contactors (50% of driving force corresponding to droplet equilibration assumed).

6b. Staged annular-flow contactors (10% of driving force corresponding to droplet equilibration assumed).

7. Single froth-flow contactor.
8. Staged froth-flow contactors.
9. Staged spray towers.

Fig. 16. Depiction of operating and investment variables for CO_2 absorbers.

In terms of investment costs alone, each of the devices, except the spray tower, appears superior to the sieve-tray column. The advantage of the spray column is primarily due to the low energy cost associated with the low pressure drop in the gas phase.

An indication of the practical meaning of the operating variable used may be obtained from the result that the high power requirement associated with the single co-current packed column with a diameter of 1.33 feet is primarily due to a calculated pressure drop in the device of 81 psi. This clearly represents an impractical operating condition.

The set of points representing the packed columns verify the hyperbolic nature of the trade-off between operating and investment costs suggested in Section V-A. On the basis of the curves drawn through these sets of points, it appears that, if the diameters are optimally selected, the multi-staged co-current packed columns would be more attractive then the single columns, since the curve representing the staged devices lies closer to the origin.

The most favorable devices, in terms both of operating and investment variables, are the single and staged froth-flow devices and, possibly, the staged annular-flow devices. The conclusion with regard to the annular-flow device is highly dependent on the approach to equilibrium which is assumed to exist between the entrained droplets and the gas phase. This may be seen by comparing the positions of point 6a representing the result when 50% of the driving force $C_e - C_a$, corresponding to droplet equilibrium with the gas to the position of point 6b, representing the result when only 10% of the full equilibrium driving force was assumed. Because of the lack of sufficiently complete

information regarding mass transfer in annular flow, the confidence with which this device can be recommended as a suitable contacting scheme is limited. The conclusion as to whether the single or multiple froth-flow contactors are more favorable depends on the relative importance of the investment and operating costs, the evaluation of which was not made.

C. HCl Absorbers

1. Basis of Evaluation

The results of the calculations of equipment sizes and pressure drops for the devices proposed for HCl absorption appear in Tables 3, 5 and 8. These devices were compared in the same general way as the CO_2 absorption devices. However, no information was found concerning commercially used absorbers operating in the same concentration and flow rate ranges as the process considered, and only general observations regarding the competitiveness of the proposed devices with equipment currently used for HCl absorption were possible.

For the AEC's Volatility process, a stripper would be required to regenerate HCl gas of a strength suitable for process use. The effects of multi-staging the absorber in altering the costs associated with the regenerator might be considerable. A consideration of the costs associated with the regenerator was not made, however, except in a qualitative way.

The variables representing investment and operating variables were calculated by the following procedures.

(1) Investment costs were considered proportional to the internal surface --excluding heads--of the devices, and no allowance for auxilliary equipment or device internals was made.

(2) The pumping requirements considered were those associated with pumping the liquid from the regenerator to the absorber and with recirculating the absorbent in the froth flow-devices. As in the CO_2 system analysis, which led to Eq. (108) to describe the energy requirement, the frictional and kinetic energy losses in the external piping were considered independent of the contactor used, and were neglected. Because the pressure difference between the regenerator and the absorber would be small, the $\Delta P/\rho_1$ term in Eq. (108) was also neglected in determining this energy requirement, but was considered in determining the pumping requirement for absorbent recirculation in the froth-flow device.

(3) Compressor requirements were calculated using Eq. (110), assuming the compressor position to be at the outlet of the absorber, compressing the outlet gas from the outlet pressure to the outlet pressure plus the pressure drop through the device or devices. Although this may not represent a compressor position at an optimal, or even necessary, point in the process stream, calculating the energy requirement in this way presents a measure of the price that may have to be paid for the pressure drop through the device.

(4) For the multiple-contactor cases, Fig. 6 shows that external heat exchangers are necessary to maintain the temperature conditions assumed for the contactors. It was assumed that the cooling in these exchangers was done by counter-current flow of water available at 21°C, and that a 5°C approach existed at the outlet of the exchanger. The cost of cooling water per hour was converted to consistent power units of KWH/hr using relative costs of electricity and cooling water of \$0.01/KWH and \$0.03/1000 gallons of water suggested by Voogt and Tielrooy.[71]

2. Results

The results of the assignment of operating and investment variables according to the above procedure are shown in Fig. 17.

A comparison between the single co-current packed columns and the multiple-column cases shows that, in contrast with the situation with CO_2 absorption, the multiple-contactor case is generally less favorable for the removal of HCl. This is because of the cost associated with inter-stage water cooling. If this cost is neglected, as point 4' indicates, the multiple contactors become more favorable. The savings in regeneration costs which might be realized in the two-column case could compensate for the cooling water costs, and make the two-column contacting scheme more favorable.

The most favorable device for the absorption of HCl is shown clearly to be the single co-current packed columns, if the sole desire is to clean an effluent gas stream. Unlike the result for CO_2 absorption, the annular-flow contactors appear relatively unfavorable, especially to the extent that the distance from the origin for the single and multiple annular-flow contactors is in the direction of increased capital requirements which, as mentioned, should be of great importance considering the high cost of materials which must be used in HCl absorbers. The multiple packed columns and the froth-flow device are potentially competitive for scrubbing HCl, even without the consideration of regenerator cost savings with the former device.

The froth-flow device, the multiple packed columns and the multiple annular-flow devices all produce an absorbent with an HCl

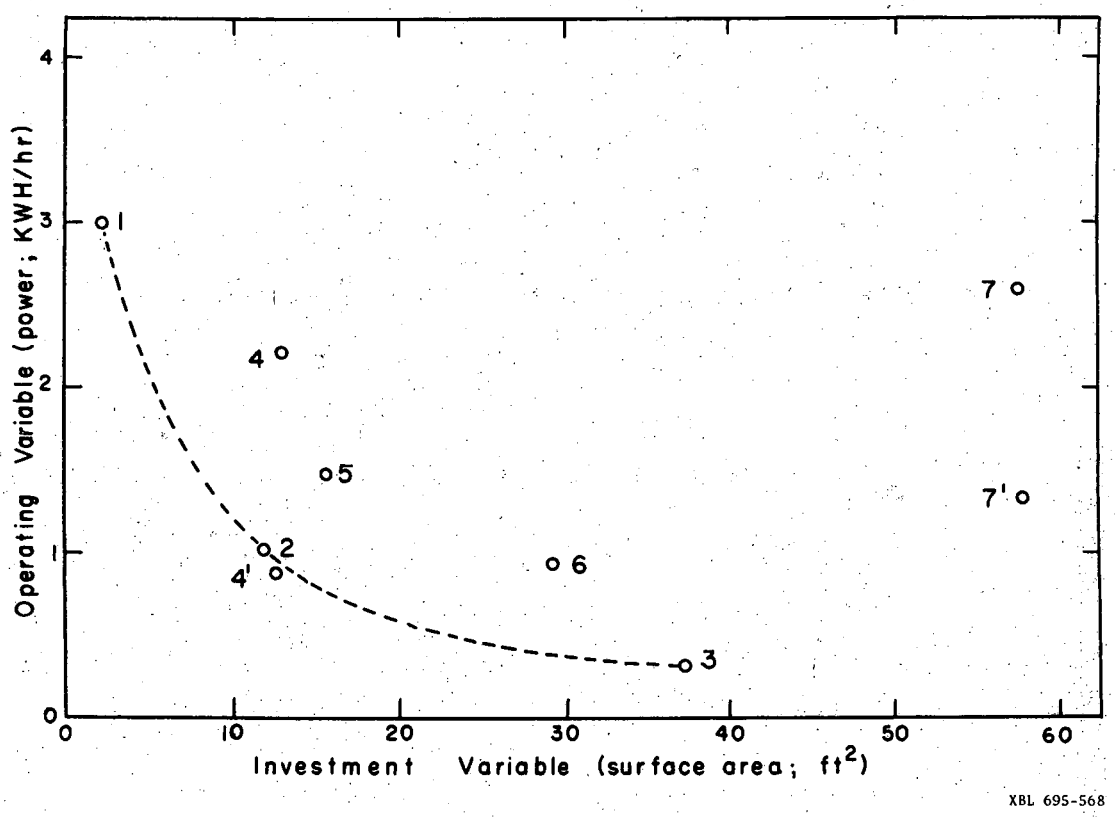

1. Single co-current packed column; D = 0.5 ft.
2. Single co-current packed column; D = 0.888 ft.
3. Single co-current packed column; D = 1.5 ft.
4. Staged co-current packed columns; D = 0.888 ft.

4'. Staged co-current packed columns; D = 0.888 ft. (cooling water costs neglected).

5. Single froth-flow contactor.
6. Single annular-flow contactor.
7. Staged annular-flow contactors.

7'. Staged annular-flow contactors (cooling water costs neglected).

Fig. 17. Depiction of operating and investment variables for HCl absorbers.

concentration considerably higher than the other devices, and of potentially valuable commercial strength. If producing an acid of high concentration is desired, the multiple packed columns and froth-flow device seem about equally attractive, with a possible edge given to the packed columns because of the lower capital costs and greater concentration of HCl produced.

Although no direct comparison between these devices and devices currently used for HCl absorption was made, certain observations may be suggested. The most commonly used commercial absorbers are cooled absorbers, which consist of bundles of tubes, through which the gas and liquid streams pass either co-currently or counter-currently. A typical installation might incorporate 100 to 300 tubes of 7/8-inch diameter.[18,19] The problems of controlling liquid distribution in such tubes are complex. It seems probable that the devices considered here would substantially reduce the capital requirements and control problems characteristic of the cooled absorbers. However, the utility of employing an adiabatic process for scrubbing gas streams of much higher concentration than was considered in this study may be limited by the high temperature rise associated with such absorptions.

D. General Conclusions

The hierarchy of attractiveness of the devices considered for the absorption of CO_2 may be listed, in an approximate order of decreasing favorableness, as

(1) Single-multiple froth-flow devices

(2) Multiple annular-flow devices

(3) Multiple co-current packed columns

(4) Single co-current packed columns

(5) Multiple spray columns

(6) Sieve-tray column.

For the removal of HCl, without consideration of the importance of the product absorbent, the approximate order is

(1) Single packed columns

(2) Froth-flow device

(3) Multiple packed columns

(4) Single annular-flow device

(5) Multiple annular-flow devices.

If the value of the product HCl absorbent is important, the best devices would be

(1) Multiple packed columns

(2) Froth-flow device

(3) Multiple annular-flow contactors.

The attractiveness of a given device for mass transfer is dependent on the system studied. Some first-order explanations of the reasons for this may be offered. The special advantage of annular-flow

contacting devices for mass transfer lies in the mechanism of interchange of droplets between the annular liquid and the gas core, with the droplets returning to the annular liquid much closer to equilibrium than the bulk liquid. Although this mechanism was important in both the HCl and CO_2 absorption cases, its importance relative to diffusional mass transfer was much greater in the CO_2 cases calculated by assuming a close approach of the droplets to equilibrium. The disadvantage of packed columns for CO_2 absorption is linked primarily to the operating costs and, more specifically, to the compressor costs associated with the pressure drops through the columns. The increase in interfacial area necessary to improve the absorption rate for this liquid-phase controlled system is at the expense of a pressure drop which, in order to reduce investment costs substantially, must be significant. The more favorable devices for CO_2 absorption, such as the froth-flow device, are able to increase the rate of absorption without necessitating as great an energy expenditure. The froth-flow devices are less desirable than the packed columns for the absorption of HCl because of the power required to recirculate the absorbent, which is more important in this case than in the CO_2 case because of the greater recycle ratio and the fact that other pumping costs in this case are small.

The potential desirability of utilizing the less common absorption devices considered for commercial processes has been shown. The areas in which necessary design information is lacking have also been outlined. The optimistic results of this study suggest the economic desirability of filling in some of these voids.

ACKNOWLEDGMENTS

Special gratitude is owed to Romesh Kumar, whose frequent comments during the course of this work were of invaluable assistance.

This work was done at the Lawrence Radiation Laboratory under the auspices of the United States Atomic Energy Commission.

APPENDIX I

A. Rate Considerations for CO_2 Absorption

The absorption of CO_2 has been extensively reviewed by Danckwerts and Sharma,[33] upon whose work much of the following discussion is based.

The pattern of chemical reaction in the absorption of carbon dioxide into catalyzed (or uncatalyzed) potassium carbonate solutions may be regarded as second-order, with the consideration of reversibility often necessary. The over-all reaction may be written as

$$K_2CO_{3(soln)} + CO_{2(g)} + H_2O = 2KHCO_{3(soln)} \qquad \text{(A-I-1)}$$

Although $CO_3^{=}$ may be regarded as the reactant, the local rate of reaction in an uncatalyzed system is proportional to the buffered concentration of hydroxide ions, which may be related to the concentrations of $CO_3^{=}$ and HCO_3^{-} by

$$(OH^-) = \frac{K_w}{K_2} \frac{(CO_3^{=})}{(HCO_3^-)} \qquad \text{(A-I-2)}$$

where $K_w = (H^+)\ (OH^-)$ (A-I-3)

$$K_2 = (H^+)\ (CO_3^{=})/(HCO_3^-) \qquad \text{(A-I-4)}$$

At infinite dilution, the equilibrium constants K_w and K_2 may be related to temperature as

$$\log_{10} K_w = -4470.99/T + 6.0875 - 0.01706\ T \quad \text{(Ref. 8)} \qquad \text{(A-I-5)}$$

K_w = gm mole^2/liter^2

$T = {}^{\circ}K$

$$\log_{10} K_2 = -2902.4/T + 6.498 - 0.0238\ T \quad \text{(Ref. 33)} \qquad \text{(A-I-6)}$$

K_2 = gm moles/liter

$T = {}^{\circ}K$

In the Vetrocoke process, the rate of reaction is also proportional to the concentration of arsenite ion, obtained from the dissociation of arsenious acid according to the reaction

$$As(OH)_3 = As(OH)_2O^- + H^+ \qquad \text{(A-I-7)}$$

Neglecting the reverse reaction, the rate of reaction of CO_2 into catalyzed potassium carbonate may be written as

$$r = k_{OH}(CO_2)(OH^-) + k_{As}(CO_2)(As(OH)_2O^-) \qquad \text{(A-I-8)}$$

where the relevant reaction rate constants are given as

$$\log_{10} k_{OH} = 13.635 - 2895.0/T \quad \text{(Ref. 33)} \qquad \text{(A-I-9)}$$

$$\log_{10} k_{As} = 12.2 - 2830.0/T \quad \text{(Ref. 33)} \qquad \text{(A-I-10)}$$

where $T = {}^{\circ}K$ and the rate constants have units of liter/gm mole sec. In the catalyzed absorption of CO_2, where the second term on the right-hand side of Eq. (A-I-8) may be expected to outweigh the first, the concentration of arsenite ion may not become significantly depleted at the interface, due to formation of undissociated arsenious acid. The rate of reaction may then be approximately first order with respect to the concentration of CO_2. An analytical solution to the diffusion equation describing the absorption process may be obtained in this case.

The solution, consistent with the Danckwerts surface renewal model, is

$$\frac{R}{k_1 C^*} = \left[1 + \frac{D_1 k_2 C_o}{k_1^2}\right]^{1/2}$$

or

$$R = C^*(k_1^{\ 2} + D_1 k_2 C_o)^{1/2} \qquad \text{(A-I-11)}$$

where: C^* = concentration of physically dissolved CO_2 in equilibrium with gas at interface, gm moles/cm^3

= HPy_i, where H is the Henry's law solubility constant, gm moles/cm^3 atm, P the total pressure, atmospheres, and y_i the interfacial gas mole fraction of solute

D_1 = diffusivity of gas in the liquid, cm^2/sec

k_1 = physical liquid phase mass-transfer coefficient, cm/sec

$k_2 C_o = k_{OH}(OH^-) + k_{As}(As(OH)_2O^-)$

R = absorption rate, gm moles/cm^2 sec

The reverse reaction may be accounted for by rewriting Eq. (A-I-11) as

$$R = (C^* - C_b)(k_1^2 + D_1 k_2 C_o)^{1/2} \qquad \text{(A-I-12)}$$

where C_b represents the concentration of dissolved but unreacted CO_2 in the bulk of the solution. The value of C_b may be determined from the first and second dissociation constants of carbonic acid, according to the equation

$$\left(CO_2\right) = C_b = \frac{K_2(HCO^-)^2}{K_1(CO_3^=)} \qquad \text{(A-I-13)}$$

where K_2 is defined by Eqs. (A-I-4) and (A-I-6), and K_1 is defined by the equation

$$K_1 = \frac{(H^+)(HCO_3^-)}{(CO_2)} \qquad \text{(A-I-14)}$$

and $\log_{10} K_1 = -3404.7/T + 14.843 - 0.03279\ T$ (Ref. 33) (A-I-15)

K_1 = gm moles/liter

$T = {}^\circ K$

Since the values of the dissociation constants K_1 and K_2 correlated by Eqs. (A-I-6) and (A-I-15) are for systems at infinite dilution, activity coefficient corrections should be applied to the ionic concentrations to account for the effects of ionic strength. No means was found in the literature to account for this effect over a suitable range, although some work in this area has been done (see Ref. 9).

The criterion for no depletion of arsenite ion, which must be satisfied correctly to represent the rate of absorption by Eq. (A-I-11) or (A-I-12), is written as[33]

$$\frac{C^*\left(\frac{1}{(CO_3^=)} + \frac{2}{(HCO_3^-)}\right)\left[\left(1 + \frac{D_1 k_{As}(As(OH)_2O^-)}{k_1^2}\right)^{1/2} - 1\right]}{1 + \frac{K_{As(OH)_3}(CO_3^=)}{K_2\ (HCO_3^-)}} << 1 \qquad \text{(A-I-16)}$$

where $K_{As(OH)_3}$ is the stoichiometric dissociation constant of $As(OH)_3$, and may be related to temperature by

$$\log_{10} pK_{As(OH)_3} = 9.614 - 0.0148\ T \quad \text{(Ref. 33)} \qquad \text{(A-I-17)}$$

$K_{As(OH)_3}$ = gm moles/liter

$T = {}^\circ C$

The constants $K_{As(OH)_3}$ and k_{As} are, like K_1 and K_2, functions of ionic strength of the solution as well as temperature.[10] This effect was, however, neglected because of the increased complexity of calculation.

It is shown in Appendix I.B that for typical conditions met in the Vetrocoke process, the assumption of no arsenite depletion at the interface is valid and, hence, that Eq. (A-I-12) is the correct rate expression.

Equation (A-I-12) may be rewritten in a form including the gas phase mass-transfer coefficient as well as the liquid-phase coefficient. It must be true that

$$Ra = a(C^* - C_b)(k_1^2 + D_1 k_2 C_o)^{1/2} = k_g a\, P(y - y_i) \qquad \text{(A-I-18)}$$

where $k_g a$ = gas phase mass-transfer coefficient, gm moles/cm^3 sec atm

P = total pressure, atmospheres

y = mole fraction of solute in bulk gas

Since $y_i = y - Ra/k_g aP$ and $C^* = HPy_i$, the rate of absorption may be rewritten as

$$Ra = \frac{a(HPy - C_b)(k_1^2 + D_1 k_2 C_o)^{1/2}}{1 + \dfrac{aH(k_1^2 + D_1 k_2 C_o)^{1/2}}{k_g a}} \qquad \text{(A-I-19)}$$

This form of the rate expression implies that it is unnecessary to know the interfacial gas composition, y_i, to calculate the rate of absorption; i.e., a pseudo-solubility, HPy may be used instead of HPy_i to calculate the concentration-driving force.

B. Test of Criterion for Treating Absorption of CO_2 into Promoted Carbonate Solutions as Pseudo First-Order

Equation to be tested: Eq. (A-I-16)

Concentrations are taken to correspond to the outlet of the high-CO_2-partial-pressure contactor of the two-contactor scheme, where the carbonate-bicarbonate ratio is the smallest.

$(CO_3^{=}) = 0.485$ gm moles/liter

$(HCO_3^{-}) = 3.31$ gm moles/liter

$C^* \cong HPy = 4.279\times10^{-3}$ gm moles/liter

$(As(OH)_3) = 1$ gm mole/liter

$k_{As} = 6.967\times10^{3}$ l gm mole/sec

$D_1 = 2.1\times10^{-5}$ cm^2/sec

$k_1 = 0.8473$ cm/sec (value corresponding to co-current packed column)

$K_{As(OH)_3} = 2.27\times10^{-9}$ gm moles/liter

$K_2 = 7.386\times10^{-11}$ gm moles/liter

Substituting into Eq. (A-I-16),

$$\text{LHS} = \frac{(4.279\times10^{-3})\left(\frac{1}{0.485}+\frac{1}{3.31}\right)\left[\left(1+\frac{(2.1\times10^{-5})(6.96\times10^{3})(1)}{0.6376}\right)^{1/2}-1\right]}{1+\frac{(2.27\times10^{-9})(0.485)}{(7.386\times10^{-11})(3.31)}}$$

$$= 2.2\times10^{-4} \ll 1$$

Thus, the system may confidently be treated as pseudo first-order.

APPENDIX II

Physical Solubility of CO_2 in K_2CO_3

It is difficult to measure the solubility of CO_2 in solutions with which it reacts. The solubility of gases in nonreacting electrolytes may be estimated[33] by

$$\log_{10}(H/H_w) = -K_s I \qquad \text{(A-II-1)}$$

where: H_w = Henry's law constant for solubility in water, gm mole/liter atm

H = Henry's law constant for solubility in given electrolyte, gm mole/liter atm

I = ionic strength, equal to half the sum of the concentrations of each species multiplied by its ionic charge squared, gm ions/liter

K_s = constant characteristic of the electrolyte and solute gas

H_w may be expressed as

$$\log_{10}H_w = 1140.0/T - 5.30 \quad \text{(Ref. 33)} \qquad \text{(A-II-2)}$$

H_w = gm moles/liter atm

T = °K

(valid for pressures of a few atmospheres or less)

Nijsing and Kramers[11] have found that for CO_2 in potassium carbonate solutions (I = 0 - 2 gm ions/liter; T = 20°C), K_s has a value of 0.063, while Sharma[12] has reported a value of 0.057 (I = 0-5 gm ions/liter; T = 25°C). The effect of temperature on K_s was not found to be great. An average value of K_s of 0.060 was used to calculate the Henry's

law constant, using Eqs. (A-II-1) and (A-II-2). The physical solubility could then be calculated from the equation

$$C^* = HPy_i \qquad \text{(A-II-3)}$$

where y_i is the interfacial gas phase solute concentration.

APPENDIX III

Chemical Equilibrium in the CO_2-K_2CO_3 System

The over-all chemical reaction occurring in the Vetrocoke absorption process is represented by Eq. (A-I-1). Bocard and Mayland[38] have expressed the equilibrium vapor pressure of CO_2 over carbonate-bicarbonate buffer solutions by the expression

$$p_{CO_2} = \frac{(\alpha^2/\beta)}{\gamma} \frac{(MKHCO_3)^2}{(MK_2CO_3)\ K} \qquad \text{(A-III-1)}$$

where: α, β, γ are activity coefficient corrections for the carbonate and bicarbonate ions and for water

MK_2CO_3 and $MKHCO_3$ are the concentrations (in molality) of the ions

K is an equilibrium constant for the reaction, calculated from the standard free energies of the products and reactants.

Bocard and Mayland constructed graphs, representing the vapor pressure of CO_2 consumed by reaction (expressed as standard cubic feet of CO_2 per gallon of solution) for various equivalent K_2CO_3 concentrations. The vapor pressure for low carbonate concentrations was predicted from Eq. (A-III-1). For high carbonate concentrations, data of the U. S. Bureau of Mines were used,[3,4] fit to equations of the form

$$\log_{10}(p_{CO_2}) = A + B/T \qquad \text{(A-III-2)}$$

where $A = a + bX + cX^2 + dX^3$

X = equivalent solution concentration (standard cubic feet of CO_2/gallon)

a,b,c,d,B = constants

T = temperature

Based on the decision to use 25%-by-weight K_2CO_3, the data of Bocard and Mayland were fit to an equation of the form of Eq. (A-III-2). The results were:

For X = 2 - 5 SCF of CO_2/gallon

$$\log_{10}(p_{CO_2}) = 7.2583 + 0.8643X - 0.11707X^2 + 0.00885X^3 - \frac{5606.84842}{T} \qquad \text{(A-III-3)}$$

For X = 5 - 6.75 SCF of CO_2/gallon

$$\log_{10}(p_{CO_2}) = 6.5882 - 0.99817X + 0.1671X^2 - 0.004X^3 - \frac{2870.91905}{T}$$

where p_{CO_2} = vapor pressure of CO_2, psia

T = °Rankine

X = SCF of CO_2/gallon of solution .

APPENDIX IV

Physical Properties—CO_2-K_2CO_3 System

1. Liquid Properties

Perry[28] gives the density of 25% K_2CO_3 at 150°F as 1.202 gm/cc, or 75.23 lb/ft^3. The effect of conversion on density is discussed by Bocard and Mayland,[38] but was neglected for most design purposes.

The liquid viscosity at this concentration and temperature is 0.91 centipoise, or 6.115×10^{-4} lb/ft sec.[38]

2. Gas Properties

The Phillips flow diagram for the Vetrocoke process, discussed in Sec. II, gives the inlet gas density as 0.24 lb/ft^3 at 150° and 150 psia. The outlet density at 140°F and 140 psia was specified as 0.079 lb/ft^3. Neglecting the compensating temperature and pressure effects, the gas density was assumed to be related linearly to the composition of CO_2, and the relationship derived was

$$\rho_g = 0.913y + 0.061 \qquad \text{(A-IV-1)}$$

where ρ_g = lb/ft^3

y = bulk gas mole fraction of CO_2

The outlet density, where the mole fraction of CO_2 was 0.01, was calculated by Eq. (A-IV-1) to be 0.07013 lb/ft^3. Design calculations were based on average densities in the stages. For the single-stage case, the average density was 0.156 lb/ft^3. For the two-contactor case, the interstage mole fraction of CO_2 was 0.07198, and the density was calculated

to be 0.1265 lb/ft^3. Thus, the average density in the first stage was 0.183 lb/ft^3 and in the second stage, 0.0983 lb/ft^3.

A gas viscosity at a temperature of 150°F and a pressure of 140 psia was estimated by the method of critical viscosities.[34] A critical viscosity, based on molar-average critical properties, is calculated as

$$\mu_c = 7.70\ \overline{M}^{1/2}\ \overline{P}_c^{\,2/3}\ \overline{T}_c^{\,-1/6} \qquad \text{(A-IV-2)}$$

where $\overline{M}$ = average molecular weight

$\overline{P}_c$ = molar average of critical pressures, atm

$\overline{T}_c$ = molar average of critical temperatures, °K

μ_c = critical viscosity, centipoise

A value of the reduced viscosity, μ/μ_c, corresponding to the reduced temperature and pressure was determined from a graph.[34] The viscosity ($\mu_c\mu_r$) was calculated as 0.01295 centipoise, or 8.702×10^{-6} lb/ft sec. This value of viscosity was assumed constant for the design calculations.

The diffusivity of CO_2 into water at 60°C is 4×10^{-5} cm^2/sec. Water at this temperature has a viscosity of 0.47 centipoise. Correcting for the viscosity and temperature of the carbonate system according to a procedure suggested by Danckwerts and Sharma[33]

$$D_{CO_2-K_2CO_3} = (4\times10^{-5})(0.47/0.91)(338.5/333)$$

$$D_1 = 2.1\times10^{-5}\ \text{cm}^2/\text{sec}$$

APPENDIX V

Algorithm for Determining Over-all Heat and Mass Balances for the Two-Contactor HCl Absorption Process

The nomenclature used to describe the algorithm may best be understood by referring to Fig. 6, in which numbers are assigned to the gas and liquid flow rates, compositions and temperatures corresponding to the inlet and outlet of the "black box" contactors R-1 and R-2. The variables discussed are

Ti = temperature at point i

y_{ji} = mole fraction in gas stream of component j at point i

G_i = total molar gas flow rate at point i

G_{ji} = molar gas flow rate of component j at point i

GI = molar flow rate of gaseous inerts

L_i = total mass liquid flow rate at point i

x_i = weight fraction in liquid of HCl at point i

The algorithm may be outlined as follows:

Given:

1. $T1$, x_1, y_{HCl1}, y_{HCl4}, G_1, $^{\dagger}P$, y_{H_2O1}
2. The assumption that the liquid and gas streams enter and leave the contactors at the same temperature as one another.
3. The assumption that the gas is saturated with water vapor at the inlet and outlet of all vessels.

---

†In this discussion, P is assumed to be 1 atmosphere, so that $p_i = y_i$. This assumption is not necessary, but the nomenclature is simplified.

4. The assumption that the liquid leaving each contactor is in equilibrium with half the actual outlet HCl mole fraction.

Procedure:

1. Guess initial values of T2 and T3, such as T2 = T3 = T1.
2. Using assumption 4 and the known value of y_{HCl4}, determine x_2.
3. Knowing x_2, y_{H_2O4} may be determined in accord with assumption 3. Since y_{HCl4} and the flow rate of gaseous inerts is known, GH_2O4 and GHCl4 may be determined algebraically.
4. Guess y_{HCl2}.
5. Determine x_3 using assumption 4. Determine y_{H_2O2} using assumption 3. Calculate the values of GH_2O2 and GHCl2 in a way similar to the calculation of GHCl4 and GH_2O4 in step 3.
6. In passing through the cooler E-1, some HCl vapor must condense, since T1 < T3. As a simplification, it was assumed that only water vapor would condense, so that GHCl2 = GHCl3. The value of y_{H_2O3} may be determined using assumption 3, since x_1 is fixed. The values of GH_2O3 and y_{HCl3} may be calculated algebraically.
7. The inlet and outlet liquid flow rates were calculated for each absorber, based on the amount of HCl absorbed, the amount of water vaporized and the change in liquid composition over each contactor. For example,

$$L_3 = \frac{(1-x_2)(GHCl1-GHCl2)M_{HCl} + x_2(GH_2O2-GH_2O1)M_{H_2O}}{x_3 - x_2} \qquad \text{(A-V-1)}$$

8. The mass balance is checked by ascertaining whether the total amount of HCl absorbed by the liquid stream, $L_3x_3 - L_1x_1$ is equal to the amount of HCl lost by the gas in R-1 plus R-2. If the mass balance does not check, a new value of y_{HCl2} is calculated, based on a value of GHCl2 that would make the mass balance check, the value of GH_2O2 determined in step 5 and the fixed value of GI. Steps 5-8 are repeated until the mass balance is satisfied.
9. After satisfying the mass balance for the assumed values of T2 and T3, the heat balance for each contactor is calculated.
10. If an imbalance exists in the heat equations, new values of T2 and T3 are chosen, the mass balance recomputed and the heat balance again checked.

The procedure for converging on temperature was a "double-false position" scheme. It was found that other methods, such as direct substitution or Newton-Raphson iteration, yielded values in the early iterations which could not be handled within the limit ranges over which the data curve fits were applicable.

Procedure:

1. If neither heat balance is satisfied, increment T2 and T3 (+ or - depending on the direction of imbalance). Continue this procedure until one of the heat balances changes sign.
2. If, for example, the heat balance over R-2 changes sign, a new value of T2 is calculated as

$$T2_{n+1} = T2_n - \Delta(\Sigma H_2)_n \left| \frac{(T2_n - T2_{n-1})}{\Delta(\Sigma H_2)_n - \Delta(\Sigma H_2)_{n-1}} \right| \qquad \text{(A-V-2)}$$

where $\Delta(\Sigma H_i)$ represents the total outlet minus the total inlet enthalpy. If the imbalance over R-1 still hasn't changed sign, increment T3 as in step 1.

3. When both balances have changed sign, though not necessarily simultaneously, calculate both new T's using Eq. (A-V-2), since the iteration should, at this time, have arrived in the neighborhood of the solution.

4. Continue until

$$\left| Ti_{n+1} - Ti_n \right| < \delta \qquad \text{(A-V-3)}$$

A measure of the effectiveness of the algorithm is the approach of the heat balances, denoted as $\Delta(\Sigma H_i)$, to zero. This solution scheme converges from initial imbalances on the order of 10^7 cal/hr, with the initially guessed values of temperature, to values less than 10 cal/hr in about 20 iterations on T, with $\delta = 10^{-5}$.

APPENDIX VI

Equilibrium in the HCl-Water System

Extensive data are available regarding the vapor pressure of HCl over its aqueous solutions.[28] Using a computer, empirical equations were derived to fit these data by solving simultaneous equations relating the logarithm of vapor pressure to polynomials in concentration and temperature.

For x_{HCl} = 2 - 20 wt%

$T = 30 - 110°C$

$$\log_{10}(p_{HCl}) = -14.18427 + 0.31101X - 0.01131X^2 + 0.00020X^3 - 1149.76879/T + 0.063182T - 0.000059T^2 \quad \text{(A-VI-1)}$$

$T = °K$

X = gms HCl/100 gms H_2O

p_{HCl} = mm Hg

For x_{HCl} = 16 - 38 wt%

$T = 30 - 80°C$

$$\log_{10}(p_{HCl}) = -48.99332973 + 0.10167621X + 0.00231592X^2 - 0.00003314X^3 + 3266.40563656/T + 0.16804229T - 0.00017038T^2$$

$T = °K$

X = wt% HCl

p = mm Hg

The data of Perry[28] and Norman[26] were used to derive similar expressions representing the vapor pressure of water over HCl solutions.

For x_{HCl} = 0 - 26 wt% HCl

$T = 20 - 110°C$

$$\log_{10}(p_{H_2O}) = 12.251601 - 0.00166X - 0.000507X^2 + 0.00000715X^3 - 2672.19272/T - 0.008665T + 0.0000078206T^2 \quad \text{(A-VI-3)}$$

$T = °K$

X = gms HCl/100 gms H_2O

p = mm Hg

For x_{HCl} = 18 - 38 wt% HCl

$T = 30 - 80\ °C$

$$\log_{10}(p_{H_2O}) = -29.12759307 + 0.01158613X - 0.00096607X^2 - 0.00000579X^3 + 1738.9320102/T + 0.11871723T - 0.0001204T^2 \quad \text{(A-VI-4)}$$

$T = °K$

X = wt% HCl

p = mm Hg

APPENDIX VII

HCl-Water System Enthalpy Data

Van Nuys[72] has presented tables and graphs representing liquid and vapor enthalpy for the system HCl-water (inert free).

The change of enthalpy associated with changing the temperature and concentration of liquid HCl solutions is due to the effects of both sensible heat change and heat of dilution. Based on values of total enthalpy and heat of dilution tabulated by Van Nuys (based on zero enthalpy at 0°C) as a function of temperature and composition, the sensible heat was implicitly defined as

$$C_p(T-273) = H_L - H_D \qquad \text{(A-VII-1)}$$

where C_p = heat capacity, cal/gm °C

T = °K

H_L = total liquid enthalpy, cal/gm

H_D = heat of dilution, cal/gm

A plot of C_p, so defined, as a function of composition and temperature indicated that it was virtually temperature independent, and was linearly dependent on concentration, according to the functionality

$$C_p = 1.00087 - 1.90X \qquad \text{(A-VII-2)}$$

where X is the weight fraction of HCl in the liquid. The heat of dilution, H_D, was fitted as

$$\log_{10}H_D = -8.514798 + 0.13633X - 0.00351X^2 + 0.00004X^3 + 0.6142T - (1.64\times10^{-4})T^2 + (1.545\times10^{-7})T^3 \qquad \text{(A-VII-3)}$$

Valid for $T = 30 - 70°C$

$X = 0 - 32\%$ HCl by weight

$T = °K$

$H_D = cal/gm$

$X = wt\%$ HCl

Thus, all the necessary data has been correlated to fit H_L as

$$H_L = C_p(T-273) + H_D \qquad \text{(A-VII-4)}$$

This procedure for curve fitting the liquid enthalpy data was expected to yield more precise results than a simple polynomial fit of the total liquid enthalpy data because, although C_p and H_D are monotonically decreasing and increasing with increasing concentration, the dependence of H_L on concentration is non-monotonic, with H_L having a minimum value at about 15% HCl.

The gas enthalpy was considered to be composed of two parts:

a) The sensible heat of the inert gases, air and H_2

b) The enthalpy of the inert free H_2O-HCl mixture, including effects of the latent heat of vaporization of the solution and the heat of absorption of HCl.

The sensible heat of the inert gases was obtained by using the mean molar heat capacities of the components. The mean-molar heat capacity, C_p^*, may be related to the molar heat capacity, $C_{p(molar)}$, by

$$C_p^*(T-TO) = \int_{TO}^{T} C_{p(molar)}\, dT \quad . \qquad \text{(A-VII-5)}$$

Since $C_{p(molar)}$ may be expressed as

$$C_{p(molar)} = a + bT + cT^2 \quad , \qquad \text{(A-VII-6)}$$

C_p^* is given by

$$C_p^* = a + b(T+TO)/2 + c(T^2+TTO+TO^2)/3 \qquad \text{(A-VII-7)}$$

and

$$Q_s = G_{mH_2} C_{pH_2}^* (T-TO) + G_{m_{air}} C_{p_{air}}^* (T-TO) \quad , \qquad \text{(A-VII-8)}$$

where Q_s = enthalpy of inert gas stream, cal/hr

G_{mi} = component molar flow rate, gm moles/hr

C_p^* = mean-molar heat capacity, cal/gm mole °C

TO = reference temperature, 298°K

$C_{p(molar)}$ = molar heat capacity, cal/gm mole °C

The constants a, b, and c in Eq. (A-VII-7) were obtained from Smith and Van Ness[73] as

Component	a	$b\times10^3$	$c\times10^6$
H_2	6.947	-0.200	0.481
Air	6.441	1.657	-0.204 (average of N_2 and O_2)

The gas enthalpy of inert free HCl-H_2O mixtures, H_g, is a linear function of composition, with temperature as a parameter defining a family of straight lines. The endpoints of these lines (at 0% HCl and 100% HCl) may readily be established. At 0% HCl,

$$H_g = (H_L+\Delta H_{vap})_{\text{at T of interest}} \text{ cal/gm} \qquad \text{(A-VII-9)}$$

ΔH_{vap} is the heat of vaporation of pure water which, based on data obtained from the Handbook of Chemistry and Physics,[39] may be related to temperature (at atmospheric pressure) by

$$\Delta H_{vap} = 597.655 - 0.586\ (T-273) \qquad \text{(A-VII-10)}$$

where ΔH_{vap} = cal/gm

T = °K

At 100% HCl,

$$H_g = 458.8 + \int_{273}^{T} C_{p_{HCl}}\ dT \text{ cal/gm} \qquad \text{(A-VII-11)}$$

in which 458.8 cal/gm is the heat of vaporization of pure HCl at 0°C and $\int_{273}^{T} C_{pHCl}\ dT$ represents the sensible heat increase from the reference temperature, 0°C, to the temperature of interest. The sensible heat term was expressed as

$$\int_{273}^{T} C_{p_{HCl}}\ dT = (1/36.47)\ [a(T-273) + b(T^2-273^2)/2 + c(T^3-273^3)/3] \qquad \text{(A-VII-12)}$$

where T = °K

$C_{p_{HCl}}$ = cal/gm °C

The necessary constants, a, b, and c are[73]

$a = 6.732$

$b = 0.433\times10^{-3}$

$c = 0.370\times10^{-6}$

The slope of a gas-enthalpy line at a given temperature may then be written as

$$s = \frac{H_g(100\%) - H_g(0\%)}{1.0} \qquad \text{(A-VII-13)}$$

so that, at a given temperature

$$H_g = H_g(0\%) + sX \text{ cal/gm} \qquad \text{(A-VII-14)}$$

in which X is the weight fraction of HCl in the gas.

Thus, the total enthalpy at any point may be expressed as

$$Q = LH_L + (G-G')\,H_g + Q_s$$

where Q = total (liquid + gas) enthalpy, cal/hr

L = liquid flow rate, gms/hr

G = total gas flow rate, gms/hr

G' = flow rate of inert gas, gms/hr

APPENDIX VIII

Physical Properties—HCl-Water System

1. Liquid Properties

The density of HCl solutions as a function of temperature and concentration is given by Perry.[28] An average value of 64.92 lb/ft^3 was taken as constant over the temperature and concentration ranges considered.

The viscosity of 31.5 wt% HCl may be obtained from a nomograph shown by Perry.[28] A tabular representation of pure water viscosity is also presented. An estimate of the liquid viscosity was made by assuming it to be an arithmetic average between pure water at 30°C and 31.5% HCl at 66°C. The error of this assumption would be compensated by the facts that the inlet viscosity would actually be lower than that assumed and the outlet viscosity larger. The estimated viscosity was 0.482 centipoise, which was taken as constant.

It will be noted that the liquid-phase properties are used only in estimating the two-phase pressure drops through the various contacting devices, since the absorption of HCl is gas phase controlled. The estimates of these properties, together with the assumptions of their constancy, are probably sufficiently accurate for this purpose.

2. Gas Properties

The gas density at any point was taken as a molar average of the individual gas densities, corrected for temperature by the ideal gas law. At 0°C[28]:

Component	Density (lb/ft^3)
HCl	0.1024
H_2	0.0056
H_2O	0.05017
Air	0.0808

At any point:

$$\rho_g = (0.1024y_{HCl} + 0.0056y_{H_2} + 0.05017_{H_2O} + 0.0808y_{Air})(273/T) \qquad \text{(A-VIII-1)}$$

where: $T = {}^oK$

$\rho_g = lb/ft^3$

y_i = mole fraction of i in the gas phase

The gas viscosity at the inlet and outlet conditions predicted by the "black box" mass balance was calculated by the method of Wilke[34]

$$\mu_{mix} = \sum_{i=1}^{n} \frac{x_i \mu_i}{\sum_{i=1}^{n} x_j \phi_{ij}} \qquad \text{(A-VIII-2)}$$

where $$\phi_{ij} = \frac{1}{\sqrt{8}} (1 + M_i/M_j)^{-1/2}[1 + (\mu_i/\mu_j)^{1/2} (M_j/M_i)^{1/4}]^2 \qquad \text{(A-VIII-3)}$$

and μ_i, μ_j = viscosities at system T + P

M_i, M_j = molecular weights of species

n = number of component

x_i, x_j = mole fractions of components .

Based on the known inlet and outlet compositions, inlet and outlet temperatures of 30 and 60°C and values of component viscosities at these temperatures interpolated from data in the Handbook of Chemistry and

Physics[39] and Perry,[28] the values of the inlet and outlet gas viscosities were determined to be 0.0175 cp and 0.01483 cp. An average viscosity of 0.01665 cp (1.11888×10^{-5} lb/ft sec) was taken as the gas viscosity, to avoid the complexity of accounting both for temperature and composition effects.

The diffusivity of HCl and H_2O in the mixture at inlet and outlet conditions was determined by estimating the values of D_{ij} for all combinations of the gas components, and averaging them in an appropriate way to determine $D_{HCl,m}$ and $D_{H_2O,m}$.

The binary diffusivities were determined from the Chapman-Enskog formula[34]

$$D_{ij} = \frac{0.0018583\,[T^3(1/M_i + 1/M_j)]^{1/2}}{P\,\sigma_{ij}^2\,\Omega_{D_{ij}}} \qquad \text{(A-VIII-4)}$$

where: T = °K

P = atm

D_{ij} = cm^2/sec

σ_{ij} = function of molecular radii, Å

$\Omega_{D_{ij}}$ = dimensionless function of temperature and intermolecular atomic field

$M_{i,j}$ = molecular weights of component i or j

For determining the mixture diffusivities, a modification of the Stefan-Maxwell equation was used. The Stefan-Maxwell equation is[34]

$$\frac{1}{CD_{i,m}} = \frac{\sum_{j=1}^{n} (1/CD_{ij})(y_j N_i - y_i N_j)}{N_i - y_i \sum_{j=1}^{n} N_j} \qquad \text{(A-VIII-5)}$$

where N_i and N_j are the molar fluxes of the components, C is the concentration, y_i and y_j are the component mole fractions, and n is the number of components. In a system of four components, if $N_2=N_3=N_4=0$, Eq. (A-VIII-5) may be rewritten as

$$D_{i,m} = \frac{1 - y_1}{\frac{y_2}{D_{12}} + \frac{y_3}{D_{13}} + \frac{y_4}{D_{14}}} \qquad \text{(A-VIII-6)}$$

Similarly, if $N_1 = -N_2$, and $N_3 = N_4 = 0$, the simplification is

$$D_{i,m} = \frac{1 + 2y_1}{\frac{y_2+y_1}{D_{12}} + \frac{y_3}{D_{13}} + \frac{y_4}{D_{14}}} \qquad \text{(A-VIII-7)}$$

The actual situation encountered in the present system, with both HCl and H_2O having non-zero fluxes, is intermediate between these two cases. Because of the high mole fraction of air, the values obtained by using Eqs. (A-VIII-6) and (A-VIII-7) were nearly the same. As a result, Eq. (A-VII-7) was used to calculate the mixture diffusivity, with a probable small degree of error. Without temperature correction, the inlet and outlet values of $D_{HCl,m}$ are 0.1807 and 0.1837 cm^2/sec, while the values for $D_{H_2O,m}$ are 0.250 and 0.265 cm^2/sec. An average value for each system was used and, assuming diffusivity to be proportional to the square of absolute temperature,[34] the diffusivities were written as:

$$D_{HCl,m} = 0.1822\ (T/303)^2\ cm^2/sec$$

$$D_{H_2O,m} = 0.2574\ (T/303)^2\ cm^2/sec$$

$$T = {}^{o}K\ .$$

APPENDIX IX

Physical Properties for Coefficient Correction

1. Liquid Properties for O_2 Desorption at 25°C, 1 atmosphere

$D_l = D_{O_2-H_2O} = 2.5\times10^{-5}$ cm^2/sec (Ref. 28)

$\mu_l = \mu_{H_2O} = 0.8937$ centipoise (Ref. 39)

$\rho_l = \rho_{H_2O} = 62.43$ lb/ft^3 (Ref. 28)

2. Gas Properties for Lean Ammonia Absorption at 21°C, 1 atmosphere

$N_{Sch} = 0.65$ (Ref. 33)

$\rho_g = \rho_{air} = 0.0749$ lb/ft^3 (Ref. 39)

$\mu_g = \mu_{air} = 182.7$ micro-poise $= 1.227\times10^{-5}$ lb/ft sec (Ref. 39) 18°C

3. HCl Absorption

a. Gas properties at 21°C, 1 atmosphere

$D_g = 0.172$ cm^2/sec (Appendix VIII)

$\rho_g = 0.0778$ lb/ft^3 (inlet composition; Appendix VIII)

$\mu_g = 171.4$ micro-poise $= 1.152\times10^{-5}$ lb/ft sec (molar average at inlet; component viscosities from Ref. 39)

b. Liquid properties at 25°C

$D_l = 3.1\times10^{-5}$ cm^2/sec (for dilute solutions)[28]

$\mu_l = 0.5868$ centipoise (average composition)[28]

$\rho_l = 62.92$ lb/ft^3 (Ref. 28)

The accuracy of these liquid properties is not critical for the gas-phase-controlled HCl absorption system.

4. CO_2 Absorption

a. Gas properties at 21°C, 1 atmosphere

$D_g = D_{H_2-CO_2} = 6.65\times10^{-4}$ ft^2/sec (estimated using Chapman-Enskog formula described in Appendix VIII)

$\mu_g = 6.389\times10^{-6}$ lb/ft sec (molar average viscosity at average composition. Component viscosities from Ref. 39)

$\rho_g = \rho_{g\ 150}(338.6/294.0)(14.7/140.0)$ ($\rho_{g\ 150}$ is the average density in the contactor of interest; see Appendix IV)

b. Liquid properties at 25°C

$D_l = 0.982\times10^{-5}$ cm^2/sec (Based on diffusivity of CO_2 in water at 25°C (Ref. 28) corrected for viscosity on the assumption that $D_l \sim \mu_l^{-0.93}$ (Ref. 33))

$\rho_l = 77.4$ lb/ft^3 (Ref. 28)

$\mu_l = 1.87$ centipoise (average composition)[38]

APPENDIX X

Fourth-Order Runge-Kutta Integration for HCl Absorption in a Packed Column

In a form suitable for numerical integration, the rate equations for HCl absorption may be written as:

$$(Lx)_{n+1} - (Lx)_n = SK_g a_{HCl} M_{HCl} P \int_n^{n+1} (y_{HCl} - y^*_{HCl})\, dz \qquad \text{(A-X-1)}$$

$$(Gy)_{n+1} - (Gy)_n = SK_g a_{H_2O} M_{H_2O} P \int_n^{n+1} (y^*_{H_2O} - y_{H_2O})\, dz \qquad \text{(A-X-2)}$$

where: L = total liquid flow, gms/hr

G = total gas flow, gms/hr

x = wt fraction of HCl in liquid

y = wt fraction of H_2O in gas

S = tower cross sectional area, ft^2

P = total pressure, atm

z = length coordinate, ft

y_j = mole fraction of component j in bulk gas

y^*_j = mole fraction of component j in equilibrium with liquid of composition x at point in column

$K_g a_j$ = mass-transfer coefficient for component j, gm moles/atm ft^3 hr

M_j = molecular weight of transferring species j

The simultaneous integration of the two rate equations is similar to a problem solved by Lapidus.[36] To perform the Runge-Kutta integration,

the equations must be capable of being rewritten as:

$$d(Lx) = F(Lx,Gy)\ dz \qquad \text{(A-X-3)}$$

$$d(Gy) = G(Lx,Gy)\ dz \qquad \text{(A-X-4)}$$

This implies that the quantities $(y_{HCl}-y^*_{HCl})$ and $(y^*_{H_2O} - y_{H_2O})$ must be expressed solely in terms of Lx and Gy. This was done through the following set of equations:

$$GHCl_{n+1} = GHCl_n - (Lx)_{n+1} + (Lx)_n \qquad \text{(A-X-5)}$$

$$GH_2O_{n+1} = GH_2O_n + (Gy)_{n+1} - (Gy)_n \qquad \text{(A-X-6)}$$

$$y_{HCl} = \frac{(GHCl)_{n+1}}{GHCl_{n+1} + GH_2O_{n+1} + GH_2 + Gair} \qquad \text{(A-X-7)}$$

$$y_{H_2O} = \frac{GH_2O_{n+1}}{GHCl_{n+1} + GH_2O_{n+1} + GH_2 + Gair} \qquad \text{(A-X-8)}$$

$$L_{n+1} = L_n + (Lx)_{n+1} - (Lx)_n + (Gy)_n - (Gy)_{n+1} \qquad \text{(A-X-9)}$$

$$x_{n+1} = \frac{(Lx)_{n+1}}{L_{n+1}} \qquad \text{(A-X-10)}$$

$$y^*_{HCl} = f(x_{n+1},T) \qquad \text{(A-X-11)}$$

$$y^*_{H_2O} = g(x_{n+1},T) \qquad \text{(A-X-12)}$$

$$G_{n+1} = G_n + (Gy)_{n+1} - (Gy)_n - (Lx)_{n+1} + (Lx)_n \qquad \text{(A-X-13)}$$

$$\Delta P/\Delta L = f(L_{n+1},\ G_{n+1},\ \text{physical and equipment properties}) \qquad \text{(A-X-14)}$$

$$K_g a_j = f(L_{n+1},\ G_{n+1},\ \Delta P/\Delta L,\ \text{physical properties}) \qquad \text{(A-X-15)}$$

where GHCl, GH_2O, GH_2, Gair are gas flow rates of component gases, gm moles/hr, T is the system temperature, and M_i is the molecular weight of component i.

Since L_o, G_o, x_o, T_o, $GHCl_o$, GH_2O_o, Gair, and GH_2 are initially set, this set of equations satisfies the requirements of Eqs. (A-X-3) and (A-X-4).

Integration is initialized by choosing Δz and guessing a value of T at a point Δz up the column. $(Lx)_{n+1}$ and $(Gy)_{n+1}$ are calculated by the scheme:

$$k_o = \Delta zF[(Lx)_n, (Gy)_n]$$
$$m_o = \Delta zG[(Lx)_n, (Gy)_n] \qquad \text{(A-X-16)}$$

$$k_1 = \Delta zF[(Lx)_n+1/2\ k_o, (Gy)_n+1/2\ m_o]$$
$$m_1 = \Delta zG[(Lx)_n+1/2\ k_o, (Gy)_n+1/2\ m_o] \qquad \text{(A-X-17)}$$

$$k_2 = \Delta zF[(Lx)_n+1/2\ k_1, (Gy)_n+1/2\ m_1]$$
$$m_2 = \Delta zG[(Lx)_n+1/2\ k_1, (Gy)_n+1/2\ m_1] \qquad \text{(A-X-18)}$$

$$k_3 = \Delta zF[(Lx)_n+k_2, (Gy)_n + m_2]$$
$$m_3 = \Delta zG[(Lx)_n+k_2\ , (Gy)_n+m_2] \qquad \text{(A-X-19)}$$

$$(Lx)_{n+1} = (Lx)_n + 1/6\ (k_o + 2k_1 + 2k_2 + k_3) \qquad \text{(A-X-19)}$$

$$(Gy)_{n+1} = (Gy)_n + 1/6\ (m_o + 2m_1 + 2m_3 + m_3) \qquad \text{(A-X-20)}$$

With the new calculated values of $(Lx)_{n+1}$ and $(Gy)_{n+1}$, the heat balance over the increment Δz is checked. If the heat balance does not

check, a new value of temperature is selected, and the values of $(Lx)_{n+1}$ and $(Gy)_{n+1}$ are recalculated. The procedure for converging on temperature was a Reguli-Falsi iteration scheme, similar to that described in Appendix V.

This procedure continues for Δz increments up the column until a selected boundary condition—such as the independently set value of the outlet HCl composition—is reached, and the sum of the Δz's represents the column height.

Since the changes in composition and temperature were greatest in the early parts of the contactors, the algorithm was made more efficient by using a variable step size, Δz, which was small at the early stage of the contactor and increased by 20% at each successive step. The performance of the technique was tested by varying the initial step size and comparing the column heights calculated.

APPENDIX XI

Flow Equations and Determination of Column Lengths for the CO_2-K_2CO_3 System

1. Flow Equations for the CO_2-K_2CO_3 System—Sample Calculation

The molalities of K_2CO_3 and $KHCO_3$ may be related to the molality of unconverted K_2CO_3 by the expressions[38]:

$$MKHCO_3 = 2Bf(MiK_2CO_3) \qquad \text{(A-XI-1)}$$

$$MK_2CO_3 = B(1-f)(MiK_2CO_3) \qquad \text{(A-XI-2)}$$

where: MiK_2CO_3 is the molality of unconverted K_2CO_3

$$f = \frac{\text{(amount of } CO_2 \text{ absorbed)}}{\text{(maximum stoichiometric amount of } CO_2 \text{ which may be absorbed by a given concentration of } K_2CO_3\text{)}}$$

= fraction conversion

B = factor to account for water consumed in the reaction of CO_2 and K_2CO_3

$$= \frac{55.51}{55.51 - f(MiK_2CO_3)} \qquad \text{(A-XI-3)}$$

At 25% K_2CO_3, the maximum stoichiometric loading of K_2CO_3 is 7.09 standard cubic feet of CO_2/gallon of solution.

Molality of unconverted 25% K_2CO_3

At 150°F sp. gr. (150/60) K_2CO_3 = 1.215

Density of H_2O at 60°F = 0.999 gm/cc

Weight of K_2CO_3 = (1.215)(0.999)(0.25) = 0.3034 gm/cc

Weight of H_2O = 1.2137 - 0.3034 = 0.9103 gm/cc

$$MiK_2CO_3 = \frac{0.3034 \text{ gms } K_2CO_3/\text{cc}}{0.9103 \text{ gms } H_2O/\text{cc}} \times \frac{1 \text{ gm mole}}{138.2 \text{ gms } K_2CO_3} \times 1000$$

$$MiK_2CO_3 = 2.4038 \frac{\text{gm moles } K_2CO_3}{1000 \text{ gms } H_2O}$$

Flow equations—co-current flow

Based on the stoichiometry of the CO_2-K_2CO_3 reaction, and neglecting density changes with reaction, the molarities of K_2CO_3 and $KHCO_3$ may be related to the molarities corresponding to the inlet absorbent loading by:

$$(KHCO_3) = (KHCO_3)_o + \frac{2}{F}\,[GCO_{2o} - GI\ y/(1-y)] \qquad \text{(A-XI-4)}$$

$$(K_2CO_3) = (K_2CO_3)_o - \frac{1}{F}\,[GCO_{2o} - GI\ y/(1-y)] \qquad \text{(A-XI-5)}$$

where: F = Absorbent flow rate, liter/hr

GCO_{2o} = initial CO_2 gas flow, gm moles/hr

GI = flow rate of gaseous inerts, gm moles/hr

y = bulk mole fraction of CO_2 in gas

Flow equations for single-contactor case

Inlet CO_2 loading = 2 SCF CO_2/gallon of solution

Therefore, f = 0.282

B = 1.0123

so that: $MKHCO_3$ = 1.3727 gm moles/1000 gm H_2O

MK_2CO_3 = 1.7468 gm moles/1000 gm H_2O

At 28% conversion, ρ_1 = 1.2217 gm/cc

Conversion to molarity:

$$\frac{1221.7 \text{ gm/liter}}{[(1.3727)(101.1) + (1.7468)(138.2) + 1000.0] \text{ gm/1000 gm } H_2O}$$

$$= 0.88516 \text{ (1000 gm } H_2O\text{)/liter}$$

$(KHCO_3)_o$ = (1.3727)(0.88516) = 1.2150 gm moles/liter

$(K_2CO_3)_o$ = (1.7468)(0.88516) = 1.5462 gm moles/liter

$$F = 232{,}638.87 \text{ Liter/hr}$$

$$GI = 314{,}637.24 \text{ gm moles/hr}$$

$$GCO_{2o} = 76{,}765.57 \text{ gm moles/hr}$$

Therefore: $(KHCO_3) = 1.8748 - 2.7047\ y/(1-y)$ gm moles/liter (A-XI-6)

$(K_2CO_3) = 1.2163 + 1.3524\ y/(1-y)$ gm moles/liter (A-XI-7)

The flow equations for the other contactor combinations may be calculated similarly.

2. Evaluation of Column Heights for CO_2 Absorption

The integrals to be evaluated in determining the height (or length) or the contactors used for CO_2 absorption were numerically integrated using Simpson's rule. Simpson's rule may be stated as

$$\int_a^b f(x)dx = \frac{h}{3}\{f(x_o) + 4[f(x_1) + f(x_3) + f(x_5) + \ldots + f(x_{m-1})] + 2[f(x_2) + f(x_4) + \ldots + f(x_{m-2})] + f(x_m)\} \quad \text{(A-XI-8)}$$

where $h = \frac{b-a}{m}$ (A-XI-9)

m = number of equal sized intervals at the ends of which the function is evaluated. According to the above notation, m is an even integer.

Co-current packed column

The integral which is to be evaluated may be written as

$$10^{-3} \int_{(CO_3^{=})_{in}}^{(CO_3^{=})_{out}} \frac{d(CO_3^{=})}{HPy-C_b} \quad \text{(A-XI-10)}$$

The variables may be related by the following equations and constants:

$$(CO_3^{=}) = A + B\ y/(1-y)\ \text{gm moles/liter} \qquad \text{(A-XI-11)}$$

$$(HCO_3^{-}) = C - D\ y/(1-y)\ \text{gm moles/liter} \qquad \text{(A-XI-12)}$$

where y is the mole fraction of CO_2 in the bulk gas and A, B, C, and D are constants (see Eqs. (A-XI-6) and A-XI-7))

$$H = H_w \times 10^{-K_s I}\ \text{gm moles/atm cm}^3 \qquad \text{(A-XI-13)}$$

in which H is the physical solubility constant and H_w is the physical solubility constant for CO_2 in water.

$$H_w = 1.16\times10^{-5}\ \text{gm moles/atm cm}^3$$

$$K_s = 0.06$$

$$I = 1/2[6(CO_3^{=}) + 2(HCO_3^{-})]\ \text{gm ions/liter} \qquad \text{(A-XI-14)}$$

$$C_b = \frac{K_2}{K_1}\frac{(HCO_3^{-})^2}{(CO_3^{=})} = 1.525\times10^{-7}\frac{(HCO_3^{-})^2}{(CO_3^{=})}\ \text{gm moles/cm}^3 \qquad \text{(A-XI-15)}$$

Procedure:

1. Knowing y_{in} and y_{out}, compute $(CO_3^{=})_{in}$ and $(CO_3^{=})_{out}$ using Eq. (A-XI-11).
2. Choose number of equal intervals, m, over which integration is to occur; define

   $$h = [(CO_3^{=})_{in} - (CO_3^{=})_{out}]/m$$

3. For $(CO_3^{=})_{in}$, $(CO_3^{=})_{in} - h$, $(CO_3^{=})_{in} - 2h$, ..., $(CO_3^{=})_{out}$, calculate y using Eq. (A-XI-11).
4. Calculate $(HCO_3^{-})_{in}$, ..., $(HCO_3^{-})_{out}$ using Eq. (A-XI-12).

5. Calculate I, H, and C_b.

6. $f(x_i) = \frac{1}{HPy-C_b}$

The evaluation procedure for the annular-flow contactor is similar, with the addition of equations relating y to C_e and C_a.

APPENDIX XII

Nomenclature

The dimensions of the nomenclature used are expressed in terms of length (L), time (t), mass (M), force (F), thermal energy (H), and temperature (T). More specific dimensions, consistent with various equations and correlations, are given in the text.

A	numerical constant
a	interfacial area per unit volume, L^{-1}
a	numerical constant
a_o	dry packing area per unit volume, L^{-1}
a_w	cylindrical area per unit volume of spray tower, L^{-1}
a'	area per unit volume associated with sprayed droplets, L^{-1}
B	factor to account for water consumed in reaction between CO_2 and K_2CO_3, dimensionless
B	numerical constant
b	numerical constant
C	numerical constant
C	concentration of component in liquid, mole/L^3
C_a	equivalent CO_2 concentration in annular liquid, mole/L^3
C_b	concentration of free carbon dioxide in the bulk of the solution, mole/L^3
C_D	drag coefficient, dimensionless
C_e	equivalent CO_2 concentration in entrained droplets, mole/L^3
C_o	reagent concentration, mole/L^3
C_p	heat capacity per unit mass, H/MT

$C_{p(molar)}$ heat capacity per mole, H/mole T

C^* concentration of physically dissolved CO_2 in equilibrium with interfacial gas concentration, mole/L^3

C_p^* mean molar heat capacity, H/mole T

c numerical constant

c_m mass concentration of entrained droplets, M/L^3

D diffusivity, L^2/t

D contactor diameter, L

D numerical constant

D_p equivalent spherical diameter of particle, L

d bubble or droplet diameter, L

d' dimensionless bubble diameter

E energy dissipation per unit volume, LF/L^3t

E_n entrainment, M/t

E_{MV} Murphree stage efficiency, dimensionless

F volumetric liquid flow rate, L^3/t

Fr Frounde number, dimensionless

f fraction conversion, dimensionless

f friction factor, dimensionless

G mass gas flow rate, M/t

G_m molar gas flow rate, mole/t

GI molar gas flow rate of gaseous inerts, mole/t

Gi molar gas flow rate of component i, mole/t

G' mass gas flow rate of gaseous inerts, M/t

g_c gravitational constant, ML/Ft^2

H	Henry's law solubility constant, mole $L^2/F\ L^3$
H_D	heat of dilution per unit mass, H/M
H_g	inert free gas enthalpy per unit mass, H/M
H_g'	enthalpy per unit mass of inert gases, H/M
H_L	liquid enthalpy, H/M
H_w	Henry's law constant for solubility in water, mole $L^2/F\ L^3$
ΔH_{vap}	heat of vaporization of water per unit mass, H/M
$\Delta(\Sigma H)$	measure of lack of closure of heat balance, H/t
h	integration interval for application of Simpson's rule
I	ionic strength, ions/L^3
I_n	interchange rate, M/Lt
In'	interchange rate, M/tL^2
j_D'	factor to account for diffusional mass transfer, dimensionless
K	proportionality constant relating y_G to R_g, dimensionless
K_1	first dissociation constant of carbonic acid, mole/L^3
K_2	second dissociation constant of carbonic acid, mole/L^3
$K_{As(OH)_3}$	stoichiometric dissociation constant of $As(OH)_3$, mole/L^3
K_g	over-all mass-transfer coefficient, L^2 mole/FL^2t
Kg'	over-all mass-transfer coefficient characterizing diffusional mass transfer in annular flow, L^2 mole/FL^2t
K_s	solubility proportionality constant, dimensionless
K_w	equilibrium constant for water dissociation, $mole^2/L^6$
k	numerical constant
k	mass-transfer coefficient for interchange, L/t
k_i	mass-transfer coefficient for steady-state interchange, L/t
k_2	second-order reaction rate constant, L^3/mole t

k_{As} rate constant for arsenite catalysis, L^3/mole t

$k_c a$ gas-phase mass-transfer coefficient, t^{-1}

k_e constant representing equilibrium approach, dimensionless

$k_g a$ gas phase mass transfer coefficient, L^2 mole/F L^3 t

k_l physical liquid phase mass-transfer coefficient, L/t

k_{OH} rate constant accounting for reaction of CO_2 with hydroxide ions, L^3/mole t

L mass liquid flow rate, M/t

L_a mass flow rate of liquid in annular film, M/t

LTU length of individual phase transfer unit, L

M molecular weight, M/mole

m numerical constant

m number of intervals in Simpson's rule integration

m_i rate of interchange mass transfer, M/L^2t

N number of dispersed spherical particles

NTU number of individual phase transfer units, dimensionless

P total pressure, F/L^2

$\Delta P/\Delta L$ pressure drop per unit length, F/L^3

$(\Delta P/\Delta L)^*$ pressure drop per unit length based on gas or liquid properties and combined phase velocities, F/L^3

p partial pressure or vapor pressure, F/L^2

Q total enthalpy per unit time, H/t

Q volumetric flow rate, L^3/t

Q_s enthalpy of inert gases per unit time, H/t

R universal gas constant, ML^2/t^2T mole

R	absorption rate, mole/L^2 t
R_d	holdup of dispersed phase, dimensionless
Re	Reynolds number, dimensionless
R_{en}	entrainment parameter, ML^2/Ft
R_g	gas holdup, dimensionless
R_l	liquid holdup, dimensionless
r	chemical reaction rate, mole/L^3t
r	radius, L
S	cross sectional area of contactor, L^2
Sch	Schmidt number, dimensionless
S_d	droplet surface area, L^2
s	slope
T	temperature, T
TO	reference temperature, T
t	time, t
U_{hom}	homogeneous velocity, L/t
U'_{hom}	modified homogeneous velocity for packed column, L/t
V	fluid velocity, L/t
V_{sl}	slip velocity, L/t
V_t	terminal velocity, L/t
We_c	critical Weber number, dimensionless
$-W_f$	energy per unit mass, LF/M
X	liquid phase concentration for correlation of physical properties, various units
x	mole or weight fraction of component in liquid, dimensionless
x_a	weight fraction of solute in annular liquid, dimensionless

x_e weight fraction of solute in entrained liquid, dimensionless

y bulk gas mole or weight fraction, dimensionless

y_i interfacial gas mole fraction, dimensionless

y_G ratio of velocity of gas to combined velocities of gas and liquid, dimensionless

y^* gas mole fraction in equilibrium with bulk liquid, dimensionless

z length coordinate, L

Z total length, L

Greek Letters

α activity coefficient correction for carbonate ions, dimensionless

α constant in Ergun equation, dimensionless

β activity coefficient correction for bicarbonate ions, dimensionless

β constant in Ergun equation, dimensionless

γ activity coefficient correction for water, dimensionless

δ convergence interval, T

ε packing void fraction, dimensionless

η $(k_1^2 + D_1 k_2 C_o)^{1/2}$, L/t

θ droplet holding time, t

Λ density parameter, dimensionless

μ viscosity, F/Lt

ρ density, M/L^3

σ surface tension, F/L

σ_{AB} function of molecular radii, L

ϕ_g Lockhart and Martinelli parameter, dimensionless

ϕ	viscosity correlation parameter, dimensionless
χ	Lockhart and Martinelli parameter, dimensionless
Ψ	viscosity and surface tension parameter, dimensionless
$\Omega_{D_{ij}}$	function of temperature and intermolecular fields, dimensionless

Subscripts

atm	corrected for atmospheric conditions
c	critical
ds	mean diameter-surface
g	gas
i	of component i
i - j	of component i in component j
i,m	of component i in mixture
l	liquid
mix	mixture
sv	mean surface-volume
tp	two phase
o	initial
50	exceeded by 50%
90	exceeded by 10%
95	exceeded by 5%

REFERENCES

1. A. L. Kohl and F. C. Riesenfeld, Gas Purification (McGraw-Hill, New York, 1960).
2. R. S. Custer, "Today's Ammonia Technology," unpublished manuscript, Bechtal Corporation.
3. H. E. Bensen, J. H. Field, and R. M. Jimeson, Chem. Eng. Prog. 50, 356 (1954).
4. H. E. Bensen, J. H. Field, and W. P. Haynes, Chem. Eng. Prog. 52, 433 (1956).
5. F. C. Riesenfeld and C. L. Blohm, Hydrocarbon Proc. and Pet. Ref. 41 (4), 123 (1962).
6. M. W. Hyman, "Computational Study of a Refinery Hydrogen Plant," M. S. Thesis, University of California, Berkeley, 1967.
7. B. O. Buch and A. R. S. Leitch, Oil and Gas J. 56, (September 22, 1958).
8. H. Wall, "Absorption and Desorption of Carbon Dioxide in Carbonate-Bicarbonate Buffer Solutions," M. S. Thesis, University of Delaware, 1966.
9. D. M. Kern, J. Chem. Educ. 37, 14 (1960).
10. P. V. Danckwerts and M. M. Sharma, Chem. Eng. Sci. 18, 729 (1963).
11. R. A. T. O. Nijsing and H. Kramers, Chem. Eng. Sci. 8, 81 (1958).
12. M. M. Sharma, "Kinetics of Gas Absorption," Ph.D. Thesis, University of Cambridge, 1964.
13. Chemical Engineering Division Research Highlights, Argonne National Laboratory, ANL-6875, 79 (May 1963 - April 1964).
14. Chemical Engineering Division Research Highlights, Argonne National Laboratory, ANL-6766, 75 (May 1962 - April 1963).

15. "Research and Development on Nonaqueous Processing," Reactor Fuel Processing 8 (1), 19 (Winter, 1964-65).

16. "Research and Development on Nonaqueous Processing," Reactor Fuel Processing 8 (2), 88 (Spring 1965).

17. "Research and Development on Nonaqueous Processing," Reactor Fuel Processing 7 (4), 241 (Fall 1964).

18. J. B. Bingeman and L. B. Reynolds, Chem. Eng. Prog. 56, 67 (1960).

19. W. M. Gaylord and M. A. Miranda, Chem. Eng. Prog. 53, 139M (1957).

20. L. P. Riess, Ind. and Eng. Chem. Process Design and Develop. 6, 486 (1967).

21. R. P. Larkins, R. R. White, and D. W. Jeffrey, A. I. Ch. E. J. 7, 231 (1961).

22. C. Y. Wen, W. S. O'Brien, and Liang-Tseng Fan, J. Chem. and Eng. Data 8, 42 (1963).

23. R. W. Lockhart and R. C. Martinelli, Chem. Eng. Prog. 45, 39 (1949).

24. S. Ergun, Chem. Eng. Prog. 48, 89 (1952).

25. P. H. Calderbank and M. B. Moo-Young, Chem. Eng. Sci. 16, 39 (1961).

26. W. S. Norman, Absorption, Distillation, and Cooling Towers (John Wiley and Sons, New York, 1961).

27. J. E. Vivian and C. J. King, A. I. Ch. E. J. 10, 220, 221 (1964).

28 John H. Perry, (ed.), Chemical Engineers' Handbook (McGraw-Hill, New York, 1963).

29. B. W. Gamson, G. Thodos, and O. A. Hougen, Trans. Am. Inst. Chem. Engrs. 39, 1 (1943).

30. R. G. Taecker and O. A. Hougen, Chem. Eng. Prog. 45, 188 (1949).

31. Jon M. Heuss, C. J. King, and C. R. Wilke, "Mass Transfer in Co-Current Gas-Liquid Flow," UCRL-11570 (1964).

32. O. E. Dwyer and B. F. Dodge, Ind. and Eng. Chem. 33, 485 (1941).

33. P. V. Danckwerts and M. M. Sharma, The Chem. Engr., CE244 (October 1966).

34. R. B. Bird, W. E. Stewart, E. N. Lightfoot, Transport Phenomena (John Wiley and Sons, New York, 1960).

35. A. S. Foust, L. A. Wenzel, C. W. Clump, L. Maus, and L. B. Andersen, Principles of Unit Operations (John Wiley and Sons, New York, 1960).

36. L. Lapidus, Digital Computation for Chemical Engineers (McGraw-Hill, New York, 1962).

37. W. James and E. Silberman, "Two-Phase Flow Studies in Horizontal Pipes with Special Reference to Bubble Mixtures," Univ. of Minn. Tech. Paper No. 26, Series B (1958).

38. J. P. Bocard and B. J. Mayland, Hydrocarbon Proc. and Pet. Ref. 41 (4), 128 (1962).

39. C. D. Hodgman (ed.), Handbook of Chemistry and Physics (Chemical Rubber Publishing Company, Cleveland, 1963).

40. A. E. Dukler and M. Wicks III, "Gas-Liquid Flow in Conduits," in Modern Chemical Engineering (Reinhold Publishing Corporation, New York, 1964) p. 349.

41. D. S. Scott, "Properties of Co-Current Gas-Liquid Flow," in Advances in Chemical Engineering (Academic Press, New York, 1964), Vol. IV.

42. William S. Gouse, Jr., An Index to the Two Phase Flow Literature, M.I.T. Report No. 9 (Riverside Press, Cambridge, 1966).

43. O. Baker, Oil and Gas J. (June 26, 1954).

44. G. A. Hughmark, Chem. Eng. Prog. 58, 62 (1962).

45. S. G. Bankoff, Trans. A. S. M. E. 82, 265 (1960).

46. A. E. Dukler, Moye Wicks III, and R. G. Cleveland, A. I. Ch. E. J. 10, 38 (1964).

47. G. A. Hughmark, Ind. and Eng. Chem. Fund. 2, 315 (1963).

48. J. M. Chenoweth and M. W. Martin, Pet. Ref. 34, 151 (October 1955).

49. H. C. McManus, Jr., "An Experimental Investigation of Liquid Distribution and Surface Character in Horizontal Annular Two-Phase Flow," Final Report, DA Project No. 59901004, AROD Project 2117-E, Sibley School of Mechanical Engineering, Cornell University (October 1961).

50. A. E. Dukler and M. Wicks III, A. I. Ch. E. J. 6, 463 (1960).

51. L. B. Cousins, W. H. Denson, and G. F. Hewitt, "Liquid Mass Transfer in Annular Two-Phase Flow," AERE-R-4926 (1965).

52. J. D. Anderson, R. E. Bollinger, and D. E. Lamb, A. I. Ch. E. J. 10, 640 (1964).

53. R. E. Bollinger, "Liquid Phase Controlled Mass Transfer in Annular Two-Phase Flow," M. S. Thesis, University of Delaware, 1960.

54. C. E. Wales, A. I. Ch. E. J. 12, 1166 (1966).

55. J. C. Jepsen, "Mass Transfer in Two-Phase Flow in Horizontal Pipelines," A. I. Ch. E. Preprint 25B, presented at Second Joint A. I. Ch. E. - IIQPR Meeting, May 1968.

56. G. A. Hughmark, Ind. and Eng. Chem. Fund. 4, 361 (1965).

57. J. M. Heuss, C. J. King, and C. R. Wilke, A. I. Ch. E. J. 11, 866 (1965).

58. D. S. Scott and W. Hayduk, Can. J. of Chem. Eng., 130 (June 1966).

59. T. Vermeulen, G. M. Williams, and G. E. Langlois, Chem. Eng. Prog. 52, 85F (1955).

60. C. J. King, Separation Processes (McGraw-Hill, New York, in press).

61. R. L. Pigford and T. K. Sherwood, Absorption and Extraction (McGraw-Hill, New York, 1952).

62. W. Strauss, Industrial Gas Cleaning (Pergamon Press, Oxford, 1966); Vol. 8 of International Series of Monographs in Chemical Engineering, P. V. Danckwerts (ed.).

63. R. V. Kleinschmidt and A. W. Anthony, Trans. Am. Soc. Mech. Engrs. 63, 349 (1941).

64. G. Nonhebel, "Centrifugal Gas Absorbers," in Gas Purification Processes, ed. by G. Nonhebel, (G. Newnes, London, 1964).

65. W. G. Bauer, A. G. Fredrickson, and W. A. Tsuchiya, Ind. and Eng. Chem. Process Design and Devel. 2, 178 (1963).

66. R. L. Pigford and C. Pyle, Ind. and Eng. Chem. 43, 1649 (1951).

67. C. F. Oldershaw, L. Simenson, T. Brown, and R. Radcliffe, Chem. Eng. Prog. 43, 371 (1947).

68. T. A. Kantyka and H. R. Hinchlieff, Trans. Inst. Chem. Engrs. 32, 236 (1954).

69. K. E. Lunde, Ind. and Eng. Chem. 50, 293 (1958).

70. J. R. Fair, "Tray Hydraulics-Perforated Trays," in B. D. Smith, Design of Equilibrium Stage Processes (McGraw-Hill, New York, 1963), Chapter 15.

71. J. Voogd and J. Tielrooy, Hydrocarbon Proc. 46 (9), 115 (1967).

72. C. C. Van Nuys, A. I. Ch. E. Trans. 39, 663 (1943).

73. J. M. Smith and H. C. Van Ness, Introduction to Chemical Engineering Thermodynamics (McGraw-Hill, New York, 1959).

74. C. J. King, personal communication.

75. M. S. Peters, Plant Design and Economics for Chemical Engineers (McGraw-Hill, New York, 1958).

LEGAL NOTICE

This report was prepared as an account of Government sponsored work. Neither the United States, nor the Commission, nor any person acting on behalf of the Commission:

A. Makes any warranty or representation, expressed or implied, with respect to the accuracy, completeness, or usefulness of the information contained in this report, or that the use of any information, apparatus, method, or process disclosed in this report may not infringe privately owned rights; or

B. Assumes any liabilities with respect to the use of, or for damages resulting from the use of any information, apparatus, method, or process disclosed in this report.

As used in the above, "person acting on behalf of the Commission" includes any employee or contractor of the Commission, or employee of such contractor, to the extent that such employee or contractor of the Commission, or employee of such contractor prepares, disseminates, or provides access to, any information pursuant to his employment or contract with the Commission, or his employment with such contractor.

TECHNICAL INFORMATION DIVISION
LAWRENCE RADIATION LABORATORY
UNIVERSITY OF CALIFORNIA
BERKELEY, CALIFORNIA 94720